Division of Pharmaceutical Chemistry
Faculty of Pharmacy
University of Helsinki
Finland

N-Glucuronidation of Drugs and Other Xenobiotics

Sanna Kaivosaari

ACADEMIC DISSERTATION

To be presented, with the permission of the Faculty of Pharmacy of the University of Helsinki, for public examination in Auditorium 1041,
Viikki Biocenter 2 (Viikinkaari 5),
on 12 February 2010, at 12 noon.

Helsinki 2010

Supervisors:

Docent Moshe Finel
Centre for Drug Research (CDR)
Faculty of Pharmacy
University of Helsinki
Helsinki, Finland

Docent Mikko Koskinen
Translational Sciences
Orion Corporation
Espoo, Finland

Reviewers:

Associate Professor Miki Nakajima
Drug Metabolism and Toxicology
Faculty of Pharmaceutical Sciences
Kanazawa University
Kanazawa, Japan

Professor Hannu Raunio
Department of Pharmacology and Toxicology
University of Kuopio
Kuopio, Finland

Opponent:

Professor Philip Lazarus
Departments of Pharmacology and Public Health Sciences
Penn State College of Medicine
Hershey, PA, USA

ISBN 978-952-10-6041-0 (paperback)
ISBN 978-952-10-6042-7 (PDF)
ISSN 1795-7079
http://ethesis.helsinki.fi/

Helsinki University Printing House
Helsinki 2010

Abstract

UDP-glucuronosyltransferases (UGTs) are a family of metabolic enzymes responsible for the detoxification of a wide range of endo- and xenobiotics, including drugs. UGT-mediated metabolism is a major determinant of the pharmacokinetic behavior of many drugs in the human body, contributing to parameters such as bioavailability and elimination. UGTs catalyze the transfer of glucuronic acid from UDP-glucuronic acid (UDPGA) to the aglycone substrates, producing water-soluble glucuronide conjugates that are mostly devoid of pharmacological activity. Some of the 19 human UGTs have the ability to conjugate different nitrogen-containing compounds, thus forming *N*-glucuronides. *N*-Glucuronidation exhibits marked differences across species. As an example, the ability to form quaternary ammonium glucuronides from tertiary amines is a reaction largely, but not completely, restricted to humans. Among the human UGTs, UGT1A4 has been considered the enzyme "specializing" in *N*-glucuronidation.

The goal of this study was to characterize species differences related to *N*-glucuronidation and to elucidate whether human UGT enzymes other than the previously reported UGT1A4 catalyze this reaction. The nitrogen-containing substrates investigated were firstly a set of 4-arylalkyl-1*H*-imidazoles, including the sedative drug dexmedetomidine [(+)-4-(*S*)-[1-(2,3-dimethylphenyl)ethyl]-1*H*-imidazole], and secondly nicotine, the addictive agent in tobacco products, along with its major metabolite cotinine. The study was performed using different *in vitro* systems, such as human and animal liver microsomes and recombinant human UGT enzymes produced in baculovirus-infected insect cells. The 4-arylalkyl-1*H*-imidazole substrates were incubated with a radiolabeled cofactor, ^{14}C-UDPGA, and the glucuronide products were analyzed by liquid chromatography using ultraviolet detection combined with a flow scintillation analyzer. Nicotine and cotinine glucuronides were quantified using liquid chromatography – mass spectrometry.

Analyses of liver microsome incubates indicated that *N*-glucuronidation of medetomidine was efficient in humans, while the glucuronidation rates measured in rat, mouse, guinea-pig, rabbit, dog, mini-pig, and monkey liver microsomes were rather low. Studies with recombinant human UGTs revealed that the "orphan enzyme" UGT2B10, which has previously demonstrated no or only very limited activity when screened against a large variety of substrates, plays an important role in the *N*-glucuronidation of the compounds investigated. More specifically, we discovered that UGT2B10 is the enzyme mainly responsible for nicotine *N*-glucuronidation in the human liver, and, furthermore, this enzyme is a major contributor to the *N*-glucuronidation of medetomidine.

Nuclear magnetic resonance (NMR) analyses revealed that the *N*-glucuronidation of medetomidine by human liver microsomes was highly regioselective, and that N_3 was the preferred site of glucuronidation. Moreover, this chiral drug was *N*-glucuronidated stereoselectively. Regio- and stereospecific *N*-glucuronidation of medetomidine in human liver microsomes was explained by complex kinetics involving two enzymes, UGT1A4 and UGT2B10. UGT2B10 was found to be a high-affinity (low K_m) enzyme towards medetomidine, while the affinity of UGT1A4 was considerably lower. Levomedetomidine

[(–)-4-(*R*)-[1-(2,3-dimethylphenyl)ethyl]-1*H*-imidazole], in particular, turned out be a high-affinity, specific substrate of UGT2B10.

The results emphasize the species differences of *N*-glucuronidation and the importance of *in vitro* studies utilizing human-derived material, along with animal studies, at the early stages of drug development. Furthermore, this study highlights the contribution of UGT2B10, along with UGT1A4, to the *N*-glucuronidation of drugs and other xenobiotics in the human liver.

Acknowledgements

The first part of this work was carried out at the Division of Pharmaceutical Chemistry, Faculty of Pharmacy, University of Helsinki, during 1998-2000. Financial support provided by the Graduate School in Pharmaceutical Research is gratefully acknowledged.

At the beginning of my academic career, I was privileged to be supervised by the late Professor Jyrki Taskinen. His broad expertise and enthusiasm and his patience in introducing me to the exciting world of drug metabolism are warmly remembered. My sincere thanks are also owed to Jarmo S. Salonen, PhD, who first suggested this topic to me. Jarmo's interest in my progress and his insightful comments throughout the process have been invaluable.

It was a pleasure to work in the warm atmosphere created by the staff of the Division of Pharmaceutical Chemistry. I am especially grateful to Leena Luukkanen, PhLic, Pia Pihlavisto, PhD, and Mika Kurkela, MSc, who among others guided me during my first steps in the *in vitro* metabolism studies.

The later part of this work was carried out at Drug Metabolism in Orion Pharma, Espoo, during 2003-2009. My warmest thanks are due to Docents Moshe Finel and Mikko Koskinen for the opportunity to work under their supervision after the early demise of Jyrki Taskinen. Moshe's enthusiasm for research and great interest in my work have been most encouraging. I could always count on his quick response to my questions, even when posed during the most unexpected hours of the day. Mikko's door was always open, and I am sincerely grateful for his sound advice and comments and also the friendly conversations, which often extended beyond the scope of this work. I also acknowledge my superiors at Orion Pharma, especially Timo Lotta, PhD, and Mika Pykäläinen, PhLic, for giving me the opportunity, means, and time to work on my thesis. It has not always been easy to divide time between studies and other duties, but your support and understanding have made my life easier.

My deepest gratitude is due to Päivi Hirvensalo (née Toivonen), MSc, whose contribution in the final stages of this work was invaluable. Her enthusiasm and friendliness made my work much more pleasant. My warmest thanks are owed to Mrs Marja Härmä, Mrs Eija Puukangas, and Mrs Satu Teliö for their skillful technical assistance. It has been a privilege to work at the metabolism lab and you truly are the hearts and souls of our lab, and have taught me a lot along the way. The inviting atmosphere in the corridors of TULA1 has made coming to work each morning a good experience. I thank all my colleagues and friends at Orion Pharma for showing interest in my work and for the countless nonscientific discussions over coffee; they really kept my spirits up.

My sincere thanks are due to my coauthors, Jonna Mortensen, MSc, Olli Aitio, MSc, Julius Sipilä, Msc, Professor Michael H. Court, and Leah M. Hesse, PhD, for their valuable contributions. Mrs Johanna Mosorin at the Division of Pharmaceutical Chemistry, University of Helsinki, is also thanked for her skillful technical assistance.

I am grateful to the official reviewers Associate Professor Miki Nakajima and Professor Hannu Raunio for their careful review and constructive comments on the thesis. Carol Ann Pelli is acknowledged for language revision of the manuscript.

My heartfelt thanks go to my parents, Anneli and Viljo, for their endless care and support. Warm thanks also to my sister Sari, my brothers Ari-Pekka and Antti, and their partners and children. You have always provided me with something else to think about and reminded me of the truly important things in life. I am sincerely grateful also to my partner Anssi's family, especially Leksa, Annikki, and Risto, for their encouragement. You have given me another family to rely on. Lastly, my deepest gratitude is owed to my dearest Anssi for unconditional love and for just being there. Words cannot describe how much you mean to me.

Nummela, January 2010

Janna Kairosaari

Contents

Abstract 3
Acknowledgements 5
Contents 7
List of original publications 9
Abbreviations and symbols 10
1. Introduction 11
2. Review of the literature 13
2.1 Drug metabolism 13
2.2 Glucuronidation and the UDP-glucuronosyltransferase (UGT) enzyme system 14
2.2.1 Overview 14
2.2.2 Glucuronidation reaction and cellular localization of the UGT enzyme 15
2.2.3 Heterogeneity and tissue localization of human UGTs 17
2.2.4 Substrate specificity of human UGTs 19
2.2.5 Comparison of human and animal UGTs 21
2.2.6 Inhibition and induction of UGTs 22
2.2.7 UGT polymorphisms 23
2.2.8 Drug and xenobiotic toxicities related to UGTs 23
2.3 *N*-Glucuronidation 24
2.3.1 Overview 24
2.3.2 Primary arylamines and hydroxylamines 26
2.3.3 Amides and sulfonamides 29
2.3.4 Tertiary aliphatic amines 30
2.3.5 Aromatic *N*-heterocycles 31
2.4 Approaches for studying drug glucuronidation 32
2.4.1 *In silico* modeling 33
2.4.2 *In vitro* approaches 34
2.4.2.1 Microsomes isolated from liver and other tissues 34
2.4.2.2 Recombinant UGTs 35
2.4.2.3 Primary hepatocytes 36
2.4.2.4 Liver cell lines 37
2.4.3 *In vivo* studies 37
2.4.4 Glucuronide analytics 38
2.4.5 Enzyme kinetics 39
2.4.6 *In vitro – in vivo* scaling (IVIVS) 41
2.5 Investigated compounds 43
2.5.1 4-Arylalkyl-1*H*-imidazoles 43
2.5.2 Nicotine and cotinine 44
3. Aims of the study 46
4. Materials and methods 47
4.1 Chemicals 47
4.2 Tissue microsomes 47
4.3 Recombinant human UGTs 48
4.4 mRNA expression of UGT enzymes in human tissues 48

4.5 *In vitro* glucuronidation assays 49
4.5.1 Glucuronidation screens 49
4.5.2 Optimization of incubation conditions 49
4.5.3 Kinetic assays 50
4.6 Liquid chromatography 51
4.6.1 Methods utilizing ^{14}C-UDP-glucuronic acid (UDPGA) (I, II, IV) 52
4.6.2 Methods utilizing ^{3}H-levomedetomidine (I, II) 52
4.6.3 Liquid chromatography – mass spectrometry (LC-MS) (III) 52
4.7 Enzyme kinetics analyses 52
4.8 Prediction of hepatic clearance via glucuronidation 53
4.9 Biosynthesis and nuclear magnetic resonance (NMR) analyses of dex- and levomedetomidine glucuronides 53
5. Results 54
5.1 Analytical methods 54
5.1.1 Methods utilizing ^{14}C-UDPGA (I, II, IV) 54
5.1.2 Methods utilizing ^{3}H-levomedetomidine (I, II) 55
5.1.3 LC-MS (III) 55
5.2 Biosynthesis and structural characterization of dex- and levomedetomidine glucuronides (IV) 56
5.3 *N*-Glucuronidation by human and animal tissue microsomes 58
5.3.1 4-Arylalkyl-1*H*-imidazoles (II, IV) 58
5.3.2 Nicotine and cotinine (III) 59
5.4 *N*-Glucuronidation by recombinant human UGTs 59
5.4.1 4-Arylalkyl-1*H*-imidazoles (II, IV) 59
5.4.2 Nicotine and cotinine (III) 61
5.5 mRNA expression of UGT enzymes in human tissues (III) 62
5.6 Optimization of incubation conditions for kinetic assays 63
5.6.1 Choice of incubation buffer and pH (unpublished data) 63
5.6.2 Latency-disrupting agents (II, IV) 63
5.6.3 Use and stability of different recombinant UGT preparations (III) 64
5.7 Kinetic characterization of glucuronidation 65
5.7.1 4-Arylalkyl-1*H*-imidazoles (II, IV) 65
5.7.2 Nicotine and cotinine (III) 69
5.8 Estimates of hepatic clearance via glucuronidation (unpublished data) 69
6. Discussion 71
6.1 Methods developed for the detection of *N*-glucuronides 71
6.2 Species- and tissue-selective *N*-glucuronidation of investigated compounds 71
6.3 Role of human UGT2B10 in catalyzing *N*-glucuronidation 72
6.4 Regio- and stereoselective *N*-glucuronidation of medetomidine 73
6.5 *In vivo* relevance of *in vitro N*-glucuronidation assays 73
7. Conclusions 74
References 75

List of original publications

This dissertation is based on the following four original publications, hereafter referred to by their Roman numerals (I-IV):

I Kaivosaari S, Salonen JS, Mortensen J, and Taskinen J (2001) High-performance liquid chromatographic method combining radiochemical and ultraviolet detection for determination of low activities of uridine 5'-diphosphate-glucuronosyltransferase. *Anal Biochem* **292**:178-187.

II Kaivosaari S, Salonen JS, and Taskinen J (2002) *N*-Glucuronidation of some 4-arylalkyl-1*H*-imidazoles by rat, dog, and human liver microsomes. *Drug Metab Dispos* **30**:295-300.

III Kaivosaari S, Toivonen P, Hesse LM, Koskinen M, Court MH, and Finel M (2007) Nicotine glucuronidation and the human UDP-glucuronosyl-transferase UGT2B10. *Mol Pharmacol* **72**:761-768.

IV Kaivosaari S, Toivonen P, Aitio O, Sipila J, Koskinen M, Salonen JS, and Finel M (2008) Regio- and stereospecific *N*-glucuronidation of medetomidine: the differences between UDP glucuronosyltransferase (UGT) 1A4 and UGT2B10 account for the complex kinetics of human liver microsomes. *Drug Metab Dispos* **36**:1529-1537.

These publications were reprinted with the kind permission of their copyright owners. In addition, some unpublished data are included.

Abbreviations and symbols

ADME	absorption, distribution, metabolism, excretion
CG	cotinine glucuronide
CL_H	hepatic clearance
CL_{int}	intrinsic clearance
CYP	cytochrome P450
DG1	N_3- glucuronide of dexmedetomidine
DG2	N_1-glucuronide of dexmedetomidine
FSA	flow scintillation analyzer
f_u	fraction unbound
GI	gastrointestinal
HIM	human intestine microsomes
HLM	human liver microsomes
IVIVS	*in vitro – in vivo* scaling
K_m	Michaelis constant
K_{si}	substrate inhibition constant
LC	liquid chromatography
LG1	N_3-glucuronide of levomedetomidine
LG2	N_1-glucuronides of levomedetomidine
MPPGL	microsomal protein per gram liver
MS	mass spectrometry
n	Hill coefficient
NG	nicotine glucuronide
NMR	nuclear magnetic resonance
N-OH-PhIP	*N*-hydroxy-2-amino-1-methyl-6-phenylimidazo[4,5-b]pyridine
Q_H	hepatic blood flow
R_B	blood-to-plasma partition ratio
S	substrate concentration
SPE	solid-phase extraction
TLC	thin-layer chromatography
UDP	uridine 5’-diphosphate
UDPGA	UDP-glucuronic acid
UGT	UDP-glucuronosyltransferase
UV	ultraviolet
v	reaction velocity
V_{max}	maximal reaction velocity
w_L	liver weight per kilogram body weight

1. Introduction

The ultimate goal of drug development is to produce safe and efficacious drugs. Elucidating the ADME properties (absorption, distribution, metabolism, excretion) of a new drug candidate is a crucial part of the drug development process contributing to both of these objectives (Lin et al., 2003; Singh, 2006). With respect to pharmacological activity, reaching the pharmacological target, such as a receptor, is a prerequisite for drug action, and ADME properties determine the fate of the drug in the human body. When given orally, the drug molecules are first released from the formulation, and only the portion that is dissolved in the intestinal fluids can be absorbed (Fig. 1). During the absorption phase, the drug permeates the cellular membranes of the intestinal wall and enters the portal vein. Enterocytes at the intestinal wall contain specific efflux proteins regulating the rate of absorption. Before reaching systemic circulation, the drug enters the liver and is subjected to metabolism. Metabolism is catalyzed by a wide variety of metabolic enzymes converting drugs to generally more water-soluble products, metabolites. The metabolites formed are usually devoid of pharmacological activity, suggesting that metabolism often ends drug action. On the other hand, some drugs (called "prodrugs") need metabolic activation to produce the pharmacologically active agent. The fraction absorbed and the rate of hepatic and intestinal "first-pass metabolism" together dictate bioavailability, i.e. the relative proportion of the drug entering systemic circulation. After reaching systemic circulation, the drug can be distributed further to tissues, including the site of action in the target tissue. The elimination phase of the pharmacokinetic process dictates the duration of drug action. Drugs can be excreted to urine or bile as such, but in most cases they are excreted as metabolites. The hydrophilic moieties introduced to the drug molecules by metabolic enzymes facilitate excretion, and, moreover, many metabolites are substrates of specific transport proteins controlling their excretion in the liver and kidney.

With respect to the safety aspect of drugs, ADME plays a role in some undesired drug responses. Some metabolic enzymes convert drugs into reactive intermediates that can be covalently bound to proteins and nucleic acids (Nassar and Lopez-Anaya, 2004; Zhou et al., 2005b). This metabolic activation has, in some cases, been shown to be related to toxic responses, such as organ toxicity or idiosyncrasies. Furthermore, some drugs have the potential to inhibit metabolic enzymes, thus increasing the exposure to other drugs taken concomitantly. Many clinically relevant drug-drug interactions are related to cytochrome P450 enzymes (CYPs) (Pelkonen et al., 2008), as a variety of drugs are metabolized by these enzymes. In addition, genetic variation in metabolic enzymes can cause large interindividual variability in drug levels, since the polymorphic variants may catalyze metabolism at highly different rates (Ingelman-Sundberg et al., 2007). CYP enzymes appear to be mostly responsible for the clinically relevant drug-drug interactions, drug-related toxicities, and interindividual variation in drug response reported thus far. The possibility for such reactions is therefore evaluated early in the drug discovery process. Furthermore, some drug companies may even try to focus on developing drugs that are preferentially eliminated via other enzymes than CYPs.

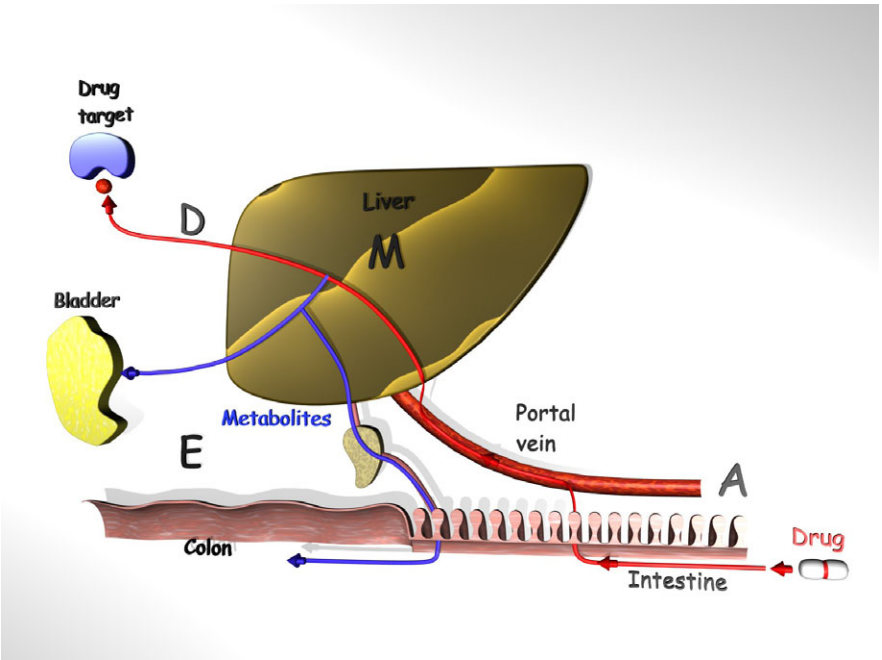

Figure 1 *ADME (absorption, distribution, metabolism, excretion) process of an oral drug.*

In the past, poor pharmacokinetics and metabolic properties have been among the most important reasons for the failure of a new drug in development (Kennedy, 1997; Roberts, 2003). As a result, ADME studies are nowadays initiated at a very early stage during the drug discovery process to ensure that the new drug candidates will not fail due to poor ADME properties. In fact, many *in vitro* approaches for drug metabolism and interaction studies have emerged to complement and in some cases even replace laborous *in vivo* studies. These *in vitro* methods are routinely used in the early testing of drug metabolism and enable the rapid screening of a large set of drug candidates in a single test. The first *in vitro* screens usually include CYP inhibition screening as an indication of the interaction potential, and metabolic stability testing using human and animal liver microsomes (Brandon et al., 2003; Plant, 2004; Pelkonen and Raunio, 2005; Pelkonen and Turpeinen, 2007). *In vitro* testing is beneficial also in terms of being able to use human-derived material already during the first steps of drug development, as large differences among species in metabolism have been reported, and interspecies extrapolations from animals to humans are often rather poor.

This study was designed to explore *N*-glucuronidation, a specific metabolic reaction playing a central role in the elimination of many drugs and xenobiotics. Different *in vitro* approaches, including human and animal liver microsomes, and recombinant human UDP-glucuronosyltransferase (UGT) enzymes were used to explore this reaction. A set of closely related 4-arylalkyl-1*H*-imidazoles and nicotine along with its major metabolite cotinine were used as test substances. Special emphasis was given to attempts to clarify the human UGTs contributing to this reaction in the human liver.

2. Review of the literature

2.1 Drug metabolism

Drug metabolism refers to the biochemical modification of drugs by specialized enzymatic systems. Overall, the role of metabolism is to protect the body against potentially harmful chemicals, including drugs and other xenobiotics, such as enviromental chemicals and food additives. Metabolism converts these chemicals generally into less toxic and more polar products, metabolites, and is therefore referred to as a detoxification system.

Drug metabolism is traditionally divided into two types of reactions, phase I (oxidation, reduction, and hydrolysis) and phase II (conjugations) (Guengerich, 2008; Remmel et al., 2008). The most common phase I and II reactions along with the enzymes catalyzing the reactions are presented in Table 1 (Ekins et al., 1999). As reviewed by Williams (2004a), approximately three-quarters of the top 200 prescribed drugs in the United States in 2002 were reported to be mainly cleared by metabolism. Whereas some drugs have one clearly dominant metabolic pathway, others have several equally important routes. The most important enzymes catalyzing phase I drug metabolism are CYPs, contributing to the clearance of two-thirds of drugs cleared by metabolism. Furthermore, many drugs are cleared predominantly by phase II reactions such as direct glucuronidation. In fact, glucuronidation, catalyzed by a family of UGT enzymes, was reported to contribute to the metabolism of approximately one-tenth of drugs (Williams et al., 2004a). In phase II reactions, an endogenous cofactor is conjugated to the drug or the newly formed phase I metabolite to form a conjugate that is usually highly polar.

Liver is quantitatively the principal organ of drug metabolism. Nonetheless, most tissues, such as the intestine, kidney, lung, and skin, have some ability to metabolize drugs. Therefore, when a drug is taken orally, it is subjected to metabolism before entering systemic circulation first during the absorption phase in the epithelial cells of the gastroinstestinal (GI) tract, and again when entering the liver via the portal vein. This process, “first-pass metabolism”, is an important determinant of the bioavailability of many oral drugs.

Table 1 *Characteristics of major drug metabolism enzymes (modified from Ekins et al, 1999).*

Enzyme	Abbreviation	Reaction	Cellular localization	Cofactor[a]
Phase I enzymes				
Cytochrome P450s	CYPs	Oxidation or reduction	Microsomal	NADPH
Flavin-containing monooxygenases	FMOs	Oxidation	Microsomal	NADPH
Monoamine oxidases	MAOs	Oxidation	Mitochondrial	
Alcohol- and aldehyde dehydrogenases	ADHs, ALDHs	Oxidation or reduction	Cytosolic	NAD^+
Phase II enzymes				
UDP-glucuronosyltransferases	UGTs	Glucuronidation	Microsomal	UDPGA
Sulfotransferases	SULTs	Sulfation	Cytosolic	PAPS
Glutathione *S*-transferases	GSTs	Glutathione conjugation	Cytosolic and microsomal	Glutathione
N-Acetyltransferases	NATs	*N*-Acetylation	Cytosolic	Acetyl-coenzyme A
Methyltransferases	MTs	Methylation	Cytosolic	*S*-Adenosyl-methionine

[a]Abbreviations of the cofactors: NADPH, β-nicotinamide adenine dinucleotide phosphate, reduced form; NAD^+, β-nicotinamide adenine dinucleotide; PAPS, 3'-phosphoadenosine 5'-phosphosulfate

2.2 Glucuronidation and the UDP-glucuronosyltransferase (UGT) enzyme system

2.2.1 Overview

Glucuronidation, catalyzed by a family of membrane-bound UGT enzymes (Burchell and Coughtrie, 1989; Miners and Mackenzie, 1991; Tukey and Strassburg, 2000; Wells et al., 2004), is a metabolic reaction converting lipophilic xeno- and endobiotics to more water-soluble metabolites, glucuronides. Substrates for UGT enzymes are compounds containing nucleophilic functional groups such as alcohols (ROH), phenols (Ar–OH), primary amines (RNH_2), secondary amines (RNR'H), tertiary and heterocyclic amines (RNR'R''), amides ($R–CO–NH_2$), thiols (RSH), and acidic carbon atoms. The clearance of some endogenous substances, such as bilirubin, steroid hormones, and bile acids, is largely dependent of UGT-mediated metabolism. In addition, a large variety of drugs are metabolized primarily by glucuronidation. Examples of extensively *O*-glucuronidated phenolic drugs include opioids (codeine, morphine, naloxone), the anaesthetic propofol, the anti-Parkinson drug entacapone, and the contraceptive ethinylestradiol (Wikberg et al., 1993; Soars et al.,

2002). Carboxylic acid drugs, which are excreted primarily by glucuronidation, include nonsteroidal anti-inflammatory drugs (ketoprofen, naproxen), the hyperlipidemia drug gemfibrozil, and the antiepileptic valproic acid (Soars et al., 2002). Readily *N*-glucuronidated drugs include antihistamines, tricyclic antipsychotics, antidepressants, antiepileptics, and antipsychotics (Dahl-Puustinen et al., 1989; Luo et al., 1991; Sinz and Remmel, 1991; Luo et al., 1995; Hawes, 1998; Kassahun et al., 1998).

Formed glucuronide conjugates are generally polar, ionized at physiologic pH (pK_a ~4), and have an increase in molecular weight (+176) (Remmel et al., 2008). All of these features facilitate biliary and/or renal excretion. However, glucuronides are generally too large and too polar to diffuse passively to bile or urine, therefore needing specific transporters, such as multidrug resistance-associated proteins MRP2 and MRP3, to aid their movement across cell membranes (Zamek-Gliszczynski et al., 2006). In general, drug glucuronides are less toxic and potent than their aglycone substrates. However, in the case of the 6-*O*-glucuronide of morphine, the glucuronide product is in fact more potent than the parent drug, suggesting that this metabolite can increase the analgesic potency of morphine (King et al., 2000). In rare cases, glucuronidation reaction has been reported to produce reactive intermediates such as acylglucuronides (Sallustio et al., 2000; Bailey and Dickinson, 2003). Nonetheless, direct evidence for the toxicity of acylglucuronides is currently scarce. Clinically relevant polymorphisms related to UGT enzymes have been reported at least for the UGT1A1 enzyme (Miners et al., 2002). Therefore, to develop safer and more efficient drugs, it is important to recognize as early as possible whether glucuronidation is involved in the clearance of the new drug candidate, what types of glucuronides are formed and at what rate, whether significant species differences exist, and which human UGT isoforms are involved in the reaction.

2.2.2 Glucuronidation reaction and cellular localization of the UGT enzyme

UGTs catalyze the transfer of glucuronic acid from UDP-glucuronic acid to the aglycone substrate (Fig. 2). Glucuronidation occurs as an S_N2 substitution reaction (Yin et al., 1994). The nucleophilic heteroatom of the substrate attacks the C_1 atom of the glucuronic acid, and both UDPGA and the aglycone substrate are bound on the active site of the enzyme. The S_N2 mechanism is supported by the inversion of the α-configuration of the C_1 atom in UDPGA to β-configuration in the glucuronide.

Within the cell, the active site of the UGT enzyme is localized in the lumen of the endoplasmic reticulum (Fig. 3) (Banhegyi et al., 1993), whereas e.g. CYPs face the cytosolic side. Single UGT enzymes have been demonstrated to form di- and tetrameric structures, i.e. two or four either similar or different UGT enzymes form an oligomeric structure (Radominska-Pandya et al., 2005b; Finel and Kurkela, 2008). Whether these enzymes actually form such oligomeric structures within the ER membrane, and their functional relevance are not fully understood.

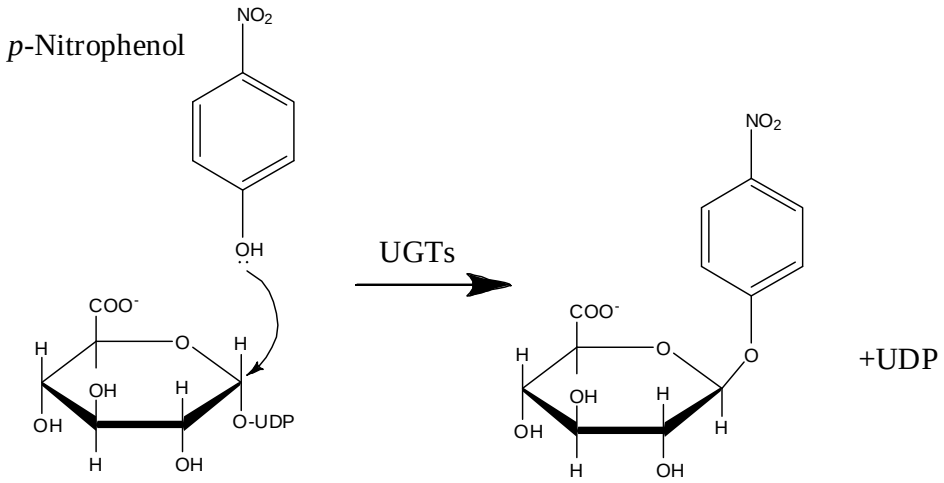

Figure 2 *Glucuronidation reaction. Conjugation of the aglycone substrate (p-nitrophenol) with glucuronic acid from UDPGA. The initial α-configuration of the glucuronic acid is converted to the β-configuration in the final glucuronide product.*

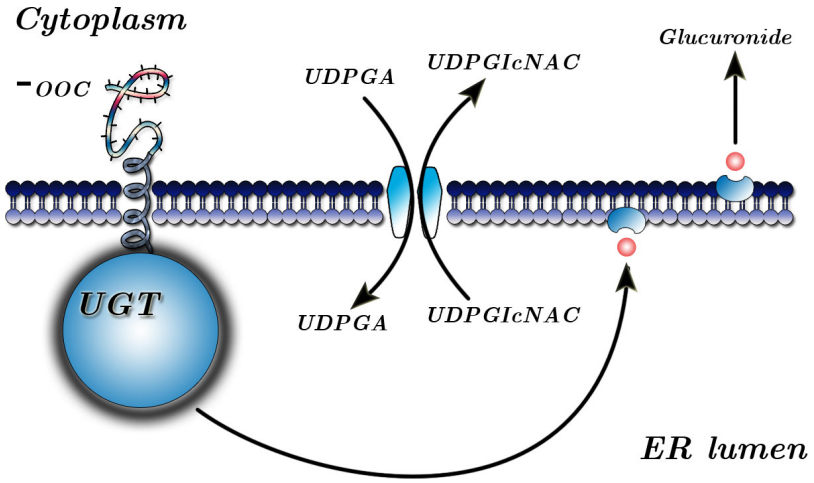

Figure 3 *Localization of the UGT enzyme in the ER membrane. UDPGA is transported into the ER and is trans-stimulated by UDP-N-acetylglucosamine (UDPGlcNAC). Modified from Clarke and Burchell (1994).*

While lipophilic xeno- and endobiotics can usually passively permeate through the ER membrane to access the active site of the enzyme, UDPGA is transported into the lumen of ER using active mechanisms (Bossuyt and Blanckaert, 1997). In the human liver, the concentration of UDPGA is 280 µM, while in extrahepatic tissues it is less than 20 µM (Lin and Wong, 2002). The physiological UDPGA concentrations in the cytosol and in the ER lumen were reported to be similar. The formed glucuronide conjugates generally need active transport through the ER membranes into the cytosol before they can be excreted out of the cell.

2.2.3 Heterogeneity and tissue localization of human UGTs

The human genome contains some 19 active UGT-encoding genes, which are divided into three subfamilies: 1A, 2A, and 2B (Mackenzie et al., 2005). According to current understanding, two of these subfamilies, 1A and 2B, are mostly responsible for the glucuronidation of drugs and xenobiotics (Tukey and Strassburg, 2000; Mackenzie et al., 2003; Ouzzine et al., 2003; Mackenzie et al., 2005). The human UGT1A enzyme family consists of nine members (UGT1A1, UGT1A3, UGT1A4, UGT1A5, UGT1A6, UGT1A7, UGT1A8, UGT1A9, and UGT1A10). Each UGT1 enzyme is encoded by a transcript that is formed by the splicing of a distinct first exon, containing the code for the substrate binding region, to exons 2-5, a set of four common downstream exons that together contain the code for the UDPGA binding site (Mackenzie et al., 2003). The UGT2A family contains three members (UGT2A1, UGT2A2, and UGT2A3), while the UGT2B family contains seven members (UGT2B4, UGT2B7, UGT2B10, UGT2B11, UGT2B15, UGT2B17, and UGT2B28). The human *UGT2A1* and *UGT2A2* genes contain unique first exons (*2A1* and *2A2*) and a shared set of five downstream exons (Mackenzie et al., 2005). All other UGT2 enzymes are encoded by separate genes, each composed of six exons.

The liver is generally considered the main drug glucuronidating organ in humans, and many UGT isoforms (1A1, 1A3, 1A4, 1A6, 1A9, 2B4, 2B7, 2B10, 2B11, 2B15, and 2B17) are abundantly expressed in the liver (Table 2) (Nakamura et al., 2008). Ohno and Nakajin (2009) recently performed an extensive quantitative mRNA measurement of UGT expressions in 23 human tissue types. They reported that the hepatic expression was highest for four members of the UGT2B family, namely 2B4, 2B7, 2B10, and 2B15, while the expression levels of UGT1A enzymes were generally somewhat lower.

Beyond the human liver, a wide variety of endo- and xenobiotics have been observed to be glucuronidated efficiently by microsomes isolated from other tissues, such as the intestine and kidney (Soars et al., 2002). Accordingly, many UGTs are expressed at considerable levels in extrahepatic tissues (Nakamura et al., 2008). The expression of UGT1A1, UGT1A10, UGT2B7, UGT2B15, and UGT2B17 was found to be particularly high along the intestine (Ohno and Nakajin, 2009). Also UGTs 1A7 and 1A8 are mainly expressed in the GI tract (Nakamura et al., 2008). Two UGT enzymes, UGT1A9 and UGT2B7, were expressed at particularly high levels in the kidney (Ohno and Nakajin, 2009). Some UGTs are expressed also in steroid-related tissues (adrenal gland, breast, ovary, uterus, and testis) in a tissue- and isoform-specific manner, indicating their role in the glucuronidation of endogenous hormones (Nakamura et al., 2008). Of the UGT2A enzymes, UGT2A1 is an extrahepatic enzyme expressed mainly in the nasal epithelium (Jedlitschky et al., 1999), suggesting that it plays a minor role in drug metabolism. UGT2A3 mRNA, by contrast, is most highly expressed in human tissues of the greatest relevance to drug clearance, including the liver, GI tract, and kidney (Court et al., 2008).

Taken together, these findings emphasize the role of several UGT2B family enzymes in the first-pass metabolism of oral drugs in both the GI tract and the liver. Moreover, these results indicate that UGT1A9 may play an important role in renal glucuronidation.

Table 2 *Typical substrates of human UGTs and UGT expression in the body.*

Enzyme	Probe substrates for hepatic UGTs[a]	Other substrates	Primary tissue(s) expression[b] and other characteristics
UGT1A1	Bilirubin Estradiol (3-*O*-gluc)[c]	Small and bulky phenols	Liver and GI tract Clinically relevant polymorphism
UGT1A3	Hexafluoro-1α,25-dihydroxyvitamin D_3	Small and bulky phenols Carboxylic acids	Liver
UGT1A4	Amitriptyline Trifluoperazine (TFP)		Liver Catalyzes *N*-glucuronidation Specific inhibitor hecogenin[d]
UGT1A5		Good substrates currently unknown	Marginally expressed in many tissues, including the liver
UGT1A6	Serotonin α-Naphthol[e]	Small, planar phenols	Kidney and liver
UGT1A7		Small and bulky phenols	Esophagus Low expression in the liver
UGT1A8		Small and bulky phenols	Marginally expressed in many tissues Not expressed in the liver
UGT1A9	Propofol[c]	Small and bulky phenols Carboxylic acids	**Kidney** and liver
UGT1A10		Small and bulky phenols	GI tract Not expressed in the liver
UGT2B4		C_{19}- and C_{21}-steroids Hyodeoxycholic acid	**Liver** and heart
UGT2B7	Carbamazepine Morphine Zidovudine	Opioids, NSAIDs Carboxylic acids C_{19}- and C_{21}-steroids Hyodeoxycholic acid	**Liver, kidney, and GI tract** Specific inhibitor fluconazole
UGT2B10[f]	Levomedetomidine	Nicotine	**Liver** Catalyzes *N*-glucuronidation
UGT2B11		Good substrates currently unknown	Marginally expressed in tissues
UGT2B15	*S*-Oxazepam	Androgens Testosterone	**Liver, GI tract**, breast, and ovary
UGT2B17		Androgens Testosterone	**GI tract**
UGT2B28		Good substrates currently unknown	Marginally expressed in tissues

[a]Potentially useful probe substrates for hepatic UGTs suggested by Burchell et al. (2005), Court (2005), and Miners et al. (2006).
[b]Primary sites of mRNA expression of each UGT enzyme according to Nakamura et al. (2008) and Ohno and Nakajin (2009). The major UGTs in the liver, kidney, and GI tract are indicated in boldface.
[c]Glucuronidated also by extrahepatic UGTs
[d]Uchaipichat et al. (2006)
[e]Glucuronidated also by other UGTs, but highest CL_{int} observed with UGT1A6.
[f] Role of UGT2B10 in *N*-glucuronidation is discussed in detail under Results and Discussion.

2.2.4 Substrate specificity of human UGTs

UGTs generally have distinct but broadly overlapping substrate specificities (Miners and Mackenzie, 1991). In other words, an individual UGT enzyme accepts multiple compounds as substrates, and a single compound is often a substrate for multiple UGT enzymes. Due to the overlapping substrate specificities, it has been a challenging task to try and find selective probe substrates for each UGT enzyme. Nonetheless, there are some "generally accepted" probe substrates and they are listed in Table 2 (Burchell et al., 2005; Court, 2005; Miners et al., 2006). UGT1A enzymes generally play a role in the *O*-glucuronidation of planar and bulky phenols (Tukey and Strassburg, 2000). Moreover, UGT1A enzymes conjugate the endogenous substrate bilirubin and are involved in the *N*-glucuronidation of various amines. UGT2B enzymes catalyze the *O*-glucuronidation of endo- and xenobiotic steroids and contribute to the conjugation of carboxylic acids such as many analgesic drugs.

Williams et al. (2004a) and Burchell et al. (2005) have postulated that seven UGT enzymes, namely 1A1, 1A3, 1A4, 1A6, 1A9, 2B4, and 2B7, are mainly responsible for hepatic drug glucuronidation (Fig. 4). More specifically, UGT2B7 was suggested to be responsible for the hepatic glucuronidation of 40% of drugs, while UGTs 1A1, 1A4, and 1A9 contribute to a further 47%. These results are not fully in line with a recent report suggesting that while many UGT2B enzymes are highly expressed in the liver, the levels of UGT1A enzymes are lower (Ohno and Nakajin, 2009). However, it is possible that UGT2B enzymes play a more significant role in the glucuronidation of endogenous compounds.

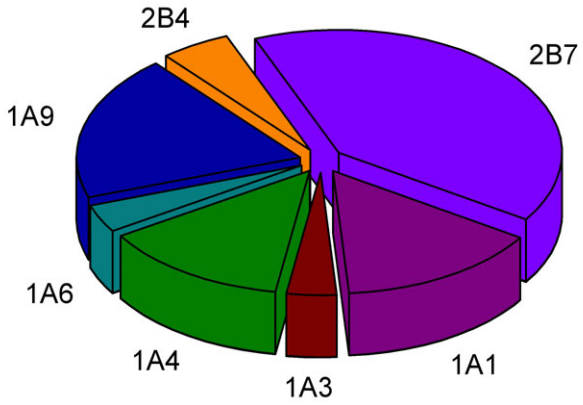

Figure 4 *Human hepatic UGT pie. Relative contributions of individual human liver UGT enzymes to the glucuronidation of 200 top prescribed drugs in the United States in 2002. Reproduced from Williams et al. (2004a) and Burchell et al. (2005).*

Phenols. Glucuronidation of small planar phenols, such as 4-nitrophenol, α-naphthol, and scopoletin, is catalyzed by most of the human UGT1A and UGT2B enzymes (Tukey and Strassburg, 2000). However, the highest activities have been observed with the UGT1

enzymes, with the exception of UGT1A4, while the activities of UGT2B enzymes towards phenolic substrates are generally 10- to 20-fold lower. Therefore, small planar phenols are often used as indicators of total UGT1A activity in human tissue microsomes. Many UGTs of subfamily 1A, such as UGT1A1, UGT1A3, UGT1A7, UGT1A8, UGT1A9, and UGT1A10, have overlapping substrate specificity in the glucuronidation of different phenols. While UGT1A6 preferentially conjugates small planar phenols, many larger, bulkier phenols are excellent substrates for UGT1A9 and the extrahepatic UGTs 1A7, 1A8, and 1A10 (Ebner and Burchell, 1993; Luukkanen et al., 2005). Based on the finding that UGT1A enzymes are expressed throughout the GI tract, these enzymes have been proposed to have evolved to serve as a defense mechanism in the detoxification of many simple and complex phenols present in the digested matter (Tukey and Strassburg, 2000).

Opioids. UGT2B7 is a major contributor to the glucuronidation of opioids (Tukey and Strassburg, 2000). When morphine glucuronidation was studied in detail, only UGT2B7 catalyzed the formation of the pharmacologically active 6-*O*-glucuronide, while also many UGT1A enzymes, in addition to UGT2B7, catalyzed the formation of the inactive 3-*O*-glucuronide (Stone et al., 2003). Interestingly, among other tissues, UGT2B7 is expressed also in the brain, indicating that the 6-*O*-glucuronide may contribute to the pharmacological activity of morphine (King et al., 2000).

Steroids. UGT2B enzymes, especially UGT2B4, UGT2B7, UGT2B15, and UGT2B17, play a central role in the glucuronidation of different endo- and xenobiotic steroids such as androgens (C_{19} steroids), estrogens (C_{18} steroids), progestins (C_{21} steroids), and bile acids (C_{24} steroids) (Tukey and Strassburg, 2000; Turgeon et al., 2001). UGT2B4 and UGT2B7 have a major role in the glucuronidation of C_{19} and C_{21} steroids and were found to be responsible for the conjugation hyodeoxycholic acid. In a recent study, UGT2A3 was also demonstrated to specifically glucuronidate bile acids (Court et al., 2008). UGT2B15 and UGT2B17 contribute significantly to the glucuronidation of testosterone and other androgens. Despite the central role of UGT2B enzymes in steroid metabolism, some UGT1A enzymes also catalyze the glucuronidation of steroids, including estrogens and androgens (Itaaho et al., 2008; Sten et al., 2009).

Carboxylic acids. The clearance of the endogenous substrate bilirubin is highly dependent on a single UGT enzyme, UGT1A1 (Senafi et al., 1994). However, bilirubin seems to be the only carboxylic acid substrate of this particular UGT enzyme. Other UGT1A enzymes, mainly UGT1A3 and UGT1A9, have a central role in the formation of acyl-*O*-glucuronides from carboxyl-containing drugs (Kuehl et al., 2005). Furthermore, UGT2B4 and UGT2B7 contribute to the glucuronidation of carboxylic acid drugs such as nonsteroidal anti-inflammatory drugs.

Amines. The contribution of various UGT enzymes to *N*-glucuronidation reactions is discussed in detail in Section 2.3. as well as under Results and Discussion.

2.2.5 Comparison of human and animal UGTs

The majority of studies on recombinant UGTs in recent years have been performed using human enzymes, with animal UGTs receiving considerably less attention. Nonetheless, many *in vitro* studies conducted using liver microsomes have revealed significant differences between humans and various animal species in their ability to catalyze different glucuronidation reactions (Soars et al., 2001a; Soars et al., 2001b; Shiratani et al., 2008). As an interesting detail, the domestic cat has a significantly lower capacity to glucuronidate many drugs and other xenobiotics than most other mammalian species (Court and Greenblatt, 2000). Overall, the reported interspecies differences and lack of animal UGT data highlight the importance of characterizing animal UGTs in more detail.

UGT1A enzymes. The *UGT1A* gene complex is largely conserved among species (Mackenzie et al., 2003). Therefore, based on the limited cross-species data available and despite a few exceptions, the substrate specificity of the UGT1A enzymes across species appears to be similar (King et al., 2000). Especially the bilirubin-conjugating enzyme UGT1A1 is functionally similar across species (King et al., 1996).

UGT1A6 gene is also highly conserved among several species, including humans, rats, mice, and rabbits (Mackenzie et al., 2005), and the respective enzyme catalyzes the glucuronidation of various simple phenolic compounds across species. However, in the domestic cat, *UGT1A6* is a pseudogene (Court and Greenblatt, 2000). This finding explains the inefficiency of the domestic cat to glucuronidate planar phenols, and, furthermore, the susceptibility of this species to the toxic effects of some phenolic analgesic drugs such as paracetamol.

Interspecies differences related to the UGT1A9 enzyme have also been reported. Propofol, a selective substrate of human UGT1A9, was glucuronidated efficiently by human, marmoset, and mouse liver microsomes, whereas its glucuronidation rate was low in the rat and undetectable in the dog (Soars et al., 2001a; Soars et al., 2001b; Shiratani et al., 2008). While human *UGT1A9* and mouse *Ugt1a9* code for functional enzymes, rat *UGT1A9* is a pseudogene, explaining the low glucuronidation rates observed in rat liver microsomes. Entacapone, another excellent human UGT1A9 substrate, is also conjugated at high efficiency by human liver microsomes (HLM), but poorly by rat liver microsomes (Lautala et al., 1997; Lautala et al., 2000). These results indicate that the rat and the dog are not predictive species of human metabolism in the case of UGT1A9 substrates.

Species differences related to the formation of quaternary ammoniumglucuronides (N^+-glucuronides) are marked. Trifluoperazine, a substrate of human UGT1A4, was extensively glucuronidated by HLM (Uchaipichat et al., 2006), whereas glucuronidation was undetectable in mouse and rat liver microsomes (Shiratani et al., 2008). This is in line with the finding that UGT1A4 is a functional enzyme in humans, while the respective genes in the rat and in the mouse are pseudogenes (Mackenzie et al., 2005). As opposed to many other animal species, the rabbit was reported to catalyze the formation of N^+-glucuronides (Bruck et al., 1997). This reaction was found to be catalyzed by rabbit UGT1A4 and UGT1A7. Interspecies differences related to *N*-glucuronidation are discussed further in Section 2.3.

UGT2B enzymes. In contrast to the UGT1A enzymes, the UGT2B enzymes are encoded by fully separate genes, and identifying orthologs of the human enzymes across species is challenging. Nonetheless, rat UGT2B1 and dog UGT2B1 appear to be orthologs of human UGT2B7. While in humans UGT2B7 catalyzes morphine 3-*O*-glucuronidation (Stone et al., 2003), rat UGT2B1 (King et al., 2000) and dog UGT2B31 (Soars et al., 2003a) play a central role in morphine glucuronidation in these species.

2.2.6 Inhibition and induction of UGTs

UGT-mediated drug-drug interactions have been reported, at least at the *in vitro* level, for many drugs, including paracetamol, codeine, zidovudine, carbamazepine, lorazepam, and propafenone (Kiang et al., 2005). A general understanding seems to be, however, that, as opposed to drugs metabolized via CYPs, the likelihood of drug-drug interactions for drugs cleared by glucuronidation is low for two reasons (Williams et al., 2004a). Firstly, in many cases multiple UGT enzymes catalyze the glucuronidation of a single drug. Secondly, many UGT-mediated reactions have relatively high Michaelis constant (K_m) values. More specifically, the K_m values are higher than those generally observed for CYP-catalyzed reactions and in most cases considerably higher than therapeutic plasma levels. As a consequence, the *in vivo* exposure to the drug metabolized via UGTs rarely increases to more than twofold in the presence of a UGT inhibitor, whereas as much as 35-fold increases have been observed for CYP-metabolized drugs in the presence of a potent CYP inhibitor. However, significant inhibitory interactions can occur when glucuronidation is a predominant metabolic elimination pathway, particularly if it is catalyzed by a single enzyme and when the therapeutic concentration of the inhibitor is close to the K_i of the target UGT (Remmel et al., 2008).

In some cases, drugs and endogenous compounds, such as bilirubin, steroid hormones, and bile acids, compete for glucuronidation by an individual UGT enzyme, which potentially increases the concentrations of one or the other in plasma. As an example, toxic accumulation of the endogenous substance bilirubin, which is a pure UGT1A1 substrate, has been reported after administration of the anticancer drug irinotecan because its active metabolite SN-38 is extensively metabolized by UGT1A1 (Tukey et al., 2002).

Unlike inhibition of metabolizing enzymes, induction is a slow regulatory process involving nuclear receptors such as pregnane X receptor (PXR), constitutive androstane receptor (CAR), and the aryl hydrocarbon (Ah) receptor (Xu et al., 2005). Activation of these regulatory elements increases the transcription of metabolizing enzymes, producing an increased amount of active enzymes. Xenobiotic nuclear receptors coordinately induce genes involved in all phases of xenobiotic metabolism, including oxidative metabolism, conjugation, and transport (Mackenzie et al., 2003; Bock and Kohle, 2004; Xu et al., 2005; Zhou et al., 2005a). The mechanisms that regulate the tissue distribution and content of an individual UGT enzyme are currently largely unknown (Mackenzie et al., 2003). The process of induction of metabolizing enzymes results in an increased clearance via this route and thus lowered drug exposure. Some classical CYP inducers, such as

phenobarbital, phenytoin, and rifampicin, also induce many UGT enzymes. In addition, typical aromatic hydrocarbon-type inducers, such as 3-methylcholanthrene and β-naphthoflavone, have been reported to induce UGT enzymes.

2.2.7 UGT polymorphisms

Genetic polymorphism has been described for several human UGT genes, including UGTs 1A1, 1A6, 1A7, 2B4, 2B7, and 2B15 (Miners et al., 2002; Burchell, 2003; Guillemette, 2003). According to current understanding, the polymorphisms related to UGT1A1 enzyme are clinically most relevant. However, also other UGT polymorphisms have been shown to greatly affect enzyme activities, as in the case of a genetic variant of UGT2B17 significantly affecting testosterone glucuronidation (Jakobsson et al., 2006). The most extreme case of the genetic variation of UGT1A1 is known as Crigler-Najjar syndrome (Mackenzie et al., 2003). Crigler-Najjar patients totally lack expression of the UGT1A1 enzyme, leading to bilirubin-induced morbidity. Gilbert's syndrome is another case of the genetic variation of UGT1A1. In this case, the polymorphic allele *UGT1A1*28* is associated with reduced UGT1A1 enzyme activity, causing mild hyperbilirubinemia. The frequency of the *UGT1A1*28* variant in Caucasians is 7-19% (Miners et al., 2002). Neonates with Gilbert's syndrome have a higher incidence of neonatal jaundice and more often require light therapy. Furthermore, Gilbert's syndrome, or UGT1A1 polymorphism, has been associated with some clinically relevant toxic drug responses. As an example, a significantly higher incidence of neutropenia caused by reduced glucuronidation of a toxic metabolite of irinotecan has been reported (Tukey et al., 2002). To this end, FDA has approved a genotyping test to test UGT1A1 polymorphism of patients receiving irinotecan therapy. Atazanavir and indinavir, inhibitors of UGT1A1 *in vitro*, are other examples of drugs associated with a higher incidence of serious hyberbilirubinemia (Zhang et al., 2005).

2.2.8 Drug and xenobiotic toxicities related to UGTs

Even though glucuronidation is generally considered a true detoxification process, some acyl and arylamine glucuronides have been associated with adverse drug effects. Acylglucuronides are formed from carboxyl-containing compounds, such as diclofenac, and other nonsteroidal anti-inflammatory drugs. It has been reported that some acylglucuronides are intrinsically reactive, i.e. they can spontaneously react at physiological pH by hydrolysis and intramolecular rearrangements (Sallustio et al., 2000; Bailey and Dickinson, 2003). These reactive metabolites can bind covalently to plasma proteins, tissue proteins, and nucleic acids, resulting in toxic reactions. Although direct evidence for the toxicity of acylglucuronides *in vivo* is scarce, acylglucuronides have been associated with many adverse drug effects, including hypersensitivity and cellular toxicity.

It has also been suggested that *N*-glucuronidation contributes to the carcinogenicity of some primary arylamines, such as the tobacco-related chemical benzidine (Zenser et al., 1998; Zenser et al., 2002). Benzidine and related substances undergo direct glucuronidation in the liver and accumulate in the bladder as *N*-glucuronides. The *N*-glucuronides are labile in the acidic pH of urine and are therefore hydrolyzed back to the initial aromatic amines. The newly formed aromatic amines are further bioactivated in the bladder to reactive species. Therefore, in this case, *N*-glucuronides seem to act as a "transport system" to deliver the toxic amines to urine, contributing to the carcinogenicity of these chemicals.

2.3 *N*-Glucuronidation

2.3.1 Overview

Compounds with nitrogen-containing nucleophilic functional groups, such as primary aromatic amines, hydroxylamines, amides, sulfonamides, tertiary aliphatic amines, and aromatic *N*-heterocycles, are subject to *N*-glucuronidation (Fig. 5). *N*-Glucuronidation represents a major elimination pathway for many drugs, including lamotrigine, olanzapine, carbamazepine, amitriptyline, retigabine, tioconazole, and ketotifen (Hawes, 1998; Kassahun et al., 1998; Breyer-Pfaff, 2004; Staines et al., 2004; Borlak et al., 2006). Aromatic *N*-heterocycles, such as imidazoles, triazoles, and tetrazoles, are common structural motifs in current drug development, and many of these new drug candidates have also been reported to be metabolized via direct *N*-glucuronidation (Stevens et al., 2001; Nakazawa et al., 2006; Yan et al., 2006). Furthermore, some toxic chemicals, e.g. primary arylamines and hydroxylamines, undergo *N*-glucuronidation. *N*-Glucuronides are generally safe, water-soluble metabolites, but, as mentioned earlier, in rare cases *N*-glucuronidation may contribute to the carcinogenicity of primary arylamines (Zenser et al., 1998; Zenser et al., 2002).

Marked differences across species have been observed in the ability to catalyze different *N*-glucuronidation reactions (Chiu and Huskey, 1998). In particular, the ability to form quaternary ammonium glucuronides (N^+-glucuronides) from aliphatic tertiary amines seems to be largely restricted to humans and higher primates (Hawes, 1998). However, a variety of *N*-glucuronidation reactions are also catalyzed, at least to some extent, by monkey, rat, dog, and rabbit UGTs (Magdalou et al., 1992; Zenser et al., 1998). Some *N*-glucuronide conjugates are formed especially efficiently by the rabbit liver (Magdalou et al., 1992; Uesawa et al., 2004; Kaji and Kume, 2005).

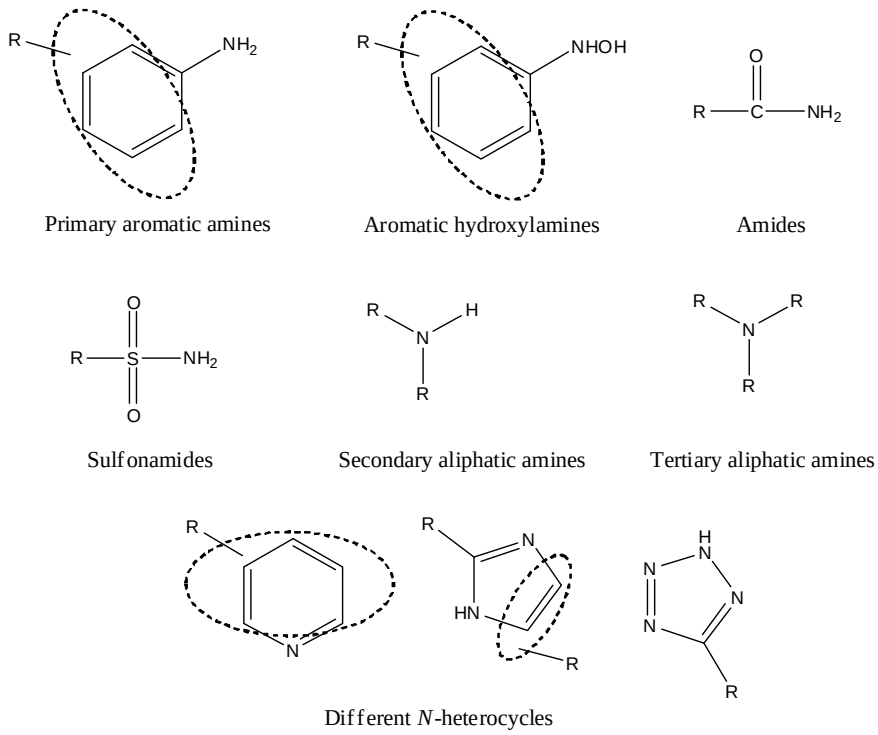

Figure 5 *Some examples of nitrogen-containing structures subject to N-glucuronidation.*

The study of interspecies differences in *N*-glucuronidation is closely related to revealing which UGT enzymes catalyze these reactions. Green et al. were the first to report that one recombinant human UGT enzyme, namely UGT1A4, catalyzes different *N*-glucuronidation reactions (Green et al., 1995; Green and Tephly, 1996; Green et al., 1998). In particular, this enzyme was found to catalyze the formation of quaternary *N*-glucuronides, the reaction limited to humans. Mainly based on these findings, UGT1A4 has generally been considered an enzyme "specialized" in *N*-glucuronidation. Nonetheless, based on recent findings, it has become evident that other enzymes, such as UGT1A1, UGT1A3, UGT1A9, UGT2B4, and UGB2B7, may play a more important role in some *N*-glucuronidation reactions (Green and Tephly, 1998; Zenser et al., 2002; Staines et al., 2004; Girard et al., 2005; Kaji and Kume, 2005; Borlak et al., 2006; Rowland et al., 2006; Omura et al., 2007; Alonen et al., 2008). In addition, based on observations on the biphasic *in vitro* kinetics of some *N*-glucuronidation reactions in HLM (Breyer-Pfaff et al., 2000; Nakajima et al., 2002b), in some cases the UGT1A4-catalyzed glucuronidation might only explain the low-affinity reaction, while another UGT enzyme is responsible for the high-affinity reaction. In the following sections, interspecies differences and the human UGTs involved in different *N*-glucuronidation reactions are discussed in detail.

2.3.2 Primary arylamines and hydroxylamines

A number of primary arylamines and hydroxylamines, including drugs and some toxic chemicals, are subject to *N*-glucuronidation (Fig. 6, Table 3). Humans and most animal species are capable of catalyzing the *N*-glucuronidation of this type of amines. More specifically, humans and dogs efficiently catalyzed the *N*-glucuronidation of primary arylamines and hydroxylamines, such as the carcinogens benzidine and *N*-hydroxy-2-amino-1-methyl-6-phenylimidazo[4,5-b]pyridine (*N*-OH-PhIP), while these reactions may be less important in the rat (Kaderlik et al., 1994; Zenser et al., 1998; Zenser et al., 2002). In fact, in the rat acetylation was the preferred pathway over *N*-glucuronidation in the metabolism of benzidine and *N*-OH-PhIP. The rabbit has also been shown to efficiently catalyze arylamine *N*-glucuronidation. As an example, the *N*-glucuronidation of afloqualone in rabbit liver microsomes was more efficient than in liver microsomes of any other species (Kaji and Kume, 2005).

Characteristic to some primary arylamine *N*-glucuronides is their lability, as they rapidly hydrolyze under acidic or alkalic conditions (Ciotti et al., 1999). As an example, *N*-glucuronide of benzidine was hydrolyzed under acidic conditions within minutes. The hydrolysis rate of benzidine *N*-glucuronide was highly dependent on pH; 50% of glucuronide was hydrolyzed at pH 5.3 (at 37°C) within 5 min, whereas at pH 7.4 the half-life of hydrolysis was >100 min. Plasma further stabilized the glucuronides, since >80% ot the conjugate remained after 4 h of incubation at 37°C. The issue of the stability of *N*-glucuronide conjugates is important in the analysis of various *in vitro* or *in vivo* samples, as for example the acidic pH of either urine or the LC eluent used may hydrolyze the labile *N*-glucuronides.

In humans, the *N*-glucuronidation of primary arylamines and hydroxylamines is primarily catalyzed by UGT1A1, UGT1A4, and UGT1A9, and possibly also by other UGT1A family enzymes, while the activities of UGT2B enzymes towards these substrates are low (Ciotti et al., 1999; Girard et al., 2005; Borlak et al., 2006). *N*-Glucuronidation of benzidine, *N*-acetylbenzidine, and 4-aminobiphenyl was shown to be catalyzed mainly by UGTs 1A9 and 1A4 (Ciotti et al., 1999). UGTs 1A1, 1A6, and 2B7 also glucuronidated these compounds, but the expression-normalized activities were low. In the case of *N*-OH-PhIP, kinetic analyses and normalized activities revealed that human UGT1A1 was the predominant enzyme involved in the formation of the N_2-glucuronide (hydroxylamine glucuronide) in the human liver, while UGT1A1 and UGT1A9 were involved in the formation of the less important N_3-glucuronide (Girard et al., 2005). Moreover, UGT1A10 was found as an important extrahepatic enzyme catalyzing *N*-OH-PhIP glucuronidation (Dellinger et al., 2007). Interestingly, N_2-glucuronide, the major metabolite in humans, was resistant to β-glucuronidase, while the N_3-glucuronide was hydrolyzed by β-glucuronidase back to *N*-OH-PhIP, thus potentially increasing the carcinogenicity of this agent *in vivo*. Retigabine was conjugated to two regio-isomeric *N*-glucuronides at the primary (N_2) and secondary (N_4) arylamine groups (Borlak et al., 2006). UGT1A9 and UGT1A1 produced the N_2-glucuronide, while the N_4-glucuronide was produced only by UGT1A9. Furthermore, UGT1A4 produced both *N*-glucuronides, but at a low rate.

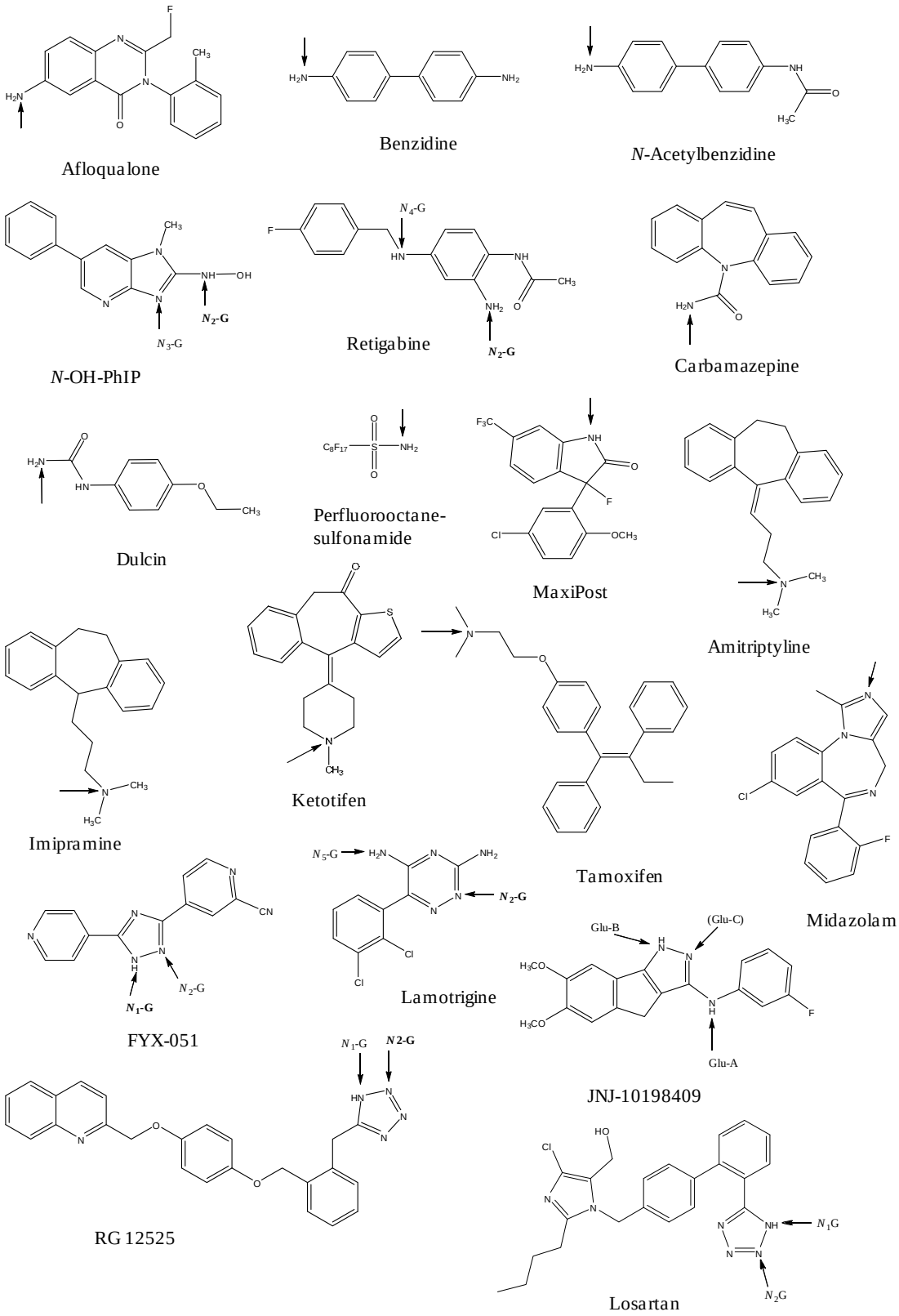

Figure 6 *Structures of N-glucuronidated drugs and xenobiotics. The glucuronidation site(s) is marked with an arrow and the major sites are indicated in boldface.*

Table 3 *Characteristics of N-glucuronidated drugs and other xenobiotics.*

Substrate	K_m, HLM (μM)	% Dose excreted in human urine	Species differences	Human UGT(s) involved	References
Primary arylamines and hydroxylamines					
Afloqualone	2019	8	*In vitro:* rabbit >> human > dog ≈ rat ≈ monkey	UGT1A4	Kaji and Kume, 2005
Benzidine	800	Major	*In vitro:* human ≈ dog > rat	UGT1A4 UGT1A9	Zenser et al., 1998; Ciotti et al., 1999
N-Acetylbenzidine	360; 1070[a]	Major	*In vitro:* human > dog > rat	UGT1A1 UGT1A4 UGT1A9	Zenser et al., 1998; Ciotti et al., 1999
N-OH-PhIP	23	Major (N_2-G)	*In vivo* (N_2-G)*:* human ≈ dog >> rat	UGT1A1 UGT1A10	Kaderlik et al., 1994; Girard et al., 2005; Dellinger et al., 2007
Retigabine	145	16 (N_2-G) 2 (N_4-G)	*In vivo:* observed in human, dog, rat	UGT1A1 UGT1A9	Hempel et al., 1999; Borlak et al., 2006
Amides and sulfonamides					
Carbamazepine	234	Major	Observed in human, rat	UGT2B7	Staines et al., 2004
Dulcin	2100	N.R.	*In vitro:* rabbit > human	UGT1A9	Uesawa et al., 2004 & 2007
Perfluorooctane-sulfonamide	143	N.R.	*In vitro:* human ≈ rat > monkey ≈dog	UGT2B7	Xu et al., 2006
MaxiPost (developmental drug)	6.4	17	*In vivo:* major in human, dog	UGT2B7	Zhang et al., 2004
Tertiary aliphatic amines					
Amitriptyline	1.4; 310[a]	3-14	*In vitro:*human, rabbit	UGT1A4	Breyer-Pfaff et al., 1997 & 2000
Imipramine	97; 700[a]	<1	N.R.	UGT1A4	Nakajima et al., 2002b
Ketotifen	1.3; 92[a]	17-24	*In vivo:* human ≈ rabbit	UGT1A4	Mey et al., 1999; Breyer-Pfaff et al., 2000
Tamoxifen	36	N.R.	*In vitro*: only in human (not in rat, mouse, guinea pig, dog, monkey)	UGT1A4	Kaku et al., 2004

Table 3 *(continued)*

Substrate	K_m, HLM (μM)	% Dose excreted in human urine	Species differences	Human UGT(s) involved	References
Aromatic N-heterocycles					
FYX-051 (developmental drug)	64	43 (N_1-G) 16 (N_2-G)	*In vivo*: human ≈ monkey >> rat	UGT1A9	Nakazawa et al,, 2006; Omura et al., 2007
JNJ-10198409 (developmental drug)	1.2 (Glu-A)	N.R.	*In vitro:* both Glu-A and Glu-B formed in human, monkey, rat	UGT1A4 UGT1A9	Yan et al., 2006
Lamotrigine	1869; 2234[a]	63 (N_2-G) Minor (N_5-G)	*In vitro*: human > rabbit >> monkey > rat	UGT1A4 UGT2B7	Magdalou et al., 1992; Rowland et al., 2006
Losartan	100	N.R.	*In vitro:* human, rabbit, rat	UGT1A1 UGT2B7	Alonen et al., 2008
Midazolam	38	N.R.	N.R.	UGT1A4	Klieber et al., 2008
RG 12525 (developmental drug)		Major (N_2-G)	*In vitro:* human ≈ monkey >> rat	UGT1A1 UGT1A3	Stevens et al., 2001

N.R. = not reported
[a]biphasic kinetics reported

2.3.3 Amides and sulfonamides

Various primary arylamides, cyclic amides, ureido compounds, and sulphonamides have been reported to undergo *N*-glucuronidation (Fig. 6, Table 3) in humans and many animal species, including rats, dogs, rabbits, and monkeys (Staines et al., 2004; Zhang et al., 2004; Xu et al., 2006). As an example, *N*-glucuronide conjugate was found as a major metabolite of the cyclic amide MaxiPost, a developmental drug, in both humans and dogs (Zhang et al., 2004). The excretion of MaxiPost *N*-glucuronide was species-dependent, as in humans this conjugate was excreted via the urine, while in the dog it was mainly found in the bile. Furthermore, the *N*-glucuronidation of perfluorooctanesulfonamide, an environmental chemical, was studied *in vitro* across species, and liver microsomes of humans, dogs, monkeys, and rats catalyzed the reaction at comparable efficiencies (Xu et al., 2006). In addition, the *N*-glucuronidation of dulcin, an ureido compound, was catalyzed by both human and rabbit liver microsomes (Uesawa et al., 2004; Uesawa et al., 2007).

Human UGT2B7 seems to play a significant role in the *N*-glucuronidation of this group of substances, including the aforementioned carbamazepine, perfluorooctane-sulfonamide, and MaxiPost (Staines et al., 2004; Zhang et al., 2004; Xu et al., 2006). More

specifically, UGT2B7, which is highly expressed in the liver, kidney, and intestine, was suggested to be a major enzyme responsible for carbamazepine *N*-glucuronidation in all of the above-mentioned tissues (Staines et al., 2004). In the case of perfluorooctanesulfonamide, UGT2B7 and UGT2B4 catalyzed its *N*-glucuronidation in humans (Xu et al., 2006). Interestingly, rat UGT2B1, which shows a strong resemblance to the human UGT2B7 enzyme, catalyzed perfluorooctanesulfonamide *N*-glucuronidation in the rat. Rat UGT1.1 and UGT2B12 also contributed to the *N*-glucuronidation of this substance. Human UGT1A family enzymes 1A1 and 1A9 catalyzed dulcin *N*-glucuronidation, while no contribution of UGT2B7 was detected (Uesawa et al., 2007). However, the affinities of the two UGT1A enzymes towards dulcin were low, suggesting the contribution of other, currently unknown UGTs in this reaction. Rabbit UGT1A7 and 2B17 also catalyzed dulcin *N*-glucuronidation (Uesawa et al., 2004; Uesawa et al., 2007).

2.3.4 Tertiary aliphatic amines

In humans, N^+-glucuronidation contributes significantly to the metabolism of many aliphatic tertiary amine drugs, such as antihistamines, tricyclic antipsychotics, and antidepressants (Luo et al., 1991; Chiu and Huskey, 1998) (Fig. 6, Table 3). While N^+-glucuronidation is efficient in humans, this reaction is generally not observed in most animal species, including rats, mice, guinea pigs, dogs, and cynomolgus monkeys (Soars et al., 2001b; Kaku et al., 2004; Shiratani et al., 2008). Nonetheless, some animal species, such as higher primates (chimpanzees), marmoset monkeys, and rabbits, have been reported to efficiently catalyze N^+-glucuronidation of a number of drugs, including cyproheptadine, ketotifen, amitriptyline, imipramine, and chlorpromazine (Coughtrie and Sharp, 1991; Chiu and Huskey, 1998; Soars et al., 2001a). These results suggest that the rabbit or the marmoset could be suitable animal models in the development of drugs that undergo N^+-glucuronidation, as they are predictive of human metabolism via this route.

Human UGT1A4 catalyzes the N^+-glucuronidation of many tertiary amine drugs, including amitriptyline, ketotifen, diphenhydramine, imipramine, and tamoxifen (Green and Tephly, 1996; Breyer-Pfaff et al., 2000; Kaku et al., 2004). Moreover, UGT1A3 has been reported to catalyze N^+-glucuronidation, but at a lower efficiency than UGT1A4 (Green et al., 1998). While catalyzing different *N*-glucuronidation reactions seems to be a major type of activity for UGT1A4, UGT1A3, a close homolog of UGT1A4, is also involved in different *O*-glucuronidation reactions. Residues 36 and 40 of UGT1A3 and UGT1A4 have been reported to be crucial for the selectivities of these enzymes towards planar phenols and tertiary amines, respectively (Kubota et al., 2007). Rabbit UGT1A4, along with UGT1A7, also catalyzed imipramine N^+-glucuronidation (Bruck et al., 1997), further supporting the similarity between humans and rabbits with respect to this metabolic route. However, in many animal species, including rats and mice, UGT1A4 is not a functional enzyme (Mackenzie et al., 2005), which in part explains the significant interspecies differences observed in N^+-glucuronidation.

Although UGT1A4 catalyzes many N^+-glucuronidation reactions, other UGT enzymes also appear to be involved in this reaction. Detailed kinetic experiments revealed that the N^+-glucuronidation of some amines, including amitriptyline, ketotifen, diphenhydramine, and imipramine, by HLM obeyed biphasic kinetics (Breyer-Pfaff et al., 1997; Mey et al., 1999; Breyer-Pfaff et al., 2000; Nakajima et al., 2002b). The measured high- and low-affinity K_m values are listed in Table 3. The biphasic kinetic curves suggested that at least two different UGT enzymes contribute to each of these reactions. Further studies conducted using different human recombinant UGT enzymes indicated that the UGT1A4-catalyzed reaction only explained the low-affinity component of the HLM-catalyzed reaction. Therefore, another, still unknown UGT enzyme probably catalyzes the high-affinity glucuronidations of these substrates in the human liver.

2.3.5 Aromatic *N*-heterocycles

A number of aromatic *N*-heterocycles containing five- and six-membered rings such as imidazoles, pyrazoles, triazines, tetrazoles, and pyridines are subject to *N*-glucuronidation (Fig. 6, Table 3). Due to the structural diversity of this group of substances, their *N*-glucuronidation across species and the human UGTs catalyzing the reactions are highly compound-dependent. Nevertheless, in many cases humans and monkeys glucuronidate aromatic *N*-heterocycles at comparable rates (Stevens et al., 2001; Nakazawa et al., 2006; Yan et al., 2006). Rats, at least in some cases, lack the ability to *N*-glucuronidate these compounds (Magdalou et al., 1992; Stevens et al., 2001; Nakazawa et al., 2006).

The *N*-glucuronidation of FYX-051, a developmental drug, was studied *in vivo* in humans, monkeys, rats, and dogs (Nakazawa et al., 2006). Triazole N_1-glucuronide was found to be the predominant metabolite in human and cynomolgus monkey urine, accounting for ~40% of the dose, whereas the N_2-glucuronide accounted for ~10-20%. In the rat, only low levels of *N*-glucuronides were detected. Interestingly, in dogs the major metabolites were N_1- and N_2-glucosides, i.e. conjugation of the triazine nitrogens with glucuronic alcohol instead of glucuronic acid. In the case of RG 12525, another developmental drug, the tetrazole N_2-glucuronide was the predominant metabolite in humans and monkeys, while only low levels of glucuronides were observed in rat hepatocytes (Stevens et al., 2001). In humans, also another regioisomeric glucuronide at the N_1 was formed, but at lower levels. Losartan, another tetrazole, was conjugated to two regioisomeric *N*-glucuronides (Alonen et al., 2008) by human, rabbit, and rat liver microsomes. Tetrazole N_2 was the preferred site of glucuronidation in all of the above-mentioned species. Furthermore, nafimidone alcohol was conjugated to an imidazole *N*-glucuronide in cynomolgus monkeys, baboons, and humans, while this metabolite was not detected in dog urine (Rush et al., 1990). Lamotrigine, an antiepileptic drug, was conjugated efficiently at the triazine ring by human, rabbit, and guinea-pig liver microsomes, whereas only low levels of glucuronide were found in Rhesus monkeys and rats (Magdalou et al., 1992). Finally, efficient *N*-glucuronidation of 1-phenylimidazole at N_3 was observed in liver microsomes of many species, including humans, rats, guinea-

pigs, rabbits, but not dogs (Vashishtha et al., 2002). The affinities in all species were, however, rather poor (K_m 0.6-4.4 mM).

Several UGT enzymes, including UGT1A1, UGT1A3, UGT1A4, UGT1A9, and UGT2B7, contribute to the glucuronidation of various *N*-heterocycles. Firstly, UGT1A4 and UGT2B7 were suggested as the primary enzymes catalyzing the *N*-glucuronidation of lamotrigine, a reaction obeying atypical kinetics in HLM (Rowland et al., 2006). While both enzymes glucuronidated lamotrigine at rather poor affinities (K_m ~2 mM), inhibition studies indicated that the UGT2B7-catalyzed reaction might dominate at low substrate concentrations. Midazolam, a sedative agent metabolized mainly by CYPs, was found to undergo *N*-glucuronidation at the tertiary imidazole group (Klieber et al., 2008). This reaction was catalyzed most efficiently, in terms of non-normalized glucuronidation rates, by UGT1A4. The role of UGT1A4 in midazolam glucuronidation was further supported by comparable K_m values of UGT1A4 and HLM, ~30-40 µM. FYX-051 glucuronidation at N_1 was catalyzed by human UGT1A9, while very low (non-normalized) activities were measured for UGT1A1 and UGT1A7 (Omura et al., 2007). However, the K_m values of UGT1A9 and HLM towards FYX-051 N_1-glucuronidation were dissimilar. UGT1A1, UGT1A3, and UGT2B7 catalyzed the formation of the tetrazole N_2-glucuronide of RG 12525 (Stevens et al., 2001), but as only a limited amount of UGT enzymes were tested and kinetic parameters were not measured, the contribution of other enzymes to this reaction cannot be excluded. Finally, UGT1A1 and UGT2B7 were the main contributors to tetrazole N_2-glucuronidation of losartan in the human liver (Alonen et al., 2008).

2.4 Approaches for studying drug glucuronidation

A schematic illustration of different approaches for studying drug glucuronidation is presented in Fig. 7. Computational ("*in silico*") methods can be used as rapid screens for the substrate selectivity of individual UGTs. However, structure–activity relations (SAR) of UGT enzymes are currently poorly understood, limiting their use. Different *in vitro* approaches, such as incubations with liver microsomes and recombinant UGT enzymes, provide the tools for reaction phenotyping and the study of interspecies differences. Using *in vitro – in vivo* scaling (IVIVS), an indication of the importance of glucuronidation on an *in vivo* scale can be produced. *In vivo* studies ultimately reveal the contribution of this metabolic route to the overall elimination of a drug.

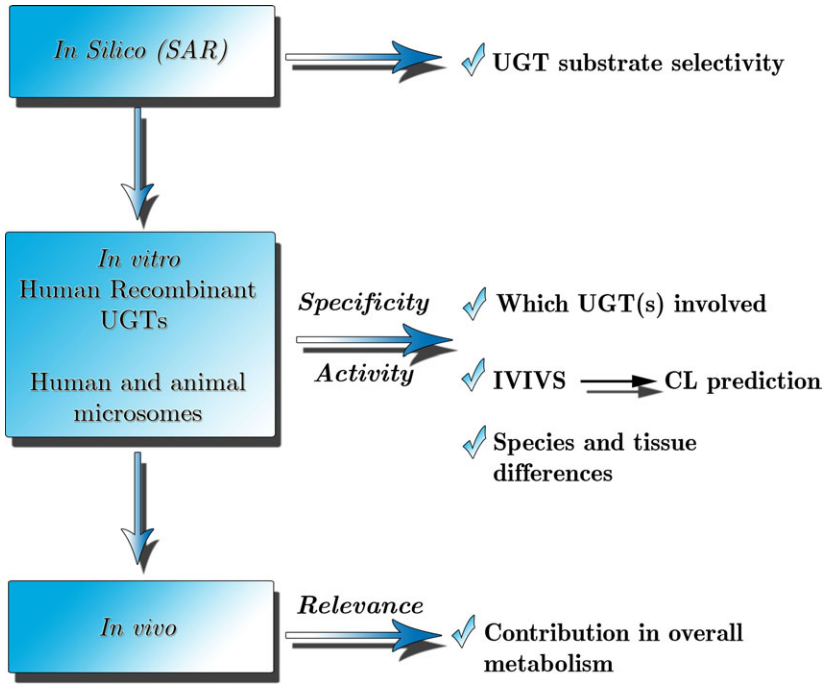

Figure 7 *A schematic illustration of drug glucuronidation studies.*

2.4.1 *In silico* modeling

Computational modeling potentially provides an economical alternative to laborous and time-consuming laboratory-based techniques for studying the structure-function relations of drug metabolism (van de Waterbeemd and Gifford, 2003). *In silico* modeling can be used as a high-throughput screen at the early stages of drug development to predict which enzymes metabolize the drug candidates. In comparison with CYP-catalyzed reactions, the structure-function relations of UGT enzymes are, however, generally poorly understood, complicating the computational prediction of UGT-mediated metabolism (Miners et al., 2004; Smith et al., 2004). The relatively small number of reports available on the modeling of UGT enzymes indicates a scarcity of appropriate experimental data for these purposes and explains why little progress has been made in this area in recent years. Moreover, existing evidence suggests that individual UGT isoforms exhibit unique, but overlapping substrate selectivity, further complicating the building of reliable models. Nonetheless, some two-dimensional (2D), quantum mechanical, and pharmacophore models permitting the classification of UGT substrates have been developed for a number of human UGTs such as 1A1, 1A4, 1A6, and 1A9 (Ethell et al., 2002; Sorich et al., 2002; Smith et al., 2003). These approaches demonstrate that computational prediction of UGT enzyme substrate selectivity is possible. The biggest obstacle for UGT modeling at present is probably that X-ray crystal structures of UGT enzymes are unavailable. Furthermore, only a few structurally or catalytically relevant amino acids have been identified in the structures of the UGT enzymes. However, crystallization technology is a rapidly developing area, and, recently, techniques to crystallize membrane-bound enzymes,

including CYPs, have been successfully utilized (Williams et al., 2003; Williams et al., 2004b). The docking of ligands into protein structures has been used in reaction phenotyping of CYP substrates, suggesting that such technologies could also be applied in the UGT field (Sorich et al., 2008).

2.4.2 *In vitro* approaches

2.4.2.1 Microsomes isolated from liver and other tissues

Microsomes are subcellular fractions isolated from hepatic and extrahepatic tissues by differential ultracentrifugation (Ekins et al., 1999). The microsomal fraction contains both UGT and CYP enzymes, as they are located in the endoplasmic reticulum of the cells. Liver microsomes are regarded as the "golden standard" of metabolic stability testing in drug development, since they contain the major drug-metabolizing enzymes as a "concentrate" (Brandon et al., 2003; Plant, 2004; Pelkonen and Raunio, 2005). Liver microsomes isolated from humans and a wide variety of animal species, as well as microsomes isolated from other tissues, such as the intestine and kidney, are currently commercially available.

Microsomal glucuronidation studies are performed by adding the drug under investigation along with the cofactor UDPGA and the enzyme source, human or animal liver microsomes, to the incubation buffer, generally phosphate or Tris buffer pH 7.4 with Mg^{2+} (Remmel et al., 2008). The samples are incubated at 37°C typically for 0.5-1 h. Many drugs and xenobiotics are highly lipophilic and therefore poorly soluble in water. Organic solvents, such as acetonitrile, methanol, or dimethyl sulfoxide, can be used to dissolve the substrates. As high concentrations of organic solvents tend to decrease microsomal UGT activities (Dehal et al., 2003), <1% solvent concentration is generally desirable. Whereas the total CYP content of the microsomes can easily be determined, no such method exists for UGTs. Therefore, the incubations are "standardized" by the addition of the same amount of protein (typically 0.25–1.0 mg protein per ml) to each incubate. In general, the enzyme is stable up to 45 min to 1 h, and an even longer incubation time may be used for slow reactions. When conducting enzyme kinetic studies, the linearity of glucuronide formation with respect to incubation time and protein concentration should be determined for each studied reaction in each studied enzyme source. It is recommended that at least ten different substrate concentrations ranging from $0.2\times K_m$ to $10\times K_m$ be used, and that less than 10% of the substrate be consumed during the incubation (Cornish-Bowden, 1995). An excess (1-5 mM) of UDPGA is added to ensure that depletion of the cofactor does not limit the reaction rates.

In contrast to the CYPs, the active site of UGTs is in the lumen of the endoplasmic reticulum (Clarke and Burchell, 1994). Therefore, at least for a portion of the isolated microsomes, the active site of the UGT enzyme remains in its "normal configuration" entrapped within the vesicle. Therefore, UGT activity in the microsomes is latent, and

maximal activity is not obtained until the integrity of the membrane is disrupted (Banhegyi et al., 1993). Disrupting the membrane will allow the cofactor UDPGA the access to the active site. Traditionally, detergents, such as Brij 58, Lubrol, or Triton X-100, or sonication have been used to remove the latency (Winsnes, 1969; Burchell and Coughtrie, 1989). However, high concentrations of detergents decrease UGT enzyme activities. The use of detergents is therefore time-consuming, as the optimal concentration has to be sought individually for each detergent – microsome – substrate combination. Recently, many investigators have switched to the use of the pore-forming 20-amino acid peptide alamethicin, which has a broader optimum concentration (typically 25-100 µg/mg protein) (Fisher et al., 2000). Alamethicin is pre-incubated together with the microsomes and buffer on ice for 30–35 min, or at 37°C for 10 min, prior to the addition of the substrate and UDPGA. Removing the latency typically increases the reaction rates from two- to fivefold (Fisher et al., 2000; Soars et al., 2003b). CYP marker activities in microsomes are reportedly unaffected by treatment with alamethicin, suggesting its usability in metabolic stability testing (Yan and Caldwell, 2003).

Saccharolactone and albumin are other agents, that can be added to the microsomal incubates in some cases. Saccharolactone inhibits microsomal β-glucuronidase from hydrolyzing the formed glucuronide conjugates. However, recent findings discourage the use of saccharolactone routinely in the incubates, as the extent of hydrolysis was found to be relatively small (9–19% of the glucuronide formation rate), and higher saccharolactone concentrations, in turn, resulted in a modest degree of inhibition of some glucuronidation reactions (Oleson and Court, 2008). Adding bovine serum albumin or fatty acid-free human serum albumin to HLM incubates was reported to decrease the K_m for zidovudine glucuronidation by an order of magnitude (Rowland et al., 2007; Rowland et al., 2008). Microsomes contain fatty acids, which were reported to act as potent competitive inhibitors of some UGTs, such as UGT2B7, and albumin “binds” these fatty acids, thus decreasing their binding to the UGT enzymes.

2.4.2.2 Recombinant UGTs

Several expression systems for different UGT enzymes have been described (Guengerich et al., 1997; Radominska-Pandya et al., 2005a). These expression systems utilize cell lines that inherently express minimal levels of the respective proteins. The mammalian-derived cell lines used for these purposes include Chinese hamster lung fibroblasts (V79), human embryonic kidney cells (HEK293), and human B-lymphoblastoid cells (AHH-1). Moreover, insect cell lines (Sf9) expressing UGTs have been developed. To produce such expression systems, the cDNA encoding an individual UGT enzyme is inserted into the cells using virus vectors, and the cells are cultured to produce sufficient amounts of the UGT enzymes. At present, several recombinant human UGT enzymes are commercially available.

The incubation conditions described earlier for liver microsomes can essentially be applied to recombinant UGT experiments. Like microsomal preparations, recombinant

UGT systems have been reported to be sensitive to the inhibitory effects of organic solvents, saccharolactone, and albumin during incubations (Dehal et al., 2003; Oleson and Court, 2008; Rowland et al., 2008). Apart from incubation conditions, many other factors, such as the transfection method (i.e. transient or stable), the cell line, and the membrane preparation (microsomes or whole-cell extracts) have an effect on the final enzyme activity of the recombinant UGT system, complicating comparison of results produced by different expression systems and laboratories (Guengerich et al., 1997; Tukey and Strassburg, 2000; Remmel et al., 2008). Insect cells transfected with baculovirus are excellent in terms of protein production, but enzyme activity tends to be low compared with mammalian cells systems. Significant amounts of inactive protein appear to be present in insect cell expression systems due to either poor membrane insertion or improper folding. Another issue regarding recombinant UGT preparates is that, as in the case of liver tissue, microsomal preparations can be isolated from these preparations; however, the yield of microsomal protein is often low. The use of whole-cell lysate as such or after sonication appears to be a good alternative and is easier than preparing microsomes.

To be able to evaluate the contribution of different UGT enzymes in the glucuronidation of a single substrate, it is important to normalize the measured UGT activities. Normalization, i.e. dividing the measured activities of each UGT enzyme by their expression levels, allows for the direct comparison of the activities. In the case of UGT1A enzymes, the expression levels can be measured by Western blotting using antibodies directed against the UGT1A constant region. However, comparison between the UGT1A and UGT2B enzymes is not possible with this method. Nonetheless, a recently described system of expressing UGTs with histidine molecule tags (His-tags) allows direct comparison of expression levels of both UGT1A and UGT2B enzymes (Kurkela et al., 2003; Kurkela et al., 2007).

Another issue complicating UGT reaction phenotyping is that the quantitative levels of different UGT enzymes in the human liver (or intestine) are currently unknown, although some estimates can be given based on mRNA levels (Nakamura et al., 2008; Ohno and Nakajin, 2009). Therefore, the best tools for determining the major UGT enzymes involved in each reaction at the moment include comparison of K_m values observed in HLM vs. different recombinant UGTs, and comparison of normalized activities of individual UGTs towards the substrate (Miners et al., 2006).

2.4.2.3 Primary hepatocytes

Primary hepatocytes are intact and fully functional cells containing the complete set of phase I and II metabolic enzymes and transporter proteins. As hepatocytes are fully functional cells, endogenous cofactors, such as UDPGA, are produced within the cells. Overall, hepatocytes provide a system with a strong resemblance to the *in vivo* liver. Hepatocytes are therefore routinely used in drug metabolism studies to evaluate the contribution of different metabolic routes, including UGT-mediated metabolism, to the

elimination of drug candidates (Vermeir et al., 2005; Hewitt et al., 2007). Hepatocyte studies are often used also in the predictions of *in vivo* hepatic clearance (McGinnity et al., 2004; Kilford et al., 2009). Culturing hepatocytes requires demanding laboratory techniques, limiting their use in routine metabolic stability testing. Moreover, the use of at least human primary hepatocytes is limited by the restricted availability of fresh liver tissue. Nonetheless, the techniques to prepare cryopreserved hepatocytes have recently developed to a point where the viabilities of cryopreserved cells are quite acceptable (LeCluyse et al., 2005). Moreover, pooled human hepatocytes from 5 or 10 donors are currently available, which decreases the variation between the batches.

2.4.2.4 Liver cell lines

Various permanent liver cell lines derived from primary tumors are less popular in drug metabolism studies mainly due to their incomplete expression of metabolic enzymes (Brandon et al., 2003; Vermeir et al., 2005). Compared with primary hepatocytes, the advantage of different cell lines is reproducibility. Moreover, cells lines are generally easier to culture and they maintain enzyme levels for a longer period. The best-characterized human hepatoma cell line is HepG2. This cell line was recently reported to express many UGT2B family enzymes, including 2B4, 2B7, 2B10, 2B11, 2B15, 2B17, and 2B28 (Nakamura et al., 2008). However, the expression of UGT1A family enzymes was limited to 1A1 and 1A3. Another human hepatoma-derived cell line, HepaRG, has also been introduced (Gripon et al., 2002). The activities of major CYPs are relatively high in this cell line, making it a very promising candidate for *in vitro* drug metabolism studies (Kanebratt and Andersson, 2008). The HepaRG cell line was also reported to catalyze some UGT-mediated reactions (Aninat et al., 2006).

2.4.3 *In vivo* studies

Even though *in vitro* studies generally predict *in vivo* metabolism quite well, *in vivo* studies are an important part of drug development to confirm the major metabolic routes of a new drug candidate, and, moreover, to identify unexpected metabolic routes (Iyer and Zhang, 2008). When glucuronide conjugates are formed *in vivo*, the portion of the conjugates excreted via bile to the GI tract is subject to hydrolysis catalyzed by bacterial β-glucuronidase in the intestinal flora. The vulnerability of the glucuronides to hydrolysis by β-glucuronidase is compound-dependent. While some glucuronides are extremely resistant to β-glucuronidase (Sinz and Remmel, 1991; Kassahun et al., 1998), others are readily hydrolyzed by this enzyme back to pharmacologically active agents (Hiller et al., 1999; Mey et al., 1999). After hydrolysis, the newly formed drugs can be absorbed back to systemic circulation. This mechanism has been reported to lead to significant enterohepatic circulation of some drugs.

Another important issue with regard to *in vivo* studies involving glucuronide conjugates is to evaluate whether the formed glucuronide conjugates are stable in plasma and excreta samples during sample pre-treatment. As an example, some glucuronides, such as the *N*-glucuronides of primary arylamines, are hydrolyzed in acidic or alkalic conditions within minutes (Ciotti et al., 1999). Furthermore, some glucuronides are rapidly hydrolyzed by bacterial β-glucuronidase present in fecal samples. If such hydrolysis occurs, the contribution of glucuronidation to the overall metabolism may be considerably underestimated.

2.4.4 Glucuronide analytics

Three basic methods have been used to analyze glucuronide conjugates from *in vitro* or *in vivo* samples (Remmel et al., 2008):

(1) Radiometric methods using either radiolabeled cofactor (^{14}C-UDPGA) or substrate followed by either thin-layer chromatography (TLC) or liquid chromatography (LC) to separate the glucuronide;
(2) LC with ultraviolet detection (UV) or mass spectrometry (MS);
(3) Fluorometric methods using fluorescent substrates, such as 1-naphthol.

Radiometric methods have been widely employed for screening assays. A major advantage of these methods is that metabolite standard is not needed for the quantitation of the formed glucuronide product(s). The universal method is to use radiolabeled ^{14}C-UDPGA as the cofactor, resulting in labeled glucuronide product(s). The glucuronides can be separated from ^{14}C-UDPGA by TLC (Bansal and Gessner, 1980) or LC (Coughtrie et al., 1986). When TLC is utilized, radioactivity on the plates is counted on a plate scanner, or by densitometric quantitation on film or a phosphoimager. In LC analyses, the glucuronides are detected using either an online flow scintillation analyzer (FSA) or fraction collection followed by liquid scintillation counting. Reversed-phase (C_{18}) columns can generally be used for the separation of the glucuronide conjugates. As an alternative to TLC and LC methods, a method utilizing ^{14}C-UDPGA and separation of the glucuronide products by solid-phase extraction (SPE) using 96-well extraction plates was recently introduced (Di Marco et al., 2005). Radiolabeled substrates can also be used instead of ^{14}C-UDPGA, but are rarely available. Radiolabeled drugs are, however, synthesized in many cases for the purpose of mass balance and excretion studies of new drug candidates.

Most glucuronides have very similar absorbance spectra as their aglycones (glucuronic acid does not contribute to UV absorption at wavelengths >210 nm), suggesting that one can construct a standard curve with the aglycone to quantitate the glucuronides during LC-UV analyses. However, this method can only be used for the estimation of glucuronide levels. For proper quantitation, an authentic glucuronide standard is required. Alternatively, the glucuronide fraction can be collected and hydrolyzed with β-glucuronidase, followed by quantitation of the glucuronide as the formed aglycone substrate. Treatment with β-glucuronidase can also be used to ensure that the peak

observed in the chromatogram is in fact a glucuronide. However, some glucuronides, such as the *N*-glucuronide conjugates of lamotrigine (Sinz and Remmel, 1991) and olanzapine (Kassahun et al., 1998), are resistant to β-glucuronidase hydrolysis.

The advantage of different LC-MS methods is that they are generally far more sensitive than any other methods. However, an authentic glucuronide standard is always needed for quantitative purposes by LC-MS. Glucuronides readily fragment, with a neutral loss of 176 amu, to produce the aglycone fragment. Glucuronides are weak acids, having a pK_a of ~4, and can thus generally be detected using negative ion mode at pH 4.5 or higher with electrospray ionization. Many glucuronides, at least when the substrate is a weak base, can also be detected using positive ion mode.

The use of fluorometric methods is limited to the cases where the aglycone substrate is fluorescent. Moreover, as the aglycone substrate and the glucuronide product are not separated, their fluorescence characteristics should be different. Fluorometric methods for some fluorescent phenolic substrates, such as 1-naphthol, have been described (Mackenzie and Hanninen, 1980), and they have been applied for continuous fluorometric monitoring of glucuronide formation.

2.4.5 Enzyme kinetics

Traditionally, the initial enzyme velocity data of *in vitro* kinetic experiments have been fitted to the classical Michaelis-Menten equation (*1*) (Cornish-Bowden, 1995):

$$v = \frac{V_{\max} \times S}{K_m + S} \qquad (1),$$

where v is the reaction velocity, $V_{\max}$ the maximum velocity, K_m the Michaelis constant, and S the substrate concentration.

However, many CYP- and UGT-catalyzed reactions have been reported to obey non-Michaelis-Menten kinetics (Houston and Kenworthy, 2000; Hutzler and Tracy, 2002; Atkins, 2004). Some of these “atypical” kinetic plots are presented in Fig. 8. Hill equation (*2*) can be used to describe sigmoidal kinetics indicating autoactivation:

$$v = \frac{V_{max} \times S^n}{K_m{}^n + S^n} \qquad (2),$$

where n is the Hill coefficient describing the degree of sigmoidicity (n>1). The mechanism of autoactivation kinetics is largely unknown, but can involve multiple substrates present in the active site of a single enzyme (Korzekwa et al., 1998).

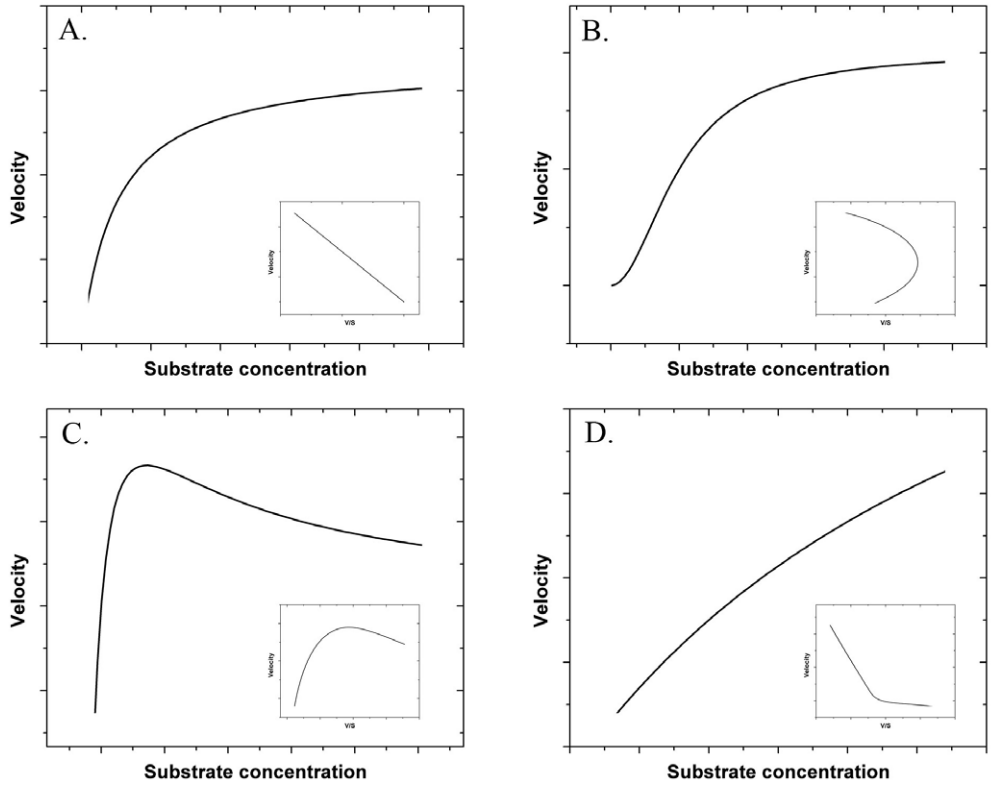

Figure 8 *Typical and atypical kinetic plots, modified from Atkins (2004). Classical hyperbolic Michaelis-Menten kinetics (A); sigmoidal kinetics (B); substrate inhibition kinetics (C); and biphasic kinetics (D). In each case, the inset is the corresponding Eadie–Hofstee plot of velocity versus velocity/substrate concentration (v/S).*

Substrate inhibition, another atypical kinetic phenomenon often observed in *in vitro* experiments, is described by the equation:

$$v = \frac{V_{\max}}{1 + (K_m / S) + (S / K_{si})} \qquad (3),$$

where K_{si} is the constant describing the substrate inhibition interaction. Although the mechanisms leading to substrate inhibition have not been fully revealed, a two-site model in which one binding site is productive and the other site is inhibitory and operable at high substrate concentrations has been suggested (Houston and Kenworthy, 2000). The operation of these two different binding sites results in decreased velocity with increasing concentrations. Detailed kinetic studies of human UGT1A enzymes have indicated another mechanism, where binding of the aglycone substrate to the enzyme-UDP complex leads to a nonproductive dead-end complex that slows the productive cycle (Luukkanen et al., 2005). Generally, the observed K_{si} values for substrate inhibition are high compared with the apparent K_m values of the reactions, suggesting that in many cases substrate inhibition may not be relevant *in vivo*.

The third atypical kinetic mechanism suggested is a biphasic saturation profile indicative of an enzyme with both low- and high-affinity binding components, described by the equation:

$$v = V_{\max 1} \times \frac{S / K_{m1}}{1 + (S / K_{m1})} + V_{\max 2} \times \frac{S / K_{m2}}{1 + (S / K_{m2})} \qquad (4),$$

where subscripts 1 and 2 denote the high- and low-affinity component of the reaction, respectively. Biphasic kinetics can be observed either when two different enzymes take part in the reaction, as frequently observed in tissues microsomes, or when a single enzyme has multiple binding regions (Houston and Kenworthy, 2000).

Whether the atypical kinetics observed with UGT-catalyzed reactions actually reflects the intrinsic properties of the enzyme(s) or whether it is an artifact arising from the incubation conditions has been debated. To this end, Soars and coworkers (2003b) performed a detailed kinetic study using different incubation conditions for a set of glucuronidated model substrates. They concluded that atypical kinetics did not originate from the incubation conditions, and recommended that equations beyond the Michaelis-Menten equation should be used to fit kinetic data to obtain an accurate estimate of *in vitro* glucuronidation, which in turn will also potentially improve the predictability of *in vivo* clearance.

2.4.6 *In vitro – in vivo* scaling (IVIVS)

The quantitative role of different metabolic pathways in the elimination of drugs can be estimated by extrapolating the measured *in vitro* kinetic data to the *in vivo* situation. Metabolic clearance (intrinsic clearance, $CL_{\text{int, in vitro}}$) is an important parameter used in the scaling, and under linear velocity conditions (when $S << K_m$) is equal to the following ratio (Houston, 1994):

$$CL_{int,in\,vitro} = \frac{V_{max}}{K_m} \qquad (5).$$

CL_{int} is a direct measure of the efficacy of an enzyme to metabolize a given substrate. When a drug is metabolized via several routes, the total clearance is the sum of these routes:

$$CL_{tot} = \sum_{i=1}^{n} CL_i \qquad (6).$$

After determining $CL_{\text{int, in vitro}}$, the first step in the IVIVS process is the use of different scaling factors (Barter et al., 2007). In the case of liver microsomal experiments, two

scaling factors, namely microsomal content per gram liver (MPPGL) and liver weight per kg body weight (w_L) , are used to obtain *in vivo* CL_{int} as follows:

$$CL_{int,in\ vivo} = CL_{int,in\ vitro} \times MPPGL \times w_L \qquad (7).$$

As only the free (unbound) drug is subject to metabolism, free fractions of the drug in blood ($f_{u,\ b}$) and microsomes ($f_{u,\ in\ vitro}$) are taken into account when the unbound *in vivo* clearance is estimated (Obach, 1997; Grime and Riley, 2006):

$$CL_{int,in\ vivo,\ u} = \frac{CL_{int,in\ vivo} \times f_{u,b}}{f_{u,in\ vitro}} \qquad (8).$$

As the free fractions are generally measured from plasma samples, the free fraction in blood can be calculated from the plasma data as follows:

$$f_{u,b} = \frac{f_{u,p}}{R_b} \qquad (9),$$

where $f_{u,\ p}$ is the free fraction in plasma and R_b the blood-to-plasma partition ratio.

Finally, an appropriate liver model is used to calculate an estimate for *in vivo* hepatic clearance, CL_H. The well-stirred model (Pang and Rowland, 1977), the simplest liver model taking into account the hepatic blood flow, Q_H, is described by the following equation:

$$CL_H = \frac{CL_{int,in\ vivo,u} \times Q_H}{CL_{int,in\ vivo,u} + Q_H} \qquad (10).$$

Both microsomal and hepatocyte data have been widely used for scaling purposes (Soars et al., 2002; McGinnity et al., 2004; Brown et al., 2007; Kilford et al., 2009). Many studies indicate that hepatocyte data give more accurate predictions of *in vivo* metabolic clearance than microsomal data (Soars et al., 2002; Brown et al., 2007). However, in many cases, both the hepatocyte and the microsomal data tend to underpredict the *in vivo* metabolic clearance. For hepatocytes, cryopreserved human cells were reported to retain on average 94% of the CL_{int} determined in fresh cells, indicating that both fresh and cryopreserved human hepatocytes may be used for the prediction of human hepatic clearance (McGinnity et al., 2004). With regard to liver microsomal data, improved predictability of microsomal data for drugs eliminated via glucuronidation was observed when alamethicin and bovine serum albumin were added to the incubates (Kilford et al., 2009). Bovine serum albumin sequesters the fatty acids released during microsomal incubations that inhibit at least UGT1A9- and UGT2B7-mediated metabolism.

2.5 Investigated compounds

2.5.1 4-Arylalkyl-1*H*-imidazoles

The studied 4-arylalkyl-1*H*-imidazoles are a family of closely related structures (Fig. 9) that mediate their pharmacological effect by either activating or inhibiting the central α_2-adrenoceptors. These compounds are rather small (molecular weight ~200) and relatively lipophilic (logP ~2.5–2.8), indicating good permeability, and thus, have the ability to pass through the blood-brain barrier. The imidazole moiety makes the compounds slightly basic, with a pK_a of ~7.0-7.2, suggesting that even though both non-ionized and ionized form are present at a physiological pH of 7.4, the non-ionized form prevails. As free bases, 4-arylalkyl-1*H*-imidazoles are poorly soluble in water, but can be dissolved in organic solvents. While a few of the studied compounds (MPV-207 AIV and MPV-295 AIV) have been used for research purposes only, others are currently used as pharmacologically active agents. The specific and selective α_2-agonists detomidine and medetomidine are in veterinary use as analgesic sedatives (Vainio, 1988; Kuusela et al., 2000). While detomidine is used for horses, cattle and other large animals, medetomidine is used for smaller domestic animals such as the dog and the cat. Atipamezole is an antagonist of the α_2-adrenoceptor, and as it rapidly reverses the sedation induced by detomidine or medetomidine, it is commonly used by veterinarians to awaken animals from sedation (Pertovaara et al., 2005).

Dexmedetomidine [(+)-4-(*S*)-[1-(2,3-dimethylphenyl)ethyl]-1*H*-imidazole], the active enantiomer of the racemic medetomidine, is currently also in human use and displays sedative, analgesic, and anxiolytic effects after intravenous administration to postsurgical patients (Bhana et al., 2000). The other enantiomer, levomedetomidine [(–)-4-(*R*)-[1-(2,3-dimethylphenyl)ethyl]-1*H*-imidazole], is practically devoid of pharmacological activity (Savola and Virtanen, 1991). The advantage of dexmedetomidine over other sedative agents in clinical use is that it produces rapid and stable sedation, while maintaining a high degree of patient rousability and anxiety reduction (Bhana et al., 2000). After a single intravenous dose to healthy volunteers, dexmedetomidine is rapidly distributed ($t_{1/2\alpha}$ 9 min) and eliminated with an elimination half-life of approximately 2 hours after extensive metabolism in the liver. Dexmedetomidine is metabolized across species via CYP-mediated hydroxylations, followed by carboxylic acid or glucuronide formations (Salonen, 1989; Salonen, 1991). However, in humans, direct glucuronidation at imidazole N_3 and N_1 (Fig. 9) represents the major metabolic pathway (data in file).

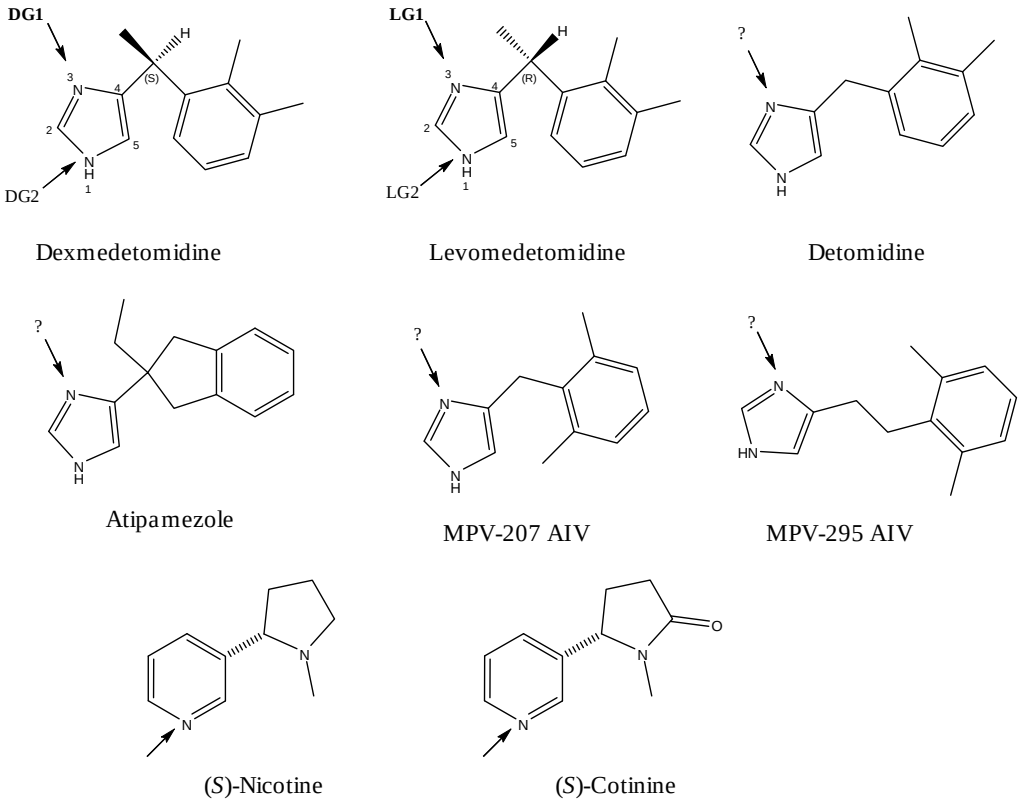

Figure 9 *Structures of the studied compounds. The N-glucuronidation site(s) is marked with an arrow and the major sites are indicated in boldface. Detomidine, atipamezole, MPV-207 AIV, and MPV-295 AIV each produced one major N-glucuronide product in HLM, and the site of glucuronidation is tentative.*

2.5.2 Nicotine and cotinine

Nicotine, a pyridine alkaloid (Fig. 9), is the addictive agent in tobacco products. The addictive properties are thought to result from increased dopamine levels in the brain (Benowitz, 2009). Nicotine addiction is the cause of continued use of tobacco products, which in turn results in exposure to the variety of carcinogenic nitroso compounds present in tobacco smoke, making tobacco the greatest preventable cause of death due to cancer. Therefore, a wide variety of products for nicotine replacement therapies are available in different formulations. Nicotine has also been studied as an active ingredient in experimental therapy for Parkinson's disease, Alzheimer's disease, and ulcerative colitis.

As a free base, nicotine is a hygroscopic, oily liquid miscible in water. Nicotine readily forms salts, which are usually solid and highly water-soluble. Nicotine is optically active, and the nicotine in tobacco is largely the levorotary (*S*)-isomer, while only 0.1-0.6% of total nicotine content is made up of the less active (*R*)-nicotine. During smoking nicotine is rapidly absorbed from the alveoli of lungs, and peak concentrations in blood are observed at the completion of cigarette smoking (Hukkanen et al., 2005; Tutka et al., 2005). The pK_a of the weakly basic nicotine is ~8.0, suggesting that the ionized form

prevails at physiological pH and also under acidic conditions such as in the GI tract. In its ionized form, the permeation of nicotine across membranes is rather poor, thus limiting the use of oral formulations in replacement therapies. Nicotine undergoes extensive first-pass metabolism in the liver, which also limits its peroral use. In humans, the elimination half-life of nicotine is ~2 h, and although 8-10% of nicotine is excreted unchanged in urine, the primary elimination pathway is hepatic metabolism. The major metabolites of nicotine are cotinine (75%), *N*'-oxide metabolite (4-7%), and a direct *N*-glucuronide (3-5%) (Hukkanen et al., 2005; Tutka et al., 2005). Cotinine, a pharmacologically inactive metabolite, is formed in a two-step reaction, the first step catalyzed by CYP2A6 and the second by the cytosolic enzyme aldehyde oxidase. Before excretion, cotinine is extensively metabolized further, mainly to a direct *N*-glucuronide conjugate and to a hydroxyl metabolite.

Large interspecies differences in the direct *N*-glucuronidation of nicotine have been observed (Ghosheh and Hawes, 2002a). While HLM catalyzed nicotine *N*-glucuronidation efficiently, the glucuronidation rates in rhesus and cynomolgus monkey microsomes were only about 7-11% of the rates measured in HLM. Furthermore, only low levels of nicotine *N*-glucuronide were detected in mini-pig and guinea-pig microsomes, and glucuronidation rates were undetectable in rats, mice, dogs, and rabbits. However, marmoset monkey liver microsomes were reported to glucuronidate nicotine (Tsai and Gorrod, 1999). Glucuronidation of cotinine, the major metabolite of nicotine, was also efficiently catalyzed by HLM. Interestingly, cotinine *N*-glucuronide was not detected in any of the above-mentioned animal species (Tsai and Gorrod, 1999; Ghosheh and Hawes, 2002a).

3. Aims of the study

Many nitrogen-containing drugs are cleared from the body predominantly as direct *N*-glucuronide conjugates, without requiring CYP enzymes. *N*-Glucuronidation, a reaction catalyzed by a family of UGT enzymes, is nonetheless an under-examined pathway. The goals of this study were to evaluate, using different *in vitro* techniques, interspecies differences in *N*-glucuronidation and to elucidate which human UGT enzymes catalyze this reaction.

More specifically, the aims were as follows:

1. To develop liquid chromatographic methods to detect low levels of *N*-glucuronide conjugates formed in *in vitro* experiments.
2. To examine interspecies differences in the *N*-glucuronidation of a set of 4-arylalkyl-*1H*-imidazole substrates, such as medetomidine, using human and animal liver microsomes.
3. To elucidate which human UGT enzymes are responsible for the *N*-glucuronidation of medetomidine enantiomers using a set of 16 recombinant UGT enzymes.
4. To investigate the regio- and stereoselective *N*-glucuronidation of medetomidine by performing detailed enzyme kinetics experiments.
5. To evaluate which UGT enzymes contribute to the *N*-glucuronidation of nicotine and its major metabolite cotinine in the human liver.

4. Materials and methods

4.1 Chemicals

Chemical structures of the substrates and their *N*-glucuronidation site(s) are presented in Fig. 9. 4-Arylalkyl-1*H*-imidazoles dexmedetomidine (II, IV), levomedetomidine (I, II, IV), ^{3}H-levomedetomidine (I, II), detomidine (II), atipamezole (II), MPV-207 AIV (II), and MPV-295 AIV (II) were kindly provided by Orion Pharma (Espoo, Finland). (*S*)-(-)-Nicotine (III) and (*S*)-(-)-cotinine (III) were obtained from Sigma-Aldrich (St. Louis, MO, USA). Metabolite standards nicotine-*N*-β-glucuronide (NG) and cotinine-*N*-β-D-glucuronide (CG), and internal standards nicotine-*N*-β-glucuronide(-methyl-d3) and (*R*,*S*)-cotinine-*N*-β-D-glucuronide(-methyl-d3) were purchased from Toronto Research Chemicals (Toronto, ON, Canada). UDPGA was obtained from Roche Molecular Biochemicals (Mannheim, Germany) (I, II) or Fluka Chemie (Buchs, Switzerland) (III, IV), while ^{14}C-UDPGA [glucuronyl-^{14}C(U)] (I, II, IV) was from Perkin Elmer Life Sciences (Boston, MA, USA). Other chemicals were mainly from Sigma-Aldrich and were of the highest purity available.

4.2 Tissue microsomes

Human and animal liver microsomes and human intestine microsomes (HIM) used in the studies are listed in Table 4. Preparation of noncommercial microsome batches are described in detail in the original publications.

Table 4 *Characteristics of human and animal tissue microsomes.*

Microsome preparation	Sex and pool size	Supplier	Publication
Human liver	Unknown	Human Biologics, Scottsdale, AZ, USA	I, II
Human liver	Mixed; n=18-30	BD Biosciences, San Jose, CA, USA	III, IV
Human intestine	Mixed; n=5	BD Biosciences	III, IV
Rat liver (Wistar)	Male; n=6	Finnish Institute of Occupational Health, Helsinki, Finland	II
Rat liver (Wistar Han)	Male; n=20	BD Biosciences	IV
Dog liver	Male; n=1	Orion Pharma, Turku, Finland	II
Dog liver	Male; n=2	Orion Pharma, Espoo, Finland	IV
Mouse liver (CD-1)	Male; n=3	Orion Pharma, Espoo, Finland	IV
Guine-pig liver	Unknown	Orion Pharma, Espoo, Finland	IV
Rabbit liver	Male; n=1	Orion Pharma, Espoo, Finland	IV
Mini-pig liver (Gottingen)	Male; n=3	BD Biosciences	IV
Monkey liver (Cynomolgus)	Male; n=6	BD Biosciences	IV

4.3 Recombinant human UGTs

Recombinant human UGTs used in the studies are listed in Table 5. Recombinant UGT1A6 and UGT1A9 used in study II were produced as detailed previously (Forsman et al., 2000). Recombinant UGT enzymes used in studies III and IV were produced as described earlier (Kurkela et al., 2003; Kurkela et al., 2007), and their relative expression levels were determined, side by side, by immunodetection using the tetra-His monoclonal antibody (QIAGEN GmbH, Hilden, Germany) as detailed elsewhere (Kurkela et al., 2007).

Table 5 *Recombinant human UGTs used in the studies.*

Human UGT	Expression system	Supplier	Publication
UGT1A3	Baculovirus-infected SF-9 insect cells	Panvera, Madison, WI, USA	II
UGT1A4	AHH-1 cells	Gentest, Woburn, MA, USA	II
UGT1A6	Semliki Forest virus-infected V79 cells	University of Helsinki, Finland	II
UGT1A9	“	“	II
UGT1A1	Baculovirus-infected SF-9 insect cells	University of Helsinki, Finland	IV
UGT1A3	“	“	IV
UGT1A4	“	“	III, IV
UGT1A5	“	“	IV
UGT1A6	“	“	IV
UGT1A7	“	“	IV
UGT1A8	“	“	IV
UGT1A9	“	“	III, IV
UGT1A10	“	“	IV
UGT2B4	“	“	IV
UGT2B7	“	“	III, IV
UGT2B10	“	“	III, IV
UGT2B11	“	“	IV
UGT2B15	“	“	IV
UGT2B17	“	“	IV
UGT2B28	“	“	IV

4.4 mRNA expression of UGT enzymes in human tissues

Gene expression levels of UGT1A4, UGT2B7, and UGT2B10 in selected human tissues (liver, kidney, stomach, small intestine, colon, trachea, lung, and brain) were determined using a quantitative RT-PCR method as detailed in publication III.

4.5 *In vitro* glucuronidation assays

4.5.1 Glucuronidation screens

The incubation mixtures for the initial screens contained 100 mM phosphate buffer pH 7.4, 5 mM $MgCl_2$, 5 mM UDPGA, and mainly 0.5 mM substrate in a total volume of 100 µl. Liver and intestine microsome incubates usually contained 0.2-0.5 mg microsomal protein per ml. Incubates of recombinant human UGTs, which were used either as cell homogenates or microsomal membranes, contained 1-3 mg protein per ml. Stock solutions (10-50 mM) of the substrates were prepared in water, provided that the water solubility of the substrate was adequate, or in organic solvent (dimethyl sulfoxide or methanol). As a result, the final incubates of some substrates contained up to 5% organic solvent. However, these amounts of organic solvents were found to inhibit each reaction by less than 10%. Consumption of the substrate was kept at <10% during the incubations. Triton X-100 (I, II) or alamethicin (III, IV) was added to liver and intestine microsome incubates to activate the glucuronidation reactions, but was not added to incubations with recombinant UGTs. Saccharolactone, the inhibitor of β-glucuronidase, was omitted since it slightly inhibited some glucuronidation reactions, as also reported by Olesen and Court (2008). The reactions were initiated by the addition of UDPGA and incubated at 37°C for 60 or 120 min. The reactions were terminated by protein precipitation. A mixture of methanol and perchloric acid was used for protein precipitation in the 4-arylalkyl-1*H*-imidazole samples, while trifluoroacetic acid was used in the nicotine and cotinine samples. Preliminary tests were performed to show that the formed glucuronide conjugates were stable in the samples after terminating the reactions. After centrifugation, the supernatants were analyzed by liquid chromatography. Further details of the incubations are presented in the original publications.

4.5.2 Optimization of incubation conditions

Before detailed kinetic assays, some preliminary tests were conducted to determine the optimal incubation conditions. Firstly, the effect of different incubation buffers adjusted to different pH values was evaluated using atipamezole as a test substrate. Atipamezole was incubated with HLM and recombinant human UGT1A4 in the following conditions: 100 mM sodium acetate buffer pH 4.5, 5.0, 5.5, and 5.8; 100 mM sodium phosphate buffer pH 6.2, 6.5, 6.8, 7.0, 7.2, and 7.4; and Tris buffer pH 7.4, 8.0, 8.5, and 9.0. Secondly, the effect of the latency-disrupting agents Triton X-100 and alamethicin was tested using dexmedetomidine as a test substrate. Dexmedetomidine was incubated with HLM and recombinant human UGT1A4 using Triton X-100, at concentrations of 0.05, 0.1, 0.2, 0.3, 0.4, and 0.5 mg per mg protein, and alamethicin, at concentrations of 12.5, 25, 37.5, 50, and 62.5 µg per mg protein. Finally, since in preliminary experiments the activity of recombinant human UGT2B10 was noted to decline during the isolation of

microsomal membranes from the cells, the rate of nicotine glucuronidation by UGT2B10 and also by UGT1A4 was tested using both microsomal membranes and lysed cell homogenates.

4.5.3 Kinetic assays

The incubation mixtures for kinetic assays by human and dog liver microsomes and recombinant human UGTs were prepared essentially as described in "Glucuronidation screens", typically using 10 different substrate concentrations and 2-4 replicate incubates. Each reaction was performed under conditions where glucuronide formation was found to be linear with respect to incubation time and protein concentration. Incubation conditions are summarized in Table 6.

Table 6 *Incubation conditions of kinetic assays.*

Substrate (and possible solvent)	*S* (µM)	Enzyme preparate	Protein concentration (mg/ml)	Triton (µg/ml)	Alamethicin (µg/ml)	Incubation time (min)
II						
Dexmedetomidine[b]	2-3500	HLM	0.2	50	-	45
	20-5000	DLM[a]	0.2-0.3	0	-	45
Levomedetomidine[b]	2-500	HLM	0.1	50	-	45
	20-3500	DLM	0.2	0	-	45
Detomidine[b]	5-1000	HLM	0.1	50	-	60
	100-10000	DLM	0.3	0	-	45
Atipamezole[b]	0.2-30	HLM	0.1	50	-	45
	50-3000	DLM	0.3	0	-	45
MPV-207 AIV (5% methanol)	2.5-1000	HLM	0.1	50	-	20
	50-5000	DLM	0.2	50	-	45
MPV-295 AIV	2.5-1000	HLM	0.1	50	-	45
	20-5000	DLM	0.1	25	-	45
III						
Nicotine	5-4000	HLM	0.2	-	20	60
	5-4000	UGT1A4	1	-	-	120
	5-4000	UGT2B10	1	-	-	60-120
Cotinine	5-4000	HLM	0.2	-	20	60
	5-4000	UGT1A4	1	-	-	120
	5-4000	UGT2B10	1	-	-	120
IV						
Dexmedetomidine[b]	2.5-2000	HLM	0.2	-	20	60
	2.5-2000	UGT1A4	1	-	-	120
	2.5-2000	UGT2B10	1	-	-	240
Levomedetomidine[c] (≤4% methanol)	2.5-2000	HLM	0.2	-	20	30
	2.5-2000	UGT1A4	2	-	-	120
	2.5-2000	UGT2B10	1	-	-	120

[a]DLM = dog liver microsomes; [b]used as hydrochloride salt; [c]used as free base

4.6 Liquid chromatography

The analytical methods and equipment used in the studies are listed in Table 7.

Table 7 *Liquid chromatographic methods used in the study.*

Substrate	t_R of glucuronide (min)	LC	Column and column oven temperature	Eluent and flow rate	Detector(s)
I and II Atipamezole Detomidine Dexmedetomidine Levomedetomidine MPV-207 AIV MPV-295 AIV	 7.2 4.8 7.0 (DG1) 9.0 (DG2) 6.5 (LG1) 9.0 (LG2) 4.7 6.6	Agilent1100 [a]	Symmetry C_{18} 150×3.9 mm[b] 40°	NaH_2PO_4 pH 3.0 (50 mM) and methanol (68:32) 1 ml/min	UV 215 nm and Model 9701 FSA[c]
I and II ^{3}H-Levomedetomidine	6.5 (LG1)	Agilent 1090	Symmetry C_{18} 150×3.9 mm 40°	"	Model 150TR FSA[d]
III Nicotine Cotinine	 6.3 8.3	Agilent 1100	Discovery C_{18} HS F5[e] 100×2.1 mm 30°	Trifluoroacetic acid pH 2.2 and methanol. A linear 15-min gradient from 5% to 30% methanol 0.2 ml/min	Model G-1946A MS, Agilent[f]
IV Dexmedetomidine Levomedetomidine	 7.0 (DG1) 9.0 (DG2) 6.5 (LG1) 9.1 (LG2)	Agilent 1100	Symmetry C_{18} 150×3.9 mm 30°	NaH_2PO_4 pH 3.0 (50 mM) and methanol (62:38) 1 ml/min	UV 215 nm and Model 500TR FSA[g]

[a]Agilent Technologies, Waldbronn, Germany
[b]Waters, Milford, MA, USA
[c]Reeve Analytical, Glasgow, UK. The flow scintillation analyzer was equipped with a heterogeneous 200-µl flow cell packed with silanized cerium-activated lithium glass (GS1/TSX).
[d]Packard, Meriden, CT, USA. The flow scintillation analyzer was equipped with a homogeneous 500-µl flow cell. Monoflow 3 scintillation fluid (National Diagnostics, Atlanta, GA, USA) was used at 3 ml/min.
[e]Sigma-Aldrich, St. Louis, MO, USA
[f]NG and CG were detected as MH^+ ions at *m/z* 339 and 353, respectively, and their methyl-d3-glucuronides were used as internal standards.
[g]Perkin Elmer Life Sciences, Waltham, MA, USA. The flow scintillation analyzer was equipped with a 0.5-ml flow cell. Ultima-Flo (Perkin Elmer Life Sciences) scintillation liquid was used at 3 ml/min.

4.6.1 Methods utilizing ^{14}C-UDP-glucuronic acid (UDPGA) (I, II, IV)

Glucuronide conjugates of 4-arylalkyl-1*H*-imidazoles formed in the *in vitro* incubates were analyzed using LC coupled with a UV detector and a flow scintillation analyzer as detailed in publication I. Briefly, along with the actual incubates, separate quantitation samples were prepared and incubated essentially as described in "Glucuronidation screens", using HLM as the enzyme source. Unlike the actual samples, the quantitation samples were incubated in the presence of both ^{14}C-UDPGA (3.7-14.8 kBq) and nonradiolabeled UDPGA (0.02-0.5 mM). The glucuronides formed in these quantitation samples were then monitored using both the UV and FSA detector equipped with either a heterogeneous or homogeneous flow cell (Table 7). Thereafter, using the data obtained from the quantitation samples by the FSA detector, a calibration curve was constructed for the UV detector [glucuronide (pmol) vs. UV peak area (mAU×s)], and the UV detector was subsequently used to quantify the glucuronides formed in the actual samples incubated only with nonradiolabeled UDPGA.

4.6.2 Methods utilizing ^{3}H-levomedetomidine (I, II)

Levomedetomidine glucuronidation by HLM in studies I and II was quantified by adding ^{3}H-levomedetomidine (18.5-55.5 MBq) to the "Glucuronidation screens" incubation mixture as detailed in publication I. The glucuronides formed were monitored using LC – FSA equipped with a heterogeneous flow cell (Table 7).

4.6.3 Liquid chromatography – mass spectrometry (LC-MS) (III)

Glucuronide conjugates of nicotine and cotinine in the *in vitro* incubates were analyzed using LC coupled with a single quadrupole mass spectrometer with atmospheric pressure electrospray ionization (Table 7). Authentic glucuronide standards and their methyl-d3-derivatives as internal standards were used for quantitation by comparing peak area ratios (analyte/internal standard) to the peak area ratios generated with a standard curve. Further details can be found in publication III.

4.7 Enzyme kinetics analyses

The enzyme kinetic parameters were estimated by nonlinear regression analysis using Leonora enzyme kinetics program version 1.0 (Cornish-Bowden, 1995) (I, II), or SigmaPlot enzyme kinetics module version 1.1 (SPSS Inc., Chicago, IL, USA) (III, IV). The initial reaction velocity data were fitted to enzyme kinetics equations *(1) – (4)* described in Section 2.4.5 using appropriate weighting factors. Goodness-of-fit to the

equations was evaluated by visual inspection of the Michaelis-Menten, Eadie-Hofstee, and residual plots, the standard errors of the parameters, and R^2 values.

4.8 Prediction of hepatic clearance via glucuronidation

Hepatic clearances were estimated from human liver microsomal data using equations *(5) – (10)* described in Section 2.4.6 and the parameters presented in Tables 8 and 9.

Table 8 *Scaling factors used for CL predictions of human liver microsomal data.*

Parameter	Value	Reference
MPPGL	32 mg per gram liver	Barter et al., 2007
w_L	25.7 g liver per kg body weight	Davies and Morris, 1993
Q_H	20.7 ml per min per kg body weight	Davies and Morris, 1993

Table 9 *Drug-dependent parameters used for CL predictions of human liver microsomal data. References are presented in parentheses.*

Parameter	Dexmedetomidine	Nicotine
$f_{u,p}$	0.06[a]	0.95 (Hukkanen et al., 2005)
R_B	0.72[a]	1.00[b]
$f_{u,b}$	0.083	0.95
$f_{u,\text{ in vitro}}$	0.50 (Toivonen, 2007)	1.00 (Toivonen, 2007)

[a]unpublished observation, Orion Pharma Study Report
[b]assumption; value not available

4.9 Biosynthesis and nuclear magnetic resonance (NMR) analyses of dex- and levomedetomidine glucuronides

Dexmedetomidine glucuronides DG1 and DG2, and levomedetomidine glucuronide LG1 were prepared using biosynthesis catalyzed by HLM, as described in detail in publication IV. The regioisomeric glucuronides were separated using SPE followed by fraction collection by LC. The final glucuronide products were lyophilized. One-dimensional and two-dimensional NOESY ^{1}H NMR spectra of the glucuronide samples dissolved in D_2O were recorded using a Varian Unity INOVA 600 MHz spectrometer (Varian, Inc., Palo Alto, CA, USA).

5. Results

5.1 Analytical methods

5.1.1 Methods utilizing ^{14}C-UDPGA (I, II, IV)

4-Arylalkyl-1*H*-imidazole glucuronides were analyzed by LC using a UV detector in series with FSA (Table 7), as detailed in Section 4.6.1. Typical LC-UV-FSA chromatograms of the separation of dexmedetomidine and its regioisomeric glucuronides DG1 and DG2 are presented in Fig. 10. Retention times of the different 4-arylalkyl-1*H*-imidazole glucuronides were between 4.8 min and 9.1 min (Table 7), whereas the aglycone substrates eluted between 10 min and 14 min. This "two-detector method" was found to be more sensitive (detection limit ~5-10 pmol) than the FSA alone (detection limit ~100–200 pmol according to Coughtrie et al., 1986).

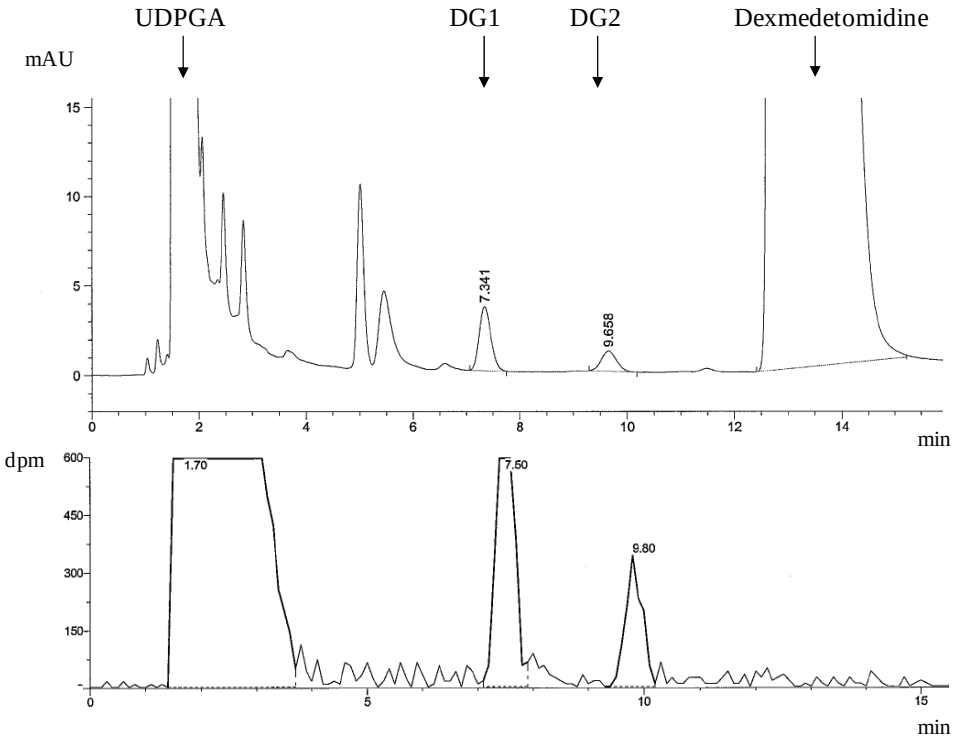

Figure 10 *Detection of dexmedetomidine glucuronidation by LC using UV detection (above) and flow scintillation analyzer (below). The chromatograms demonstrate the detection of DG1 and DG2 produced by incubation of dexmedetomidine (0.5 mM) with HLM.*

5.1.2 Methods utilizing ^{3}H-levomedetomidine (I, II)

Along with the method utilizing ^{14}C-UDPGA, a method utilizing ^{3}H-labeled aglycone substrate was developed for the levomedetomidine glucuronidation experiments. ^{3}H-levomedetomidine was added to the *in vitro* incubates and the glucuronides formed were analyzed by LC-FSA (Table 7). This method was found to be highly applicable for *in vitro* kinetic assays. Since the relative proportion of the radiolabel was higher, this method was more sensitive than the method utilizing ^{14}C-UDPGA. The limitation of this method is that radiolabeled substrates are rarely available, whereas the method utilizing ^{14}C-UDPGA can be used universally.

5.1.3 LC-MS (III)

Nicotine and cotinine glucuronides were analyzed by LC-MS using authentic glucuronide standards and their methyl-d3-derivatives as internal standards. Typical LC-MS chromatograms of nicotine and cotinine incubations with human UGT1A4 and UGT2B10 are presented in Fig. 11. Separation of the glucuronides from the unreacted aglycone substrates was performed using a novel pentafluorophenylpropyl-bonded column and a trifluoroacetic acid – methanol gradient (Table 7). Good retention was obtained for these highly hydrophilic glucuronides, which have very poor retention by conventional C_{18} columns. The retention times of nicotine and cotinine glucuronides were approximately 6.3 and 8.3 min, respectively, whereas their aglycone substrates eluted between 11 min and 13 min. In the course of the study, the retention times of the glucuronides were not constant (variation at least ± 1 min between batches), probably due to instability of the column used. However, quantitation was reliable, as the internal standards always eluted at the same retention time as the respective glucuronides. The limit of detection was 0.5 or 1.0 pmol for NG and CG, respectively, showing a clearly improved sensitivity over the LC-UV-FSA system used for 4-arylalkyl-1*H*-imidazole glucuronides. The limitation of this method is that authentic glucuronide standards as well as respective internal standards are needed for reliable quantitation by MS.

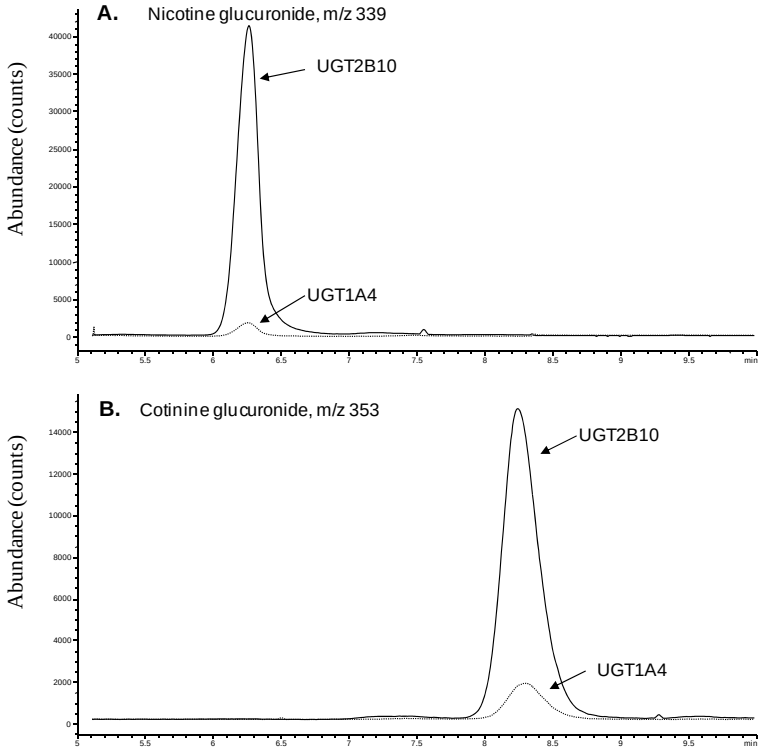

Figure 11 *LC-MS chromatograms of nicotine (A) or cotinine (B) (0.5 mM) incubation with human UGT1A4 or UGT2B10. NG and CG were detected as MH^+ ions at m/z 339 and 353, respectively.*

5.2 Biosynthesis and structural characterization of dex- and levomedetomidine glucuronides (IV)

The 4-arylalkyl-1*H*-imidazoles investigated are subject to glucuronidation at the two imidazole ring nitrogens, N_1 and N_3 (Fig. 9). Accordingly, when dexmedetomidine was incubated with HLM, two *N*-glucuronide products were detected in the respective LC-UV chromatogram (Fig. 10). The peak area ratio of these two regioisomeric glucuronides ("G1:G2") was ~4:1. However, when the other 4-arylalkyl-1*H*-imidazoles (Fig. 9) were incubated with HLM, primarily one glucuronide product, named "G1" according to the elution order, was formed, while the formation of the later eluting glucuronide, "G2", was negligible (<5%). The G1 and G2 peaks were isolated from the HLM incubates of dex- and levomedetomidine and analyzed by LC-MS. An MH^+ ion at *m/z* 377 was observed in all four samples, indicating the formation of two regioisomeric monoglucuronides from both dex- and levomedetomidine by HLM.

For further structural characterization, dex- and levomedetomidine regiomeric glucuronides were produced using biosynthesis by HLM, and the purified, lyophilized regioisomers were subjected to NMR analyses (IV). The samples for NMR contained 0.25 mg DG1, 0.13 mg DG2, or 1.6 mg LG1. The LG1 sample contained ~5% of

levomedetomidine N_1-glucuronide (LG2) as an “impurity” since it was considered unnecessary to separate these regioisomers after the HLM incubation due to the low relative proportion of LG2.

Inter-glycosidic NOE correlations indicated that DG1 and DG2 are the N_3- and N_1-glucuronides of dexmedetomidine, respectively, and LG1 is the N_3-glucuronide of levomedetomidine. Thus, N_3 was shown to be the preferred glucuronidation site of these 4-arylalkyl-1*H*-imidazoles, at least in the cases of dex- and levomedetomidine. The proposed 3D structures of the glucuronides are presented in Fig. 12.

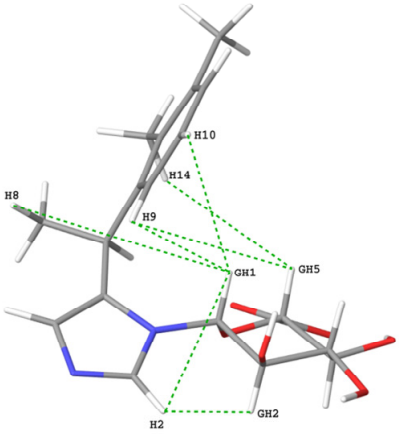

DG1

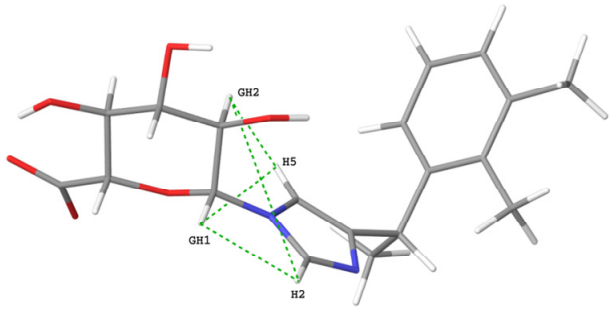

DG2

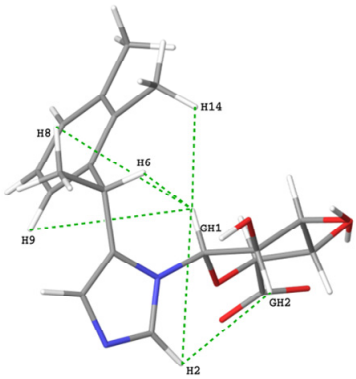

LG1

Figure 12 *Proposed structures of DG1 (N_3-glucuronide of dexmedetomidine); DG2 (N_1-glucuronide of dexmedetomidine); and LG1 (N_3-glucuronide of levomedetomidine) based on experimental 1D and 2D NMR data. Key NOE correlations used in the identification of the different glucuronides are indicated by dashed lines. All distances between correlating protons are smaller than 5Å in the depicted structures.*

5.3 *N*-Glucuronidation by human and animal tissue microsomes

5.3.1 4-Arylalkyl-1*H*-imidazoles (II, IV)

Differences across species in the *N*-glucuronidation of 4-arylalkyl-1*H*-imidazoles were investigated using dex- and levomedetomidine as model substrates. Human and animal liver microsomes were incubated with the model substrates using a 0.5 mM substrate concentration, and the formation of the stereo-/regioisomeric glucuronides DG1, DG2, LG1, and LG2 was analyzed. HLM catalyzed the glucuronidation of dex- and levomedetomidine more actively than the liver microsomes of any other species (Table 10). Besides HLM, only dog liver microsomes glucuronidated medetomidine at considerable rates. Human intestine microsomes were also tested, and they catalyzed the *N*-glucuronidation of medetomidine at a very low rate, only 0.1-2% of the rate found in HLM.

Table 10 *N-Glucuronidation of the compounds studied by human and animal liver microsomes and by human intestine microsomes.*

The substrate concentration in the assays was 0.5 mM. Activities were measured in duplicate (<15% difference), and mean data are presented. Note that while the same batch of HLM was used for all substrates, the batch of HIM used for dex-and levomedetomidine incubations was different from the batch used for nicotine and cotinine incubations; thus the HIM results are not directly comparable.

	Human liver	Human intestine	Rat liver	Mouse liver	Guinea-pig liver	Rabbit liver	Dog liver	Mini-pig liver	Monkey liver
	UGT activity (pmol/min/mg)								
Dexmedetomidine									
DG1	801	11	1.1	N.D.	13	2.1	108	1.2	3.9
DG2	185	2.2	2.0	N.D.	11	1.3	8.6	N.D.	38
Levomedetomidine									
LG1	1410	N.D.	N.D.	N.D.	15	N.D.	381	N.D.	2.8
LG2	67	1.6	5.8	N.D.	5.0	N.D.	N.D.	N.D.	19
Nicotine	220	0.077	N.M.	N.M.	N.M.	N.M.	N.M.	N.M.	N.M.
Cotinine	108	N.D.	N.M.	N.M.	N.M.	N.M.	N.M.	N.M.	N.M.

N.D. = activity below quantification limit (0.2 pmol/min/mg for DG1, DG2, LG1, and LG2, and 0.04 and 0.08 pmol/min/mg for NG and CG, respectively).
N.M. = not measured

HLM catalyzed the *N*-glucuronidation of dex- and levomedetomidine regioselectively, and N_3-glucuronide (i.e. DG1 or LG1) was the prevailing product (Table 10). Especially levomedetomidine conjugation by HLM was highly regioselective, producing 95% LG1, while 80% DG1 was formed from dexmedetomidine. Essentially similar high preference for the G1 regioisomer formation (>95% G1) was seen with the other 4-arylalkyl-1*H*-

imidazole substrates, including atipamezole (unpublished observation). In these cases, the site of glucuronidation (N_3 or N_1) was not characterized by NMR analyses. It is, however, tempting to suggest based on the structural characterization of dex- and levomedetomidine glucuronides that also other 4-arylalkyl-1*H*-imidazoles investigated are preferentially glucuronidated at N_3 (Fig. 9). Also dog liver microsomes preferentially catalyzed the formation of DG1 and LG1, while the regioselectivity of Cynomolgus monkey liver microsomes was different, as relatively much more of each G2 glucuronide was formed and only low levels of DG1 and LG1 were detected.

5.3.2 Nicotine and cotinine (III)

The *N*-glucuronidation of nicotine and cotinine was screened only in human liver and intestine microsomes. HLM catalyzed nicotine and cotinine glucuronidation at moderate rates; the rates were, however, lower than those measured for dex- and levomedetomidine glucuronidation (Table 10). HIM catalyzed nicotine glucuronidation at a very low rate, which was only ~0.1% of the rate found in the liver. Cotinine glucuronidation by HIM was not detected.

5.4 *N*-Glucuronidation by recombinant human UGTs

5.4.1 4-Arylalkyl-1*H*-imidazoles (II, IV)

In the first set of experiments (study II), *N*-glucuronidation activity of human recombinant UGTs 1A3, 1A4, 1A6, and 1A9 towards medetomidine enantiomers and atipamezole was tested. Only UGT1A4 catalyzed the *N*-glucuronidation of these substrates, and the observed activities were low (II: Table 2). In the same experiment, UGT1A4 was shown to efficiently catalyze the *N*-glucuronidation of 4-aminobiphenyl, a known substrate of UGT1A4 (Green and Tephly, 1996). In fact, 4-aminobiphenyl glucuronidation rate by UGT1A4 was 25-fold that of levomedetomidine, whereas the difference in the V_{max} values of levomedetomidine and 4-aminobiphenyl glucuronidation by HLM was much smaller (1.89 vs. 5.07 nmol/min/mg) (II: Table 1). These results indicated that, in addition to UGT1A4, another UGT isoenzyme(s) contributes to the glucuronidation of medetomidine and other 4-arylalkyl-1*H*-imidazoles in the human liver.

In the search for the “missing” UGT, a set of recombinant UGTs encoding two different UGT enzymes simultaneously was prepared (unpublished data). Based on previous findings from the coexpression of different UGTs (Kurkela et al., 2007), it was speculated that hetero-oligomerization of UGT1A4 with another UGT enzyme could stimulate the activity of UGT1A4 to the level observed in HLM. The glucuronidation experiments were performed using lysed cell homogenate preparates, and the usual step of

isolating the microsomal membranes was skipped. When levomedetomidine (50 µM) was incubated with cells coinfected with UGT1A4 and UGT2B10, the formation of LG1 was unexpectedly observed to be 10 times more efficient than in any other coinfection sample. Moreover, a high preference for LG1 formation (97%) was observed in this "UGT1A4+UGT2B10" sample, while in all other samples the relative proportion of LG1 was ~80%. This finding indicated that UGT2B10, either alone or as a hetero-oligomer with UGT1A4, could catalyze the *N*-glucuronidation of the compounds investigated.

Sixteen recombinant human UGT enzymes, including the newly discovered UGT2B10, were then tested for their ability to catalyze the *N*-glucuronidation of dex- and levomedetomidine. Recombinant UGTs were used as cell homogenates since preliminary experiments showed that the activity of UGT2B10 declined upon the isolation of microsomal membranes, as detailed in Section 5.6.3. Four different human UGTs, namely 1A3, 1A4, 2B7, and 2B10, catalyzed to different degrees the *N*-glucuronidation of medetomidine enantiomers (Fig. 13). The highest (normalized) activity towards dexmedetomidine was exhibited by UGT1A4, while lower activities were observed with the three other enzymes, in the order UGT2B10 >> UGT1A3 ≈ UGT2B7. In the case of levomedetomidine, the highest glucuronidation rate was measured with UGT2B10, whereas the activities of the other UGTs were considerably lower. Thus, according to the first screen against 16 human UGTs, UGT1A4 and UGT2B10 in particular seemed to play a major role in medetomidine glucuronidation, while the contributions of UGTs 1A3 and 2B7 were minor.

Levomedetomidine glucuronidation by UGT2B10 was highly regioselective, as only LG1 was formed (Fig. 13). On the contrary, UGT1A4 produced both LG1 and LG2 in a ratio of 2:1. In the case of dexmedetomidine, UGT1A4 showed a preference for DG1 formation (87%), while UGT2B10 activity showed no significant regioselectivity. *N*-Glucuronidation of atipamezole, another 4-arlylalkyl-1*H*-imidazole, by UGT2B10 produced only the G1 glucuronide, whereas both G1 and G2 were formed by UGT1A4 at a low rate (unpublished observation).

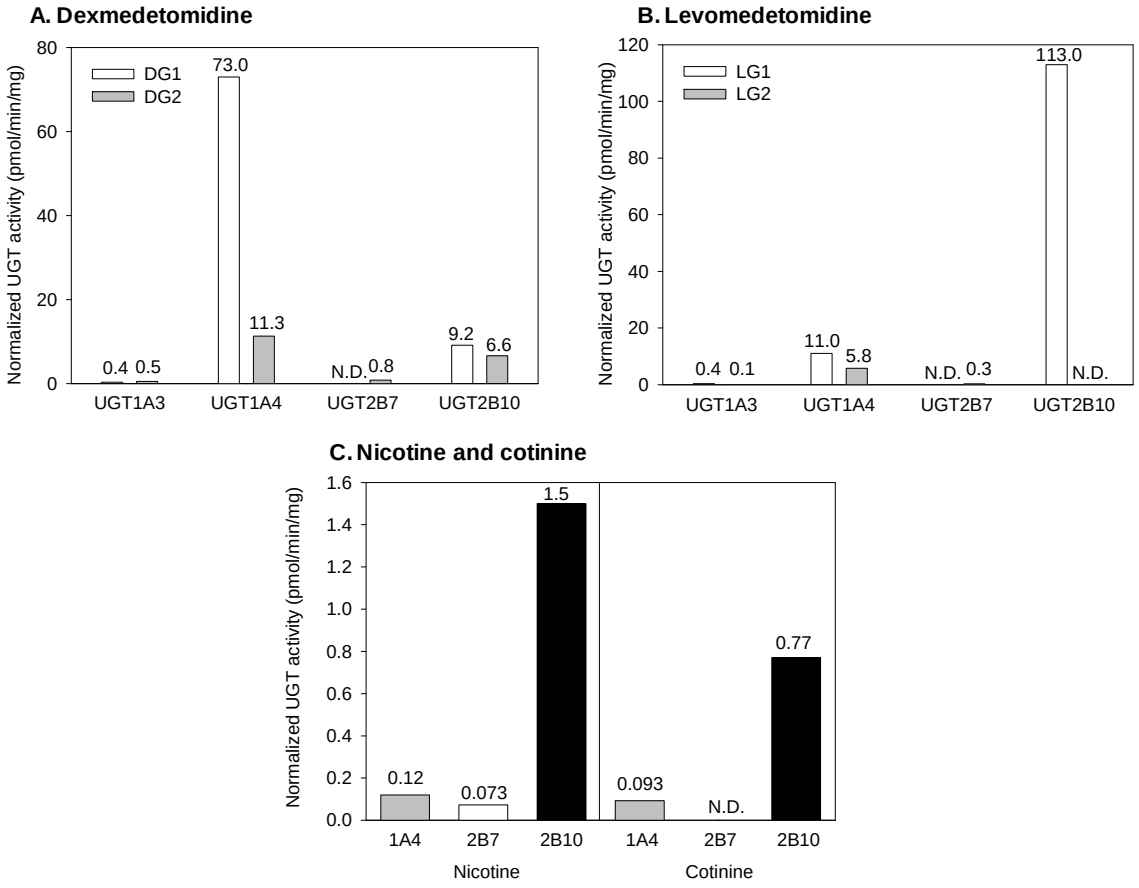

Figure 13 *N-Glucuronidation of studied compounds by human recombinant UGTs. The activity values are directly comparable, as they are normalized to the expression level of each UGT batch.*

The substrate concentration in the assays was 0.5 mM. Dex- and levomedetomidine *N*-glucuronidation by UGTs 1A1, 1A5, 1A6-1A10, 2B4, 2B11, 2B15, 2B17, and 2B28 was also tested, but no activity was observed. Nicotine and cotinine *N*-glucuronidation by UGT1A9 was also assayed, but no activity was observed. Activities were measured in duplicate (<15% difference), and the mean data are presented. The relative expression levels per milligram of protein in different UGT batches were 25.87, 1.96, 2.90, and 0.26 for UGTs 1A3, 1A4, 2B7, and 2B10, respectively, when dex- and levomedetomidine glucuronidations were assayed, and 0.80, 1.51, and 1.56 for UGTs 1A4, 2B7, and 2B10 when nicotine and cotinine glucuronidations were assayed.

5.4.2 Nicotine and cotinine (III)

UGT1A4 and UGT1A9 were previously reported to catalyze nicotine glucuronidation (Kuehl and Murphy, 2003), although the measured activities were rather low. Also UGT2B7 was shown to catalyze some *N*-glucuronidation reactions (Zhang et al., 2004; Xu et al., 2006). Based on these findings, *N*-glucuronidation of nicotine and cotinine was screened using recombinant human UGT1A4, UGT1A9, and UGT2B7, along with UGT2B10. The glucuronidation experiments were conducted using cell homogenates to preserve the activity of UGT2B10 (see Section 5.6.3 for details). The results indicated

that, in terms of normalized activity, UGT2B10 is the most active human UGT in both nicotine and cotinine *N*-glucuronidation (Fig. 13). UGT1A4 catalyzed nicotine and cotinine *N*-glucuronidation at a lower but detectable rate. UGT1A9 showed no activity towards nicotine or cotinine, but a low level of nicotine glucuronidation by UGT2B7 was detected. Cotinine glucuronidation by UGT2B7 was not observed.

5.5 mRNA expression of UGT enzymes in human tissues (III)

The mRNA expression levels of three *N*-glucuronidating UGT enzymes, UGT1A4, UGT2B7, and UGT2B10, were determined in selected human tissues using a quantitative RT-PCR method. The levels of UGT1A4, UGT2B7, and UGT2B10 in the human liver were comparable (Fig. 14). The UGT2B10 gene was exclusively expressed, at least at the level of mRNA, in the liver, while it was not expressed, for example, in the small intestine (detection limit 0.05% of the liver level). UGT1A4 and UGT2B7, on the other hand, were expressed at significant levels in several other tissues, including the small intestine. These results are in good agreement, at least with respect to UGT2B7 and UGT2B10, with a recent report on the expression levels of 15 UGT enzymes in various human tissues (Ohno and Nakajin, 2009). However, compared with the results presented here, somewhat lower expression levels of UGT1A4 in the liver were reported by Ohno and Nakajin.

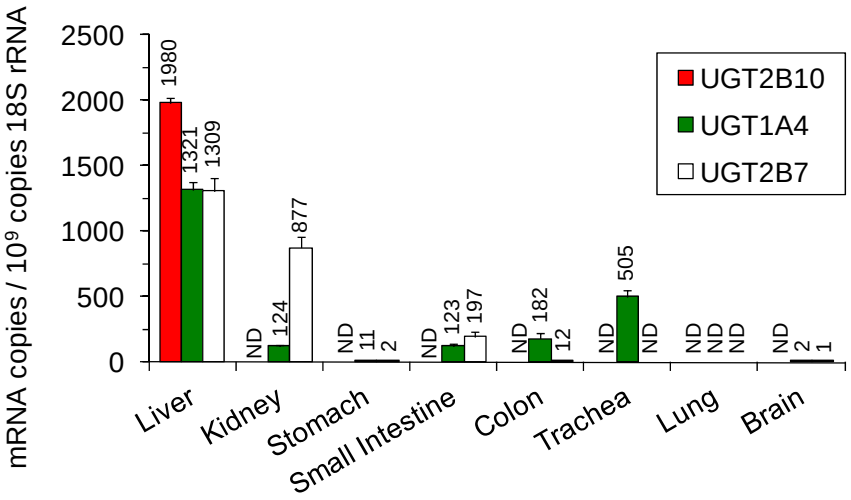

Figure 14 *mRNA expression levels of N-glucuronidating enzymes in human tissues.*

5.6 Optimization of incubation conditions for kinetic assays

5.6.1 Choice of incubation buffer and pH (unpublished data)

Atipamezole glucuronidation by HLM and human UGT1A4 was tested at 13 different pH values, ranging from 4.5 to 9.0. While both regioisomeric atipamezole glucuronides, G1 and G2, were formed by UGT1A4, only G1 was formed by HLM. The relative glucuronidation rate of atipamezole was highest at pH 8.0 in both enzyme preparations (Fig. 15). However, the glucuronidation rates at pH 7.4 were only 10-30% lower than at pH 8.0. Glucuronidation of other 4-arylalkyl-1*H*-imidazoles, such as dex- and levomedetomidine, as a function of pH was highly similar to atipamezole (data not shown). Atipamezole *N*-glucuronidation rates were comparable in different incubation buffers, Tris or phosphate buffer pH 7.4. Based on these findings, phosphate buffer pH 7.4 was used in subsequent kinetic assays.

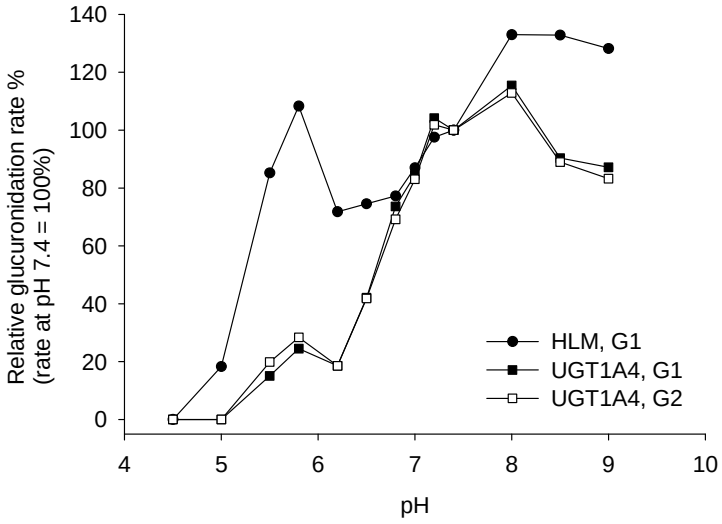

Figure 15 *Atipamezole N-glucuronidation by HLM and human UGT1A4 as a function of pH. Atipamezole concentration in the incubations was 50 µM (HLM) or 1 mM (UGT1A4). The formation rate of G2 was below the detection limit in all HLM samples.*

5.6.2 Latency-disrupting agents (II, IV)

The effect of two commonly used latency-disrupting agents, the detergent Triton and the pore-forming peptide alamethicin, on dexmedetomidine glucuronidation by HLM and UGT1A4 was tested. Interestingly, Triton activated DG1 and DG2 formations in these enzyme preparations differently. Firstly, the optimal concentration of Triton (0.4 mg per mg protein) activated HLM-catalyzed DG2 formation sevenfold, while the activation of DG1 formation was only threefold (Fig. 16). Furthermore, while Triton activated DG2

formation by UGT1A4 about twofold, DG1 formation was significantly decreased already at the lowest concentrations of Triton. Alamethicin, on the other hand, activated both DG1 and DG2 formations by HLM equally, about fourfold (IV: Fig. 3), and maximal activation was observed at an alamethicin concentration of ≥25 µg per mg protein. However, alamethicin had no effect, activation or inhibition, on dexmedetomidine glucuronidation by UGT1A4. As expected, the effect of Triton on dexmedetomidine glucuronidation was overall highly concentration-dependent, while the effect of alamethicin was constant after reaching the full activation. The use of alamethicin seemed therefore beneficial, and alamethicin was used in the kinetic assays of liver microsome incubations. As alamethicin did not activate glucuronidation by recombinant UGT preparations, it was not added to these incubates.

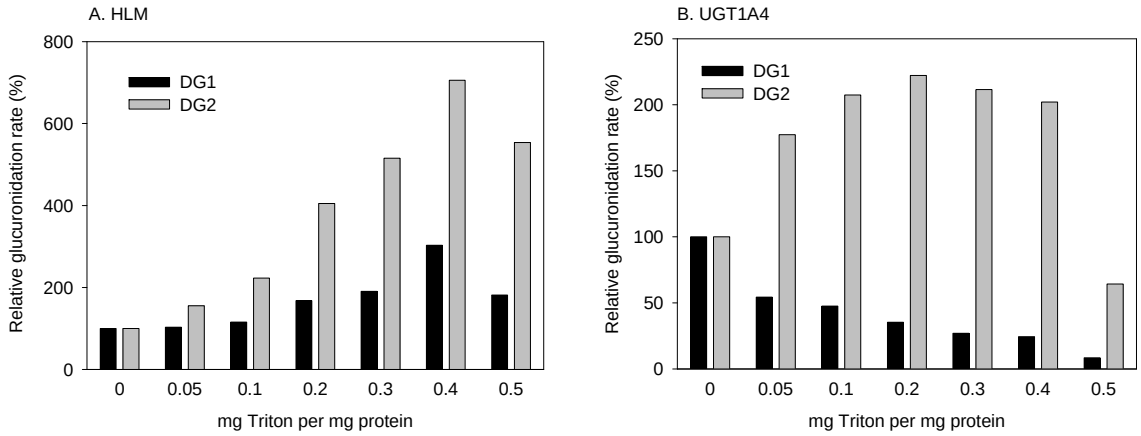

Figure 16 *Effect of Triton on dexmedetomidine (0.5 mM) glucuronidation by HLM and recombinant human UGT1A4 (relative glucuronidation rate; rate without Triton = 100%).*

5.6.3 Use and stability of different recombinant UGT preparations (III)

Recombinant UGTs are generally used as microsomal preparates, as these enzymes are located within the endoplasmic reticulum of cells. Another option is to use insect cells as a lysed cell homogenate without isolation of microsomal membranes. When the UGT2B10 cell homogenate was tested along with microsomal membranes prepared from the same UGT batch, the normalized levomedetomidine glucuronidation rate was almost fourfold higher in the cell homogenate than in the microsomal membrane (unpublished observation). In addition, a 2.5-fold higher glucuronidation rate in cell homogenate vs. microsomal membrane was detected when nicotine was used as the substrate (III: Fig. 3). This suggests that the activity of UGT2B10 declines with isolation of microsomal membranes and can partly explain why the *N*-glucuronidation activity of this enzyme has not been previously discovered. Furthermore, preliminary experiments indicate that the activity of UGT2B10 preparates decreases, at least to some extent, during storage at -80°C. In the case of UGT1A4, however, the normalized activities of cell homogenate and

microsomal membrane towards nicotine glucuronidation were very similar (III: Fig. 3). Therefore, UGT2B10 was used as a cell homogenate in further kinetic assays, while UGT1A4 incubations were conducted using either the cell homogenate or the microsomal membrane.

5.7 Kinetic characterization of glucuronidation

5.7.1 4-Arylalkyl-1*H*-imidazoles (II, IV)

The glucuronidation screens revealed that *N*-glucuronides of 4-arylalkyl-1*H*-imidazoles were formed only in human and dog liver microsomes (Table 10). Therefore, detailed kinetic assays were performed using liver microsomes of these two species. HLM generally catalyzed these reactions much more efficiently than dog liver microsomes (II: Table 1). The apparent K_m values for the formation of five different 4-arylalkyl-1*H*-imidazole *N*-glucuronides by HLM, ranging from 4.0 µM (atipamezole) to 78 µM (detomidine), indicated rather high affinity. On the other hand, dog liver microsomes catalyzed the *N*-glucuronidation of 4-arylalkyl-1*H*-imidazoles at a rather poor affinity (apparent K_m values between 279 µM and 1640 µM).

Further kinetic characterization of dexmedetomidine glucuronidation by HLM indicated biphasic kinetics, strongly suggesting the involvement of two different UGTs in this reaction (Fig. 17). The apparent K_{m1} values (the high-affinity components) for DG1 and DG2 formations by HLM were both below 10 µM, while the K_{m2} values (the low-affinity components) were much higher, >1 mM (Table 11). The apparent V_{max} values indicated a preference for DG1 formation. In the case of levomedetomidine, the kinetics of the prevailing regioisomer, LG1, by HLM was significantly different from LG2 formation. LG1 formation by HLM exhibited monophasic kinetics with a high affinity, K_m 14 µM, along with substrate inhibition observed at high concentrations (Fig. 18, Table 11). LG2, by contrast, was formed by HLM at a low rate and at a poor affinity.

When *N*-glucuronidation kinetics of dexmedetomidine by recombinant UGTs was assayed, large differences between UGT1A4 and UGT2B10 were observed. The affinity of UGT1A4 was low, K_m 0.6-0.7 mM, for both DG1 and DG2 formation, but the normalized V_{max} values, particularly in the case of DG1, were relatively high (Table 12). By contrast, UGT2B10 exhibited much higher affinity for dexmedetomidine, K_m values between 10 µM and 20 µM for both DG1 and DG2 formations, but the normalized V_{max} values were low. While the V_{max} values observed with HLM and recombinant UGTs are not directly comparable, as the amounts of the UGT enzymes per mg protein in these preparates are not equal, comparison of K_m values can be made. When the K_m values of dexmedetomidine glucuronidation by HLM, UGT1A4, and UGT2B10 are compared, the K_m values of UGT2B10 were very close to the high-affinity K_{m1}s observed in HLM, while the K_ms of UGT1A4 resembled the low-affinity K_{m2}s in HLM (Tables 11 and 12).

The kinetics of levomedetomidine *N*-glucuronidation by UGT2B10 highly resembled the kinetics observed in HLM (Fig. 18). Firstly, only N_3-glucuronide (i.e. LG1) was formed, and, moreover, the reaction showed a high affinity, K_m 7.4 µM, and a mild substrate inhibition (Table 12), which was the case also with HLM. By contrast, the affinity of UGT1A4 towards both LG1 and LG2 formations was rather poor. The normalized V_{max} of UGT2B10 in LG1 formation was also considerably higher than that of UGT1A4.

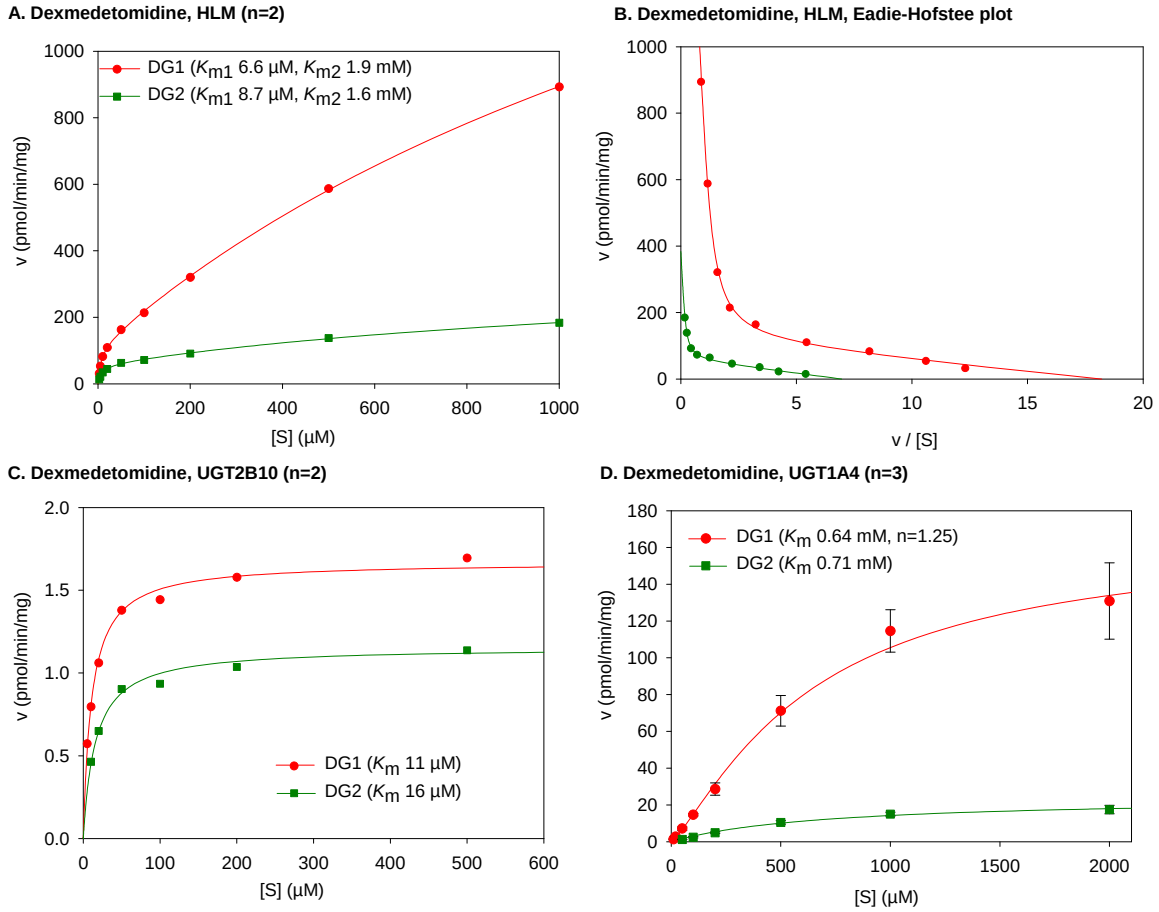

Figure 17 *Representative kinetic plots for dexmedetomidine N-glucuronidation by HLM (A; and Eadie-Hofstee plot; B); human UGT2B10 (C); and human UGT1A4 (D).*
The incubation conditions were as presented in Table 6. The glucuronidation rates represent the mean of two independent determinations, or the mean (±S.D.) of three independent determinations. The glucuronidation rates by recombinant UGTs presented here are not normalized according to the relative expression levels.

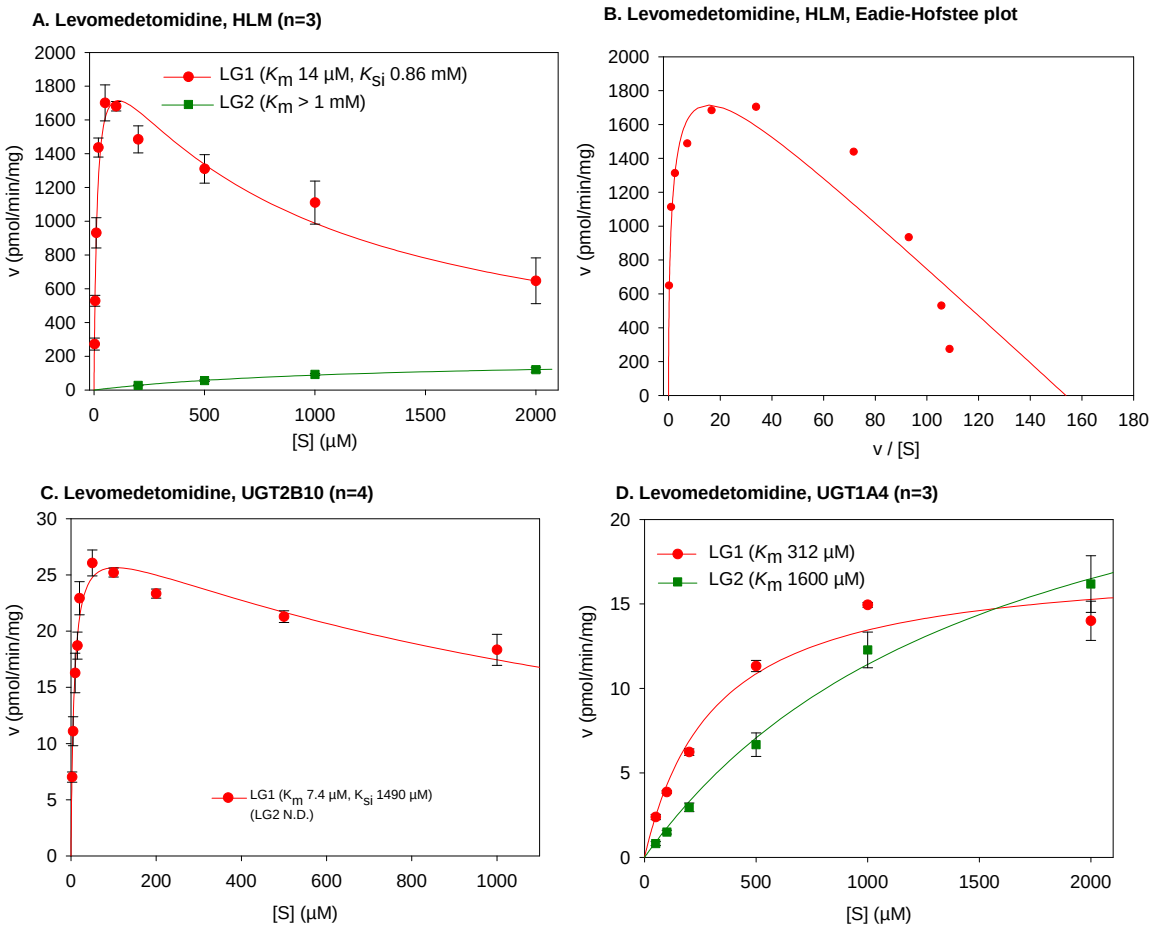

Figure 18 *Representative kinetic plots for levomedetomidine N-glucuronidation by HLM (A; and Eadie-Hofstee plot; B); human UGT2B10 (C); and human UGT1A4 (D).*

The incubation conditions were as presented in Table 6. The glucuronidation rates represent the mean (±S.D.) of three of four independent determinations. The glucuronidation rates by recombinant UGTs presented here are not normalized according to the relative expression levels.

Table 11 *Kinetic parameters for glucuronidation of studied compounds by HLM.*
The data are presented as mean ± standard error of parameter fit.

	HLM			
	K_{m1}	K_{m2}	V_{max1}	V_{max2}
	µM	*µM*	*pmol/min/mg*	*pmol/min/mg*
Dexmedetomidine				
DG1 [a]	6.61±1.10	1930±190	12±7	2290±140
DG2[a]	8.73±1.23	1590±380	59.0±3.3	325 ± 43
Levomedetomidine				
LG1 [b]	14.0±0.4		2150 ± 28	
LG2 [c]	>1000		121 ± 15	
Nicotine	331±26		290±7	
Cotinine	1250±190		370±23	

[a]Two-enzyme equation (Eq. 4, see Section 2.4.5)
[b]Substrate inhibition equation (Eq. 3), K_{si} 860±30 µM;
[c]Kinetic constants could not be determined with confidence. In this case, the V_{max} value indicates the highest observed glucuronidation rate at 2 mM substrate concentration.

Table 12 *Kinetic parameters for glucuronidation of studied compounds by human UGT1A4 and UGT2B10.*
The data are presented as mean ± standard error of parameter fit.

	UGT1A4			UGT2B10		
	K_m	V_{max}	V_{max} (normal) [a]	K_m	V_{max}	V_{max} (normal)[a]
	µM	*pmol/min/mg*		*µM*	*pmol/min/mg*	
Dexmedetomidine						
DG1	644±132[b]	167±17	85.0±8.7	10.8±0.8	1.67±0.03	1.67±0.03
DG2	706±116	24.3±1.7	12.4±0.9	15.7±1.5	1.15±0.02	1.15±0.02
Levomedetomidine						
LG1	312±44	17.7±0.8	9.01±0.42	7.42±0.64[c]	29.3±0.8	29.3±0.8
LG2	1600±300	29.7±3.0	15.1±1.6	N.D.		
Nicotine	2420±360	3.99±0.30	0.302±0.023	288±15	3.30±0.05	3.30±0.05
Cotinine	1540±200	14.9±0.8	1.13±0.06	1030±90	19.3±0.6	19.3±0.6

N.D. = activity below quantification limit (0.2 pmol/min/mg for dex- and levomedetomidine, and 0.04 and 0.08 pmol/min/mg for nicotine and cotinine, respectively).
[a]Normalized V_{max} values were calculated by dividing the V_{max} value (pmol/min/mg) by the relative expression level of the UGTs. The relative expression levels of UGT1A4 cell homogenate used for levo-and dexmedetomide, UGT1A4 microsomal membrane used for nicotine and cotinine, and UGT2B10 cell homogenate used for all substrates were 1.96, 13.21, and 1.00, respectively.
[b]Hill equation (Eq. 2, see Section 2.4.5), n=1.25
[c]Substrate inhibition equation (Eq. 3), K_{si} 1490±190 µM

5.7.2 Nicotine and cotinine (III)

Kinetic assays of nicotine and cotinine *N*-glucuronidation indicated that HLM catalyzed nicotine glucuronidation at a higher affinity (K_m 0.33 mM) than cotinine (K_m 1.3 mM), while the V_{max} values were comparable (Table 11). The observed kinetic parameters corresponded reasonably well with previously reported results (Ghosheh et al., 2001; Ghosheh and Hawes, 2002b; Nakajima et al., 2002c). When kinetic analyses were performed using recombinant human UGTs, the K_m of UGT2B10 towards nicotine, 0.29 mM, was very similar to the value observed in HLM, while the affinity of UGT1A4 was markedly lower (2.4 mM) (Table 12). In the case of cotinine glucuronidation, the K_m values of UGT1A4, UGT2B10, and HLM were all close to each other (1.0-1.5 mM). Despite this, the expression-normalized V_{max} of recombinant UGT2B10 in cotinine glucuronidation was significantly higher than that of UGT1A4.

5.8 Estimates of hepatic clearance via glucuronidation (unpublished data)

The kinetic data obtained from dexmedetomidine and nicotine glucuronidation experiments by HLM (Table 11) were used for *in vitro – in vivo* scaling. The estimates of intrinsic clearances, $CL_{int,\ in\ vitro}$ (i.e. V_{max}/K_m ratios), and hepatic clearances via glucuronidation, $CL_{H,\ gluc}$, are presented in Table 13. In the case of dexmedetomidine, the estimated intrinsic clearances for DG1 and DG2 formations by the high-affinity component (catalyzed by UGT2B10) were at least tenfold those of the low-affinity component (catalyzed by UGT1A4) indicating that UGT2B10 is mostly responsible for the hepatic glucuronidation of dexmedetomidine. The calculated $CL_{H,\ gluc}$ of dexmedetomidine was 24% of the observed *in vivo* clearance in blood (12.5 ml/min/kg) (data in file), whereas in the case of nicotine the calculated $CL_{H,\ gluc}$ was ~5% of the total clearance (14.5 ml/min/kg) (Hukkanen et al., 2005). These estimates correlate well with the *in vivo* situation since it has been reported that 3-5% of nicotine is eliminated as a direct glucuronide conjugate (Hukkanen et al., 2005), while 30-40% of dexmedetomidine has been estimated to be excreted in human urine as N_3- and N_1-glucuronides (data in file).

Table 13 *Estimated hepatic clearances via glucuronidation, $CL_{H,\ gluc}$, for dexmedetomidine and nicotine calculated from human liver microsomal data (Table 11).*

	$CL_{int,\ in\ vitro}$ high-affinity component[a] *µl/min/mg*	$CL_{int,\ in\ vitro}$ low-affinity component[b] *µl/min/mg*	$\Sigma CL_{int,\ in\ vitro}$ *µl/min/mg*	$CL_{H,\ gluc}$ (predicted) *ml/min/kg*	$CL_{in\ vivo}$ (observed) *ml/min/kg*
Dexmedetomidine			25[c]	2.9 (24%[d])	12.5[e]
DG1	17	1.2			
DG2	6.8	0.20			
Nicotine	0.88		0.88	0.67 (5%)	14.5[f]

[a] V_{max1}/K_{m1} for reactions obeying biphasic kinetics and V_{max}/K_m for reactions obeying Michaelis-Menten kinetics

[b] V_{max2}/K_{m2} for reactions obeying biphasic kinetics

[c] sum of $CL_{int,\ in\ vitro}$ for the high- and low-affinity formations of DG1 and DG2

[d] % of the observed clearance

[e] *In vivo CL* of dexmedetomidine in human plasma after intravenous administration was 9.0 ml/min/kg (data in file). *CL* in blood was calculated by dividing plasma clearance with R_B (Table 9).

[f] *In vivo CL* of nicotine in human plasma after intravenous administration was approximately 14.5 ml/min/kg (Hukkanen et al., 2005). *CL* in blood was calculated by dividing plasma clearance with R_B (Table 9).

6. Discussion

6.1 Methods developed for the detection of *N*-glucuronides

4-Arylalkyl-1*H*-imidazoles glucuronides were analyzed by LC using flow scintillation analyzer in series with a UV detector (Table 7). The reasons leading to the development of this particular method were severalfold. Firstly, authentic glucuronide standards were not available, and therefore, the development of a universal method utilizing radiolabeled cofactor, ^{14}C-UDPGA, for the detection of a number of 4-arylalkyl-1*H*-imidazole glucuronides was pursued. Furthermore, the applicability of biosynthetic approaches to produce the *N*-glucuronides was limited since sufficient amounts of these *N*-glucuronides were formed only by HLM. The formation of the two regioisomeric glucuronides from each substrate also complicated the purification process. During development of the analytical methods it was noticed that the low levels of the regioisomeric *N*-glucuronide conjugates formed in the *in vitro* samples could not be detected by the flow scintillation analyzer alone. The UV detector was therefore coupled is series with the FSA, yielding a better sensitivity (~0.2-1 pmol/min/mg) (Fig. 10).

Nicotine and cotinine glucuronides were analyzed by LC-MS using commercially available glucuronide standards along with the respective internal standards (Table 7). In previous studies, clear difficulties emerged in measuring these activities due to the combination of low *N*-glucuronidation rates of nicotine and cotinine by recombinant UGTs and the use of less sensitive LC-UV and LC-FSA methods (Ghosheh and Hawes, 2002b; Nakajima et al., 2002a). Developing the LC method for these analytes proved challenging, as both the glucuronides and the aglycone substrates are highly polar. Nonetheless, using a novel column suitable for hydrophilic analytes and gradient elution, good retention and separation were obtained (Fig. 11). This method enabled the detection of low levels (<0.1 pmol/min/mg) of nicotine and cotinine glucuronides in the recombinant UGT samples.

6.2 Species- and tissue-selective *N*-glucuronidation of investigated compounds

While many primary arylamines are generally *N*-glucuronidated by humans and a wide variety of animal species (Zenser et al., 1998), the *N*-glucuronidation of aliphatic tertiary amines is mostly limited to humans (Chiu and Huskey, 1998). In the case of aromatic *N*-heterocycles, however, the *N*-glucuronidation across species is highly compound-dependent due to the structural diversity of this group of substances (Soars et al., 2001b; Kaku et al., 2004; Shiratani et al., 2008). In this study, the results of the human and animal liver microsome incubations indicated that the *N*-glucuronidation of the imidazole compound medetomidine is largely limited to humans (Table 10). Similarly, the *N*-

glucuronidation of nicotine and cotinine has been previously reported to be mostly restricted to humans (Ghosheh and Hawes, 2002a). These results suggested that these substrates might be metabolized by the same, human-specific UGT.

The *N*-glucuronidation of the compounds investigated was also tissue-selective. While HLM efficiently glucuronidated medetomidine, nicotine, and cotinine, the glucuronidation rates in human intestinal microsomes were <2% of the rates measured in HLM (Table 10). This finding strongly suggests that the human UGT enzyme responsible for the glucuronidation of these compounds is highly expressed in the human liver, but not in the intestine.

6.3 Role of human UGT2B10 in catalyzing *N*-glucuronidation

Four human UGTs catalyzed the *N*-glucuronidation of the compounds studied. The initial screens indicated that the contribution of UGT1A3 and UGT2B7 to these reactions is not significant, while the contributions of UGT1A4 and particularly UGT2B10 are fundamental (Fig. 13).

Evidence that UGT2B10 plays a major role in the *N*-glucuronidation of the studied compounds, including nicotine, cotinine, and dex- and levomedetomidine, was supported by several findings. Firstly, the activity assays of recombinant UGTs clearly demonstrated that the normalized activity of UGT2B10 towards these compounds is much higher than the activity of any other enzyme, including UGT1A4 (Fig. 13). Only in the case of dexmedetomidine was the normalized activity of UGT1A4 higher than that of UGT2B10. Secondly, kinetic analyses revealed that the kinetics of UGT2B10 towards these substrates highly resembled the kinetics observed in HLM (Tables 11 and 12). UGT2B10 and HLM catalyzed the *N*-glucuronidation of dex- and levomedetomidine at high affinities, the estimated K_m values ranging between 7 µM and 16 µM, while nicotine and cotinine were lower affinity substrates. The UGT1A4-catalyzed reactions generally showed markedly lower affinities. Furthermore, the regioselectivity of UGT2B10 in dex- and levomedetomidine *N*-glucuronidation highly resembled the regioselectivity observed in HLM (Figs. 17 and 18). Finally, the measured mRNA levels in human tissues, although not a direct measure for the protein levels of the UGTs, suggested that the amount of UGT2B10 in the liver is considerable and in the same range as UGT1A4, if not higher (Fig. 14). Moreover, UGT2B10 was not expressed in the human intestine, which is in accordance with the finding that the compounds studied were very poorly glucuronidated by HIM (Table 10). Taken together, these results highlight the importance of UGT2B10 in the *N*-glucuronidation of these four substrates in the human liver.

The finding that UGT2B10 catalyzes nicotine and cotinine *N*-glucuronidation was made simultaneously by our laboratory (III) and by Chen and coworkers (2007). UGT2B10 was found to be responsible also for the *N*-glucuronidation of some carcinogenic tobacco-specific nitrosamines such as 4-(methylnitrosamino)-1-(3-pyridyl)-1-butanol (NNAL) (Chen et al., 2008b), suggesting that this enzyme plays an important role in the detoxification of some harmful chemicals. A functional single-nucleotide

polymorphism, UGT2B10^{67Tyr} variant, was reported to be related to reduced *N*-glucuronidation rates by HLM (Chen et al., 2008a), indicating that polymorphism of this enzyme may result in interindividual variation in the glucuronidation of UGT2B10 substrates.

6.4 Regio- and stereoselective *N*-glucuronidation of medetomidine

N-Glucuronidation of both dex- and levomedetomidine produced two regioisomeric glucuronides, at N_3 and N_1 of the imidazole ring. Structural characterization by NMR revealed that DG1 and LG1, the prevailing dex- and levomedetomidine glucuronides, respectively, are both conjugated at N_3 (Fig. 9). *N*-Glucuronidation of levomedetomidine by HLM and the major UGT enzyme 2B10 was highly regioselective, producing almost exclusively LG1, while dexmedetomidine glucuronidation by HLM yielded also DG2 (~20%), the N_1-glucuronide, along with DG1.

Kinetic analyses showed that the *N*-glucuronidation of medetomidine was also stereoselective. While the affinities of the UGT enzymes toward both enantiomers were comparable with the high affinity of UGT2B10 and a lower affinity of UGT1A4 (Table 12), the stereoselectivity mainly originated from the highly different turnover rates. Whereas UGT2B10 catalyzed levomedetomidine glucuronidation at a superior normalized rate relative to dexmedetomidine, UGT1A4 was more active towards dexmedetomidine.

6.5 *In vivo* relevance of *in vitro N*-glucuronidation assays

The goals here were to evaluate, using different *in vitro* techniques, the interspecies differences in *N*-glucuronidation and to elucidate which human UGT enzymes catalyze these reactions. The results demonstrated that the *N*-glucuronidation of the 4-arylalkyl-1*H*-imidazoles investigated was largely limited to humans, while the human-specific *N*-glucuronidation of nicotine and cotinine has been reported earlier (Ghosheh and Hawes, 2002a; Kuehl and Murphy, 2003). IVIVS of human liver microsomal data was performed to estimate the role of glucuronidation in the hepatic elimination of dexmedetomidine and nicotine (Table 13). The accuracy of the predictions indicated that this type of kinetic data can be used also for scaling purposes. Expression-normalized glucuronidation rates and kinetic characterization were found to be important tools in interpreting the results of recombinant human UGT experiments. Based on these assays, UGT2B10 was shown to be mainly responsible for the *N*-glucuronidation of medetomidine enantiomers, nicotine, and cotinine in the human liver, while the role of UGT1A4 was less important. It is tempting to speculate that UGT2B10 is also responsible for the glucuronidation of a wide variety of other nitrogen-containing drugs and xenobiotics. UGT2B10 may overall play a role in the human-specificity of many *N*-glucuronidation reactions.

7. Conclusions

1. LC-UV combined with radioisotope detection and LC-MS methods were developed to analyze *N*-glucuronide conjugates from different *in vitro* samples, including human and animal liver microsomes and recombinant human UGTs (I, III, IV).
2. *N*-Glucuronidation of medetomidine enantiomers was shown to be largely restricted to the human liver, while the glucuronidation activities measured in the human intestine and in the rat, mouse, guinea-pig, rabbit, dog, mini-pig, and monkey liver were rather low or below detection limits (IV).
3. Human UGT2B10 was found to catalyze different *N*-glucuronidation reactions in the human liver. This previously little-studied enzyme turned out to be the predominant UGT enzyme catalyzing the *N*-glucuronidation of nicotine and its major metabolite cotinine (III).
4. In addition, UGT2B10 was shown to be a major contributor to the *N*-glucuronidation of dex- and levomedetomidine in the human liver (IV).
5. Recombinant UGT2B10 enzyme produced in baculovirus-infected insect cells loses activity during the isolation of microsomal membranes and during freeze-thaw cycling. The use of freshly prepared cell homogenates, when possible, is thus recommended (III, IV).
6. *N*-Glucuronidation of medetomidine was observed to be highly regio- and stereospecific. In the human liver and in human recombinant UGT2B10, both medetomidine enantiomers are conjugated mainly at the N_3 of the imidazole ring (IV).
7. Regio- and stereospecific *N*-glucuronidation of medetomidine was explained by complex kinetics observed in human UGT1A4 and UGT2B10. UGT2B10 was found to be a high-affinity (low K_m) enzyme towards medetomidine, while affinity of UGT1A4 was considerably lower (IV).
8. The results indicate the potential importance of human UGT2B10, along with UGT1A4, in the hepatic glucuronidation of various nitrogen-containing drugs and xenobiotics.

References

Alonen A, Finel M, and Kostiainen R (2008) The human UDP-glucuronosyltransferase UGT1A3 is highly selective towards N2 in the tetrazole ring of losartan, candesartan, and zolarsartan. *Biochem Pharmacol.* **76:**763-772.

Aninat C, Piton A, Glaise D, Le Charpentier T, Langouet S, Morel F, Guguen-Guillouzo C, and Guillouzo A (2006) Expression of cytochromes P450, conjugating enzymes and nuclear receptors in human hepatoma HepaRG cells. *Drug Metab Dispos.* **34:**75-83.

Atkins WM (2004) Implications of the allosteric kinetics of cytochrome P450s. *Drug Discov Today.* **9:**478-484.

Bailey MJ and Dickinson RG (2003) Acyl glucuronide reactivity in perspective: biological consequences. *Chem Biol Interact.* **145:**117-137.

Banhegyi G, Garzo T, Fulceri R, Benedetti A, and Mandl J (1993) Latency is the major determinant of UDP-glucuronosyltransferase activity in isolated hepatocytes. *FEBS Lett.* **328:**149-152.

Bansal SK and Gessner T (1980) A unified method for the assay of uridine diphosphoglucuronyltransferase activities toward various aglycones using uridine diphospho[U-14C]glucuronic acid. *Anal Biochem.* **109:**321-329.

Barter ZE, Bayliss MK, Beaune PH, Boobis AR, Carlile DJ, Edwards RJ, Houston JB, Lake BG, Lipscomb JC, Pelkonen OR, Tucker GT, and Rostami-Hodjegan A (2007) Scaling factors for the extrapolation of in vivo metabolic drug clearance from in vitro data: reaching a consensus on values of human microsomal protein and hepatocellularity per gram of liver. *Curr Drug Metab.* **8:**33-45.

Benowitz NL (2009) Pharmacology of nicotine: addiction, smoking-induced disease, and therapeutics. *Annu Rev Pharmacol Toxicol.* **49:**57-71.

Bhana N, Goa KL, and McClellan KJ (2000) Dexmedetomidine. *Drugs.* **59:**263-270.

Bock KW and Kohle C (2004) Coordinate regulation of drug metabolism by xenobiotic nuclear receptors: UGTs acting together with CYPs and glucuronide transporters. *Drug Metab Rev.* **36:**595-615.

Borlak J, Gasparic A, Locher M, Schupke H, and Hermann R (2006) N-Glucuronidation of the antiepileptic drug retigabine: results from studies with human volunteers, heterologously expressed human UGTs, human liver, kidney, and liver microsomal membranes of Crigler-Najjar type II. *Metabolism.* **55:**711-721.

Bossuyt X and Blanckaert N (1997) Carrier-mediated transport of uridine diphosphoglucuronic acid across the endoplasmic reticulum membrane is a prerequisite for UDP-glucuronosyltransferase activity in rat liver. *Biochem J.* **323:**645-648.

Brandon EF, Raap CD, Meijerman I, Beijnen JH, and Schellens JH (2003) An update on in vitro test methods in human hepatic drug biotransformation research: pros and cons. *Toxicol Appl Pharmacol.* **189:**233-246.

Breyer-Pfaff U (2004) The metabolic fate of amitriptyline, nortriptyline and amitriptylinoxide in man. *Drug Metab Rev.* **36:**723-746.

Breyer-Pfaff U, Fischer D, and Winne D (1997) Biphasic kinetics of quaternary ammonium glucuronide formation from amitriptyline and diphenhydramine in human liver microsomes. *Drug Metab Dispos.* **25:**340-345.

Breyer-Pfaff U, Mey U, Green MD, and Tephly TR (2000) Comparative N-glucuronidation kinetics of ketotifen and amitriptyline by expressed human UDP-glucuronosyltransferases and liver microsomes. *Drug Metab Dispos.* **28:**869-872.

Brown HS, Griffin M, and Houston JB (2007) Evaluation of cryopreserved human hepatocytes as an alternative in vitro system to microsomes for the prediction of metabolic clearance. *Drug Metab Dispos.* **35:**293-301.

Bruck M, Li Q, Lamb JG, and Tukey RH (1997) Characterization of rabbit UDP-glucuronosyltransferase UGT1A7: tertiary amine glucuronidation is catalyzed by UGT1A7 and UGT1A4. *Arch Biochem Biophys.* **348:**357-364.

Burchell B (2003) Genetic variation of human UDP-glucuronosyltransferase: implications in disease and drug glucuronidation. *Am J Pharmacogenomics.* **3:**37-52.

Burchell B and Coughtrie MW (1989) UDP-glucuronosyltransferases. *Pharmacol Ther.* **43:**261-289.

Burchell B, Lockley DJ, Staines A, Uesawa Y, and Coughtrie MW (2005) Substrate specificity of human hepatic udp-glucuronosyltransferases. *Methods Enzymol.* **400:**46-57.

Chen G, Blevins-Primeau AS, Dellinger RW, Muscat JE, and Lazarus P (2007) Glucuronidation of nicotine and cotinine by UGT2B10: loss of function by the UGT2B10 Codon 67 (Asp>Tyr) polymorphism. *Cancer Res.* **67:**9024-9029.

Chen G, Dellinger RW, Gallagher CJ, Sun D, and Lazarus P (2008a) Identification of a prevalent functional missense polymorphism in the UGT2B10 gene and its association with UGT2B10 inactivation against tobacco-specific nitrosamines. *Pharmacogenet Genomics.* **18:**181-191.

Chen G, Dellinger RW, Sun D, Spratt TE, and Lazarus P (2008b) Glucuronidation of tobacco-specific nitrosamines by UGT2B10. *Drug Metab Dispos.* **36:**824-830.

Chiu SH and Huskey SW (1998) Species differences in N-glucuronidation. *Drug Metab Dispos.* **26:**838-847.

Ciotti M, Lakshmi VM, Basu N, Davis BB, Owens IS, and Zenser TV (1999) Glucuronidation of benzidine and its metabolites by cDNA-expressed human UDP-glucuronosyltransferases and pH stability of glucuronides. *Carcinogenesis.* **20:**1963-1969.

Clarke DJ and Burchell B (1994) The uridine diphosphate glucuronosyltransferase multigene family: function and regulation, in: *Conjugation-Deconjugation Reactions in Drug Metabolism and Toxicity.* (Kaufman FC ed), pp 3-43., Springer-Verlag, New York.

Cornish-Bowden A (1995) *Fundamentals of Enzyme Kinetics, revised ed.*, Portland Press, London, UK.

Coughtrie MW, Burchell B, and Bend JR (1986) A general assay for UDPglucuronosyltransferase activity using polar amino-cyano stationary phase HPLC and UDP[U-14C]glucuronic acid. *Anal Biochem.* **159:**198-205.

Coughtrie MW and Sharp S (1991) Glucuronidation of imipramine in rabbit and human liver microsomes: assay conditions and interaction with other tertiary amine drugs. *Biochem Pharmacol.* **42:**1497-1501.

Court MH (2005) Isoform-selective probe substrates for in vitro studies of human UDP-glucuronosyltransferases. *Methods Enzymol.* **400:**104-116.

Court MH and Greenblatt DJ (2000) Molecular genetic basis for deficient acetaminophen glucuronidation by cats: UGT1A6 is a pseudogene, and evidence for reduced diversity of expressed hepatic UGT1A isoforms. *Pharmacogenetics.* **10:**355-369.

Court MH, Hazarika S, Krishnaswamy S, Finel M, and Williams JA (2008) Novel polymorphic human UDP-glucuronosyltransferase 2A3: cloning, functional characterization of enzyme variants, comparative tissue expression, and gene induction. *Mol Pharmacol.* **74:**744-754.

Dahl-Puustinen ML, Aberg-Wistedt A, and Bertilsson L (1989) Glucuronidation of amitriptyline in man in vivo. *Pharmacol Toxicol.* **65:**37-39.

Davies B and Morris T (1993) Physiological parameters in laboratory animals and humans. *Pharm Res.* **10:**1093-1095.

Dehal SS, Gagne PV, Crespi CL, and Patten CJ (2003) Differential effect of common organic solvents on human UGT enzyme activities., in: *8th European ISSX Meeting*, pp 60, Drug Metabolism Reviews, Dijon, France.

Dellinger RW, Chen G, Blevins-Primeau AS, Krzeminski J, Amin S, and Lazarus P (2007) Glucuronidation of PhIP and N-OH-PhIP by UDP-glucuronosyltransferase 1A10. *Carcinogenesis.* **28:**2412-2418.

Di Marco A, D'Antoni M, Attaccalite S, Carotenuto P, and Laufer R (2005) Determination of drug glucuronidation and UDP-glucuronosyltransferase selectivity using a 96-well radiometric assay. *Drug Metab Dispos.* **33:**812-819.

Ebner T and Burchell B (1993) Substrate specificities of two stably expressed human liver UDP-glucuronosyltransferases of the UGT1 gene family. *Drug Metab Dispos.* **21:**50-55.

Ekins S, Mäenpää J, and Wrighton SA (1999) In vitro metabolism: Subcellular fractions, in: *Handbook of Drug Metabolism* (Woolf TF ed), pp 363-400., Marcel Dekker, Inc., New York.

Ethell BT, Ekins S, Wang J, and Burchell B (2002) Quantitative structure activity relationships for the glucuronidation of simple phenols by expressed human UGT1A6 and UGT1A9. *Drug Metab Dispos.* **30:**734-738.

Finel M and Kurkela M (2008) The UDP-glucuronosyltransferases as oligomeric enzymes. *Curr Drug Metab.* **9:**70-76.

Fisher MB, Campanale K, Ackermann BL, VandenBranden M, and Wrighton SA (2000) In vitro glucuronidation using human liver microsomes and the pore-forming peptide alamethicin. *Drug Metab Dispos.* **28:**560-566.

Forsman T, Lautala P, Lundstrom K, Monastyrskaia K, Ouzzine M, Burchell B, Taskinen J, and Ulmanen I (2000) Production of human UDP-glucuronosyltransferases 1A6 and 1A9 using the Semliki Forest virus expression system. *Life Sci.* **67:**2473-2484.

Ghosheh O and Hawes EM (2002a) Microsomal N-glucuronidation of nicotine and cotinine: human hepatic interindividual, human intertissue, and interspecies hepatic variation. *Drug Metab Dispos.* **30:**1478-1483.

Ghosheh O and Hawes EM (2002b) N-glucuronidation of nicotine and cotinine in human: formation of cotinine glucuronide in liver microsomes and lack of catalysis by 10 examined UDP-glucuronosyltransferases. *Drug Metab Dispos.* **30:**991-996.

Ghosheh O, Vashishtha SC, and Hawes EM (2001) Formation of the quaternary ammonium-linked glucuronide of nicotine in human liver microsomes: identification and stereoselectivity in the kinetics. *Drug Metab Dispos.* **29:**1525-1528.

Girard H, Thibaudeau J, Court MH, Fortier LC, Villeneuve L, Caron P, Hao Q, von Moltke LL, Greenblatt DJ, and Guillemette C (2005) UGT1A1 polymorphisms are important determinants of dietary carcinogen detoxification in the liver. *Hepatology.* **42:**448-457.

Green MD, Bishop WP, and Tephly TR (1995) Expressed human UGT1.4 protein catalyzes the formation of quaternary ammonium-linked glucuronides. *Drug Metab Dispos.* **23:**299-302.

Green MD, King CD, Mojarrabi B, Mackenzie PI, and Tephly TR (1998) Glucuronidation of amines and other xenobiotics catalyzed by expressed human UDP-glucuronosyltransferase 1A3. *Drug Metab Dispos.* **26:**507-512.

Green MD and Tephly TR (1996) Glucuronidation of amines and hydroxylated xenobiotics and endobiotics catalyzed by expressed human UGT1.4 protein. *Drug Metab Dispos.* **24:**356-363.

Green MD and Tephly TR (1998) Glucuronidation of amine substrates by purified and expressed UDP-glucuronosyltransferase proteins. *Drug Metab Dispos.* **26:**860-867.

Grime K and Riley RJ (2006) The impact of in vitro binding on in vitro-in vivo extrapolations, projections of metabolic clearance and clinical drug-drug interactions. *Curr Drug Metab.* **7:**251-264.

Gripon P, Rumin S, Urban S, Le Seyec J, Glaise D, Cannie I, Guyomard C, Lucas J, Trepo C, and Guguen-Guillouzo C (2002) Infection of a human hepatoma cell line by hepatitis B virus. *Proc Natl Acad Sci U S A.* **99:**15655-15660.

Guengerich FP (2008) Oxidative, reductive and hydrolytic metabolism of drugs., in: *Drug metabolism in drug design and development* (Zhang D, Zhu M and Humphreys WG eds), pp 15-36., Hoboken, New Jersey, Wiley Interscience.

Guengerich FP, Parikh A, Johnson EF, Richardson TH, von Wachenfeldt C, Cosme J, Jung F, Strassburg CP, Manns MP, Tukey RH, Pritchard M, Fournel-Gigleux S, and Burchell B (1997) Heterologous expression of human drug-metabolizing enzymes. *Drug Metab Dispos.* **25:**1234-1241.

Guillemette C (2003) Pharmacogenomics of human UDP-glucuronosyltransferase enzymes. *Pharmacogenomics J.* **3:**136-158.

Hawes EM (1998) N+-glucuronidation, a common pathway in human metabolism of drugs with a tertiary amine group. *Drug Metab Dispos.* **26:**830-837.

Hempel R, Schupke H, McNeilly PJ, Heinecke K, Kronbach C, Grunwald C, Zimmermann G, Griesinger C, Engel J, and Kronbach T (1999) Metabolism of retigabine (D-23129), a novel anticonvulsant. *Drug Metab Dispos.* **27:**613-622.

Hewitt NJ, Lechon MJ, Houston JB, Hallifax D, Brown HS, Maurel P, Kenna JG, Gustavsson L, Lohmann C, Skonberg C, Guillouzo A, Tuschl G, Li AP, LeCluyse E, Groothuis GM, and Hengstler JG (2007) Primary hepatocytes: current understanding of the regulation of metabolic enzymes and transporter proteins, and pharmaceutical practice for the use of hepatocytes in metabolism, enzyme induction, transporter, clearance, and hepatotoxicity studies. *Drug Metab Rev.* **39:**159-234.

Hiller A, Nguyen N, Strassburg CP, Li Q, Jainta H, Pechstein B, Ruus P, Engel J, Tukey RH, and Kronbach T (1999) Retigabine N-glucuronidation and its potential role in enterohepatic circulation. *Drug Metab Dispos.* **27:**605-612.

Houston JB (1994) Utility of in vitro drug metabolism data in predicting in vivo metabolic clearance. *Biochem Pharmacol.* **47:**1469-1479.
Houston JB and Kenworthy KE (2000) In vitro-in vivo scaling of CYP kinetic data not consistent with the classical Michaelis-Menten model. *Drug Metab Dispos.* **28:**246-254.
Hukkanen J, Jacob P, 3rd, and Benowitz NL (2005) Metabolism and disposition kinetics of nicotine. *Pharmacol Rev.* **57:**79-115.
Hutzler JM and Tracy TS (2002) Atypical kinetic profiles in drug metabolism reactions. *Drug Metab Dispos.* **30:**355-362.
Ingelman-Sundberg M, Sim SC, Gomez A, Rodriguez-Antona C, Johansson I, and Karlgren M (2007) Influence of cytochrome P450 polymorphisms on drug therapies: pharmacogenetic, pharmacoepigenetic and clinical aspects. New approaches and applications in chemical biology. *Pharmacol Ther.* **116:**496-526.
Itaaho K, Mackenzie PI, Ikushiro S, Miners JO, and Finel M (2008) The configuration of the 17-hydroxy group variably influences the glucuronidation of beta-estradiol and epiestradiol by human UDP-glucuronosyltransferases. *Drug Metab Dispos.* **36:**2307-2315.
Iyer R and Zhang D (2008) Role of drug metabolism in drug development, in: *Drug metabolism in drug design and development* (Zhang D, Zhu M and Humphreys WG eds), pp 261-285., Hoboken, New Jersey, Wiley Interscience.
Jakobsson J, Ekstrom L, Inotsume N, Garle M, Lorentzon M, Ohlsson C, Roh HK, Carlstrom K, and Rane A (2006) Large differences in testosterone excretion in Korean and Swedish men are strongly associated with a UDP-glucuronosyl transferase 2B17 polymorphism. *J Clin Endocrinol Metab.* **91:**687-693.
Jedlitschky G, Cassidy AJ, Sales M, Pratt N, and Burchell B (1999) Cloning and characterization of a novel human olfactory UDP-glucuronosyltransferase. *Biochem J.* **340:**837-843.
Kaderlik KR, Mulder GJ, Turesky RJ, Lang NP, Teitel CH, Chiarelli MP, and Kadlubar FF (1994) Glucuronidation of N-hydroxy heterocyclic amines by human and rat liver microsomes. *Carcinogenesis.* **15:**1695-1701.
Kaji H and Kume T (2005) Characterization of afloqualone N-glucuronidation: species differences and identification of human UDP-glucuronosyltransferase isoform(s). *Drug Metab Dispos.* **33:**60-67.
Kaku T, Ogura K, Nishiyama T, Ohnuma T, Muro K, and Hiratsuka A (2004) Quaternary ammonium-linked glucuronidation of tamoxifen by human liver microsomes and UDP-glucuronosyltransferase 1A4. *Biochem Pharmacol.* **67:**2093-2102.
Kanebratt KP and Andersson TB (2008) Evaluation of HepaRG cells as an in vitro model for human drug metabolism studies. *Drug Metab Dispos.* **36:**1444-1452.
Kassahun K, Mattiuz E, Franklin R, and Gillespie T (1998) Olanzapine 10-N-glucuronide. A tertiary N-glucuronide unique to humans. *Drug Metab Dispos.* **26:**848-855.
Kennedy T (1997) Managing the drug discovery/development interface. *Drug Discovery Today* **2:**436-444.
Kiang TK, Ensom MH, and Chang TK (2005) UDP-glucuronosyltransferases and clinical drug-drug interactions. *Pharmacol Ther.* **106:**97-132.
Kilford PJ, Stringer R, Sohal B, Houston JB, and Galetin A (2009) Prediction of drug clearance by glucuronidation from in vitro data: use of combined cytochrome P450

and UDP-glucuronosyltransferase cofactors in alamethicin-activated human liver microsomes. *Drug Metab Dispos.* **37:**82-89.

King CD, Green MD, Rios GR, Coffman BL, Owens IS, Bishop WP, and Tephly TR (1996) The glucuronidation of exogenous and endogenous compounds by stably expressed rat and human UDP-glucuronosyltransferase 1.1. *Arch Biochem Biophys.* **332:**92-100.

King CD, Rios GR, Green MD, and Tephly TR (2000) UDP-glucuronosyltransferases. *Curr Drug Metab.* **1:**143-161.

Klieber S, Hugla S, Ngo R, Arabeyre-Fabre C, Meunier V, Sadoun F, Fedeli O, Rival M, Bourrie M, Guillou F, Maurel P, and Fabre G (2008) Contribution of the N-glucuronidation pathway to the overall in vitro metabolic clearance of midazolam in humans. *Drug Metab Dispos.* **36:**851-862.

Korzekwa KR, Krishnamachary N, Shou M, Ogai A, Parise RA, Rettie AE, Gonzalez FJ, and Tracy TS (1998) Evaluation of atypical cytochrome P450 kinetics with two-substrate models: evidence that multiple substrates can simultaneously bind to cytochrome P450 active sites. *Biochemistry.* **37:**4137-4147.

Kubota T, Lewis BC, Elliot DJ, Mackenzie PI, and Miners JO (2007) Critical roles of residues 36 and 40 in the phenol and tertiary amine aglycone substrate selectivities of UDP-glucuronosyltransferases 1A3 and 1A4. *Mol Pharmacol.* **72:**1054-1062.

Kuehl GE, Lampe JW, Potter JD, and Bigler J (2005) Glucuronidation of nonsteroidal anti-inflammatory drugs: identifying the enzymes responsible in human liver microsomes. *Drug Metab Dispos.* **33:**1027-1035.

Kuehl GE and Murphy SE (2003) N-glucuronidation of nicotine and cotinine by human liver microsomes and heterologously expressed UDP-glucuronosyltransferases. *Drug Metab Dispos.* **31:**1361-1368.

Kurkela M, Garcia-Horsman JA, Luukkanen L, Morsky S, Taskinen J, Baumann M, Kostiainen R, Hirvonen J, and Finel M (2003) Expression and characterization of recombinant human UDP-glucuronosyltransferases (UGTs). UGT1A9 is more resistant to detergent inhibition than other UGTs and was purified as an active dimeric enzyme. *J Biol Chem.* **278:**3536-3544.

Kurkela M, Patana AS, Mackenzie PI, Court MH, Tate CG, Hirvonen J, Goldman A, and Finel M (2007) Interactions with other human UDP-glucuronosyltransferases attenuate the consequences of the Y485D mutation on the activity and substrate affinity of UGT1A6. *Pharmacogenet Genomics.* **17:**115-126.

Kuusela E, Raekallio M, Anttila M, Falck I, Molsa S, and Vainio O (2000) Clinical effects and pharmacokinetics of medetomidine and its enantiomers in dogs. *J Vet Pharmacol Ther.* **23:**15-20.

Lautala P, Ethell BT, Taskinen J, and Burchell B (2000) The specificity of glucuronidation of entacapone and tolcapone by recombinant human UDP-glucuronosyltransferases. *Drug Metab Dispos.* **28:**1385-1389.

Lautala P, Kivimaa M, Salomies H, Elovaara E, and Taskinen J (1997) Glucuronidation of entacapone, nitecapone, tolcapone, and some other nitrocatechols by rat liver microsomes. *Pharm Res.* **14:**1444-1448.

LeCluyse EL, Alexandre E, Hamilton GA, Viollon-Abadie C, Coon DJ, Jolley S, and Richert L (2005) Isolation and culture of primary human hepatocytes. *Methods Mol Biol.* **290:**207-229.

Lin J, Sahakian DC, de Morais SM, Xu JJ, Polzer RJ, and Winter SM (2003) The role of absorption, distribution, metabolism, excretion and toxicity in drug discovery. *Curr Top Med Chem.* **3:**1125-1154.

Lin JH and Wong BK (2002) Complexities of glucuronidation affecting in vitro in vivo extrapolation. *Curr Drug Metab.* **3:**623-646.

Luo H, Hawes EM, McKay G, Korchinski ED, and Midha KK (1991) N(+)-glucuronidation of aliphatic tertiary amines, a general phenomenon in the metabolism of H1-antihistamines in humans. *Xenobiotica.* **21:**1281-1288.

Luo H, Hawes EM, McKay G, Korchinski ED, and Midha KK (1995) N(+)-glucuronidation of aliphatic tertiary amines in human: antidepressant versus antipsychotic drugs. *Xenobiotica.* **25:**291-301.

Luukkanen L, Taskinen J, Kurkela M, Kostiainen R, Hirvonen J, and Finel M (2005) Kinetic characterization of the 1A subfamily of recombinant human UDP-glucuronosyltransferases. *Drug Metab Dispos.* **33:**1017-1026.

Mackenzie PI, Bock KW, Burchell B, Guillemette C, Ikushiro S, Iyanagi T, Miners JO, Owens IS, and Nebert DW (2005) Nomenclature update for the mammalian UDP glycosyltransferase (UGT) gene superfamily. *Pharmacogenet Genomics.* **15:**677-685.

Mackenzie PI, Gregory PA, Gardner-Stephen DA, Lewinsky RH, Jorgensen BR, Nishiyama T, Xie W, and Radominska-Pandya A (2003) Regulation of UDP glucuronosyltransferase genes. *Curr Drug Metab.* **4:**249-257.

Mackenzie PI and Hanninen O (1980) A sensitive kinetic assay for UDPglucuronosyltransferase using 1-naphthol as substrate. *Anal Biochem.* **109:**362-368.

Magdalou J, Herber R, Bidault R, and Siest G (1992) In vitro N-glucuronidation of a novel antiepileptic drug, lamotrigine, by human liver microsomes. *J Pharmacol Exp Ther.* **260:**1166-1173.

McGinnity DF, Soars MG, Urbanowicz RA, and Riley RJ (2004) Evaluation of fresh and cryopreserved hepatocytes as in vitro drug metabolism tools for the prediction of metabolic clearance. *Drug Metab Dispos.* **32:**1247-1253.

Mey U, Wachsmuth H, and Breyer-Pfaff U (1999) Conjugation of the enantiomers of ketotifen to four isomeric quaternary ammonium glucuronides in humans in vivo and in liver microsomes. *Drug Metab Dispos.* **27:**1281-1292.

Miners JO, Knights KM, Houston JB, and Mackenzie PI (2006) In vitro-in vivo correlation for drugs and other compounds eliminated by glucuronidation in humans: pitfalls and promises. *Biochem Pharmacol.* **71:**1531-1539.

Miners JO and Mackenzie PI (1991) Drug glucuronidation in humans. *Pharmacol Ther.* **51:**347-369.

Miners JO, McKinnon RA, and Mackenzie PI (2002) Genetic polymorphisms of UDP-glucuronosyltransferases and their functional significance. *Toxicology.* **181-182:**453-456.

Miners JO, Smith PA, Sorich MJ, McKinnon RA, and Mackenzie PI (2004) Predicting human drug glucuronidation parameters: application of in vitro and in silico modeling approaches. *Annu Rev Pharmacol Toxicol.* **44:**1-25.

Nakajima M, Kwon JT, Tanaka E, and Yokoi T (2002a) High-performance liquid chromatographic assay for N-glucuronidation of nicotine and cotinine in human liver microsomes. *Anal Biochem.* **302:**131-135.

Nakajima M, Tanaka E, Kobayashi T, Ohashi N, Kume T, and Yokoi T (2002b) Imipramine N-glucuronidation in human liver microsomes: biphasic kinetics and characterization of UDP-glucuronosyltransferase isoforms. *Drug Metab Dispos.* **30:**636-642.

Nakajima M, Tanaka E, Kwon JT, and Yokoi T (2002c) Characterization of nicotine and cotinine N-glucuronidations in human liver microsomes. *Drug Metab Dispos.* **30:**1484-1490.

Nakamura A, Nakajima M, Yamanaka H, Fujiwara R, and Yokoi T (2008) Expression of UGT1A and UGT2B mRNA in human normal tissues and various cell lines. *Drug Metab Dispos.* **36:**1461-1464.

Nakazawa T, Miyata K, Omura K, Iwanaga T, and Nagata O (2006) Metabolic profile of FYX-051 (4-(5-pyridin-4-yl-1h-[1,2,4]triazol-3-yl)pyridine-2-carbonitrile) in the rat, dog, monkey, and human: identification of N-glucuronides and N-glucosides. *Drug Metab Dispos.* **34:**1880-1886.

Nassar AE and Lopez-Anaya A (2004) Strategies for dealing with reactive intermediates in drug discovery and development. *Curr Opin Drug Discov Devel.* **7:**126-136.

Obach RS (1997) Nonspecific binding to microsomes: impact on scale-up of in vitro intrinsic clearance to hepatic clearance as assessed through examination of warfarin, imipramine, and propranolol. *Drug Metab Dispos.* **25:**1359-1369.

Ohno S and Nakajin S (2009) Determination of mRNA expression of human UDP-glucuronosyltransferases and application for localization in various human tissues by real-time reverse transcriptase-polymerase chain reaction. *Drug Metab Dispos.* **37:**32-40.

Oleson L and Court MH (2008) Effect of the beta-glucuronidase inhibitor saccharolactone on glucuronidation by human tissue microsomes and recombinant UDP-glucuronosyltransferases. *J Pharm Pharmacol.* **60:**1175-1182.

Omura K, Nakazawa T, Sato T, Iwanaga T, and Nagata O (2007) Characterization of N-glucuronidation of 4-(5-pyridin-4-yl-1H-[1,2,4]triazol-3-yl) pyridine-2-carbonitrile (FYX-051): a new xanthine oxidoreductase inhibitor. *Drug Metab Dispos.* **35:**2143-2148.

Ouzzine M, Barre L, Netter P, Magdalou J, and Fournel-Gigleux S (2003) The human UDP-glucuronosyltransferases: structural aspects and drug glucuronidation. *Drug Metab Rev.* **35:**287-303.

Pang KS and Rowland M (1977) Hepatic clearance of drugs. I. Theoretical considerations of a "well-stirred" model and a "parallel tube" model. Influence of hepatic blood flow, plasma and blood cell binding, and the hepatocellular enzymatic activity on hepatic drug clearance. *J Pharmacokinet Biopharm.* **5:**625-653.

Pelkonen O and Raunio H (2005) In vitro screening of drug metabolism during drug development: can we trust the predictions? *Expert Opin Drug Metab Toxicol.* **1:**49-59.

Pelkonen O and Turpeinen M (2007) In vitro-in vivo extrapolation of hepatic clearance: biological tools, scaling factors, model assumptions and correct concentrations. *Xenobiotica.* **37:**1066-1089.

Pelkonen O, Turpeinen M, Hakkola J, Honkakoski P, Hukkanen J, and Raunio H (2008) Inhibition and induction of human cytochrome P450 enzymes: current status. *Arch Toxicol.* **82:**667-715.

Pertovaara A, Haapalinna A, Sirvio J, and Virtanen R (2005) Pharmacological properties, central nervous system effects, and potential therapeutic applications of atipamezole, a selective alpha2-adrenoceptor antagonist. *CNS Drug Rev.* **11:**273-288.

Plant N (2004) Strategies for using in vitro screens in drug metabolism. *Drug Discov Today.* **9:**328-336.

Radominska-Pandya A, Bratton S, and Little JM (2005a) A historical overview of the heterologous expression of mammalian UDP-glucuronosyltransferase isoforms over the past twenty years. *Curr Drug Metab.* **6:**141-160.

Radominska-Pandya A, Ouzzine M, Fournel-Gigleux S, and Magdalou J (2005b) Structure of UDP-glucuronosyltransferases in membranes. *Methods Enzymol.* **400:**116-147.

Remmel RP, Nagar S, and Argikar U (2008) Conjugative metabolism of drugs, in: *Drug metabolism in drug design and development* (Zhang D, Zhu M and Humphreys WG eds), pp 37-62., Hoboken, New Jersey, Wiley Interscience.

Roberts SA (2003) Drug metabolism and pharmacokinetics in drug discovery. *Curr Opin Drug Discov Devel.* **6:**66-80.

Rowland A, Elliot DJ, Williams JA, Mackenzie PI, Dickinson RG, and Miners JO (2006) In vitro characterization of lamotrigine N2-glucuronidation and the lamotrigine-valproic acid interaction. *Drug Metab Dispos.* **34:**1055-1062.

Rowland A, Gaganis P, Elliot DJ, Mackenzie PI, Knights KM, and Miners JO (2007) Binding of inhibitory fatty acids is responsible for the enhancement of UDP-glucuronosyltransferase 2B7 activity by albumin: implications for in vitro-in vivo extrapolation. *J Pharmacol Exp Ther.* **321:**137-147.

Rowland A, Knights KM, Mackenzie PI, and Miners JO (2008) The "albumin effect" and drug glucuronidation: bovine serum albumin and fatty acid-free human serum albumin enhance the glucuronidation of UDP-glucuronosyltransferase (UGT) 1A9 substrates but not UGT1A1 and UGT1A6 activities. *Drug Metab Dispos.* **36:**1056-1062.

Rush WR, Alexander OF, Hall DJ, Dow RJ, Tokes L, Kurz L, and Graham DJ (1990) The metabolism of nafimidone hydrochloride in the dog, primates and man. *Xenobiotica.* **20:**123-132.

Sallustio BC, Sabordo L, Evans AM, and Nation RL (2000) Hepatic disposition of electrophilic acyl glucuronide conjugates. *Curr Drug Metab.* **1:**163-180.

Salonen JS (1989) Pharmacokinetics of medetomidine. *Acta Vet Scand Suppl.* **85:**49-54.

Salonen JS (1991) Tissue-specificity of hydroxylation and N-methylation of arylalkylimidazoles. *Pharmacol Toxicol.* **69:**1-4.

Savola JM and Virtanen R (1991) Central alpha 2-adrenoceptors are highly stereoselective for dexmedetomidine, the dextro enantiomer of medetomidine. *Eur J Pharmacol.* **195:**193-199.

Senafi SB, Clarke DJ, and Burchell B (1994) Investigation of the substrate specificity of a cloned expressed human bilirubin UDP-glucuronosyltransferase: UDP-sugar specificity and involvement in steroid and xenobiotic glucuronidation. *Biochem J.* **303:**233-240.

Shiratani H, Katoh M, Nakajima M, and Yokoi T (2008) Species differences in UDP-glucuronosyltransferase activities in mice and rats. *Drug Metab Dispos.* **36:**1745-1752.

Singh SS (2006) Preclinical pharmacokinetics: an approach towards safer and efficacious drugs. *Curr Drug Metab.* **7:**165-182.
Sinz MW and Remmel RP (1991) Isolation and characterization of a novel quaternary ammonium-linked glucuronide of lamotrigine. *Drug Metab Dispos.* **19:**149-153.
Smith PA, Sorich MJ, Low LS, McKinnon RA, and Miners JO (2004) Towards integrated ADME prediction: past, present and future directions for modelling metabolism by UDP-glucuronosyltransferases. *J Mol Graph Model.* **22:**507-517.
Smith PA, Sorich MJ, McKinnon RA, and Miners JO (2003) Pharmacophore and quantitative structure-activity relationship modeling: complementary approaches for the rationalization and prediction of UDP-glucuronosyltransferase 1A4 substrate selectivity. *J Med Chem.* **46:**1617-1626.
Soars MG, Burchell B, and Riley RJ (2002) In vitro analysis of human drug glucuronidation and prediction of in vivo metabolic clearance. *J Pharmacol Exp Ther.* **301:**382-390.
Soars MG, Fettes M, O'Sullivan AC, Riley RJ, Ethell BT, and Burchell B (2003a) Cloning and characterisation of the first drug-metabolising canine UDP-glucuronosyltransferase of the 2B subfamily. *Biochem Pharmacol.* **65:**1251-1259.
Soars MG, Riley RJ, and Burchell B (2001a) Evaluation of the marmoset as a model species for drug glucuronidation. *Xenobiotica.* **31:**849-860.
Soars MG, Riley RJ, Findlay KA, Coffey MJ, and Burchell B (2001b) Evidence for significant differences in microsomal drug glucuronidation by canine and human liver and kidney. *Drug Metab Dispos.* **29:**121-126.
Soars MG, Ring BJ, and Wrighton SA (2003b) The effect of incubation conditions on the enzyme kinetics of udp-glucuronosyltransferases. *Drug Metab Dispos.* **31:**762-767.
Sorich MJ, Smith PA, McKinnon RA, and Miners JO (2002) Pharmacophore and quantitative structure activity relationship modelling of UDP-glucuronosyltransferase 1A1 (UGT1A1) substrates. *Pharmacogenetics.* **12:**635-645.
Sorich MJ, Smith PA, Miners JO, Mackenzie PI, and McKinnon RA (2008) Recent advances in the in silico modelling of UDP glucuronosyltransferase substrates. *Curr Drug Metab.* **9:**60-69.
Staines AG, Coughtrie MW, and Burchell B (2004) N-glucuronidation of carbamazepine in human tissues is mediated by UGT2B7. *J Pharmacol Exp Ther.* **311:**1131-1137.
Sten T, Bichlmaier I, Kuuranne T, Leinonen A, Yli-Kauhaluoma J, and Finel M (2009) UDP-glucuronosyltransferases (UGTs) 2B7 and UGT2B17 display converse specificity in testosterone and epitestosterone glucuronidation, whereas UGT2A1 conjugates both androgens similarly. *Drug Metab Dispos.* **37:**417-423.
Stevens JC, Fayer JL, and Cassidy KC (2001) Characterization of 2-[[4-[[2-(1H-tetrazol-5-ylmethyl)phenyl]methoxy]methyl]quinoline N-glucuronidation by in vitro and in vivo approaches. *Drug Metab Dispos.* **29:**289-295.
Stone AN, Mackenzie PI, Galetin A, Houston JB, and Miners JO (2003) Isoform selectivity and kinetics of morphine 3- and 6-glucuronidation by human udp-glucuronosyltransferases: evidence for atypical glucuronidation kinetics by UGT2B7. *Drug Metab Dispos.* **31:**1086-1089.

Toivonen P (2007) Erilaisten in vitro-menetelmien vertailu in vivo metabolisen puhdistuman ennustamisessa., in: *Pro gradu tutkielma, Department of Pharmaceutical Chemistry*, pp 103, University of Helsinki, Helsinki.

Tsai MC and Gorrod JW (1999) Evidence for the biosynthesis of A glucuronide conjugate of (S)-(-)-nicotine, but not (S)-(-)-cotinine or (+/-)-trans-3'-hydroxycotinine by marmoset hepatic microsomes. *Drug Metabol Drug Interact.* **15:**223-237.

Tukey RH and Strassburg CP (2000) Human UDP-glucuronosyltransferases: metabolism, expression, and disease. *Annu Rev Pharmacol Toxicol.* **40:**581-616.

Tukey RH, Strassburg CP, and Mackenzie PI (2002) Pharmacogenomics of human UDP-glucuronosyltransferases and irinotecan toxicity. *Mol Pharmacol.* **62:**446-450.

Turgeon D, Carrier JS, Levesque E, Hum DW, and Belanger A (2001) Relative enzymatic activity, protein stability, and tissue distribution of human steroid-metabolizing UGT2B subfamily members. *Endocrinology.* **142:**778-787.

Tutka P, Mosiewicz J, and Wielosz M (2005) Pharmacokinetics and metabolism of nicotine. *Pharmacol Rep.* **57:**143-153.

Uchaipichat V, Mackenzie PI, Elliot DJ, and Miners JO (2006) Selectivity of substrate (trifluoperazine) and inhibitor (amitriptyline, androsterone, canrenoic acid, hecogenin, phenylbutazone, quinidine, quinine, and sulfinpyrazone) "probes" for human udp-glucuronosyltransferases. *Drug Metab Dispos.* **34:**449-456.

Uesawa Y, Staines AG, Lockley D, Mohri K, and Burchell B (2007) Identification of the human liver UDP-glucuronosyltransferase involved in the metabolism of p-ethoxyphenylurea (dulcin). *Arch Toxicol.* **81:**163-168.

Uesawa Y, Staines AG, O'Sullivan A, Mohri K, and Burchell B (2004) Identification of the rabbit liver UDP-glucuronosyltransferase catalyzing the glucuronidation of 4-ethoxyphenylurea (dulcin). *Drug Metab Dispos.* **32:**1476-1481.

Vainio O (1988) Detomidine. *Vet Rec.* **123:**655.

van de Waterbeemd H and Gifford E (2003) ADMET in silico modelling: towards prediction paradise? *Nat Rev Drug Discov.* **2:**192-204.

Vashishtha SC, Hawes EM, McCann DJ, Ghosheh O, and Hogg L (2002) Quaternary ammonium-linked glucuronidation of 1-substituted imidazoles by liver microsomes: interspecies differences and structure-metabolism relationships. *Drug Metab Dispos.* **30:**1070-1076.

Vermeir M, Annaert P, Mamidi RN, Roymans D, Meuldermans W, and Mannens G (2005) Cell-based models to study hepatic drug metabolism and enzyme induction in humans. *Expert Opin Drug Metab Toxicol.* **1:**75-90.

Wells PG, Mackenzie PI, Chowdhury JR, Guillemette C, Gregory PA, Ishii Y, Hansen AJ, Kessler FK, Kim PM, Chowdhury NR, and Ritter JK (2004) Glucuronidation and the UDP-glucuronosyltransferases in health and disease. Pharmacogenomics of human UDP-glucuronosyltransferase enzymes. *Drug Metab Dispos.* **32:**281-290.

Wikberg T, Vuorela A, Ottoila P, and Taskinen J (1993) Identification of major metabolites of the catechol-O-methyltransferase inhibitor entacapone in rats and humans. *Drug Metab Dispos.* **21:**81-92.

Williams JA, Hyland R, Jones BC, Smith DA, Hurst S, Goosen TC, Peterkin V, Koup JR, and Ball SE (2004a) Drug-drug interactions for UDP-glucuronosyltransferase substrates: a pharmacokinetic explanation for typically observed low exposure (AUCi/AUC) ratios. *Drug Metab Dispos.* **32:**1201-1208.

Williams PA, Cosme J, Vinkovic DM, Ward A, Angove HC, Day PJ, Vonrhein C, Tickle IJ, and Jhoti H (2004b) Crystal structures of human cytochrome P450 3A4 bound to metyrapone and progesterone. *Science.* **305:**683-686.

Williams PA, Cosme J, Ward A, Angove HC, Matak Vinkovic D, and Jhoti H (2003) Crystal structure of human cytochrome P450 2C9 with bound warfarin. *Nature.* **424:**464-468.

Winsnes A (1969) Studies on the activation in vitro of glucuronyltransferase. *Biochim Biophys Acta.* **191:**279-291.

Xu C, Li CY, and Kong AN (2005) Induction of phase I, II and III drug metabolism/transport by xenobiotics. *Arch Pharm Res.* **28:**249-268.

Xu L, Krenitsky DM, Seacat AM, Butenhoff JL, Tephly TR, and Anders MW (2006) N-glucuronidation of perfluorooctanesulfonamide by human, rat, dog, and monkey liver microsomes and by expressed rat and human UDP-glucuronosyltransferases. *Drug Metab Dispos.* **34:**1406-1410.

Yan Z and Caldwell GW (2003) Metabolic assessment in liver microsomes by co-activating cytochrome P450s and UDP-glycosyltransferases. *Eur J Drug Metab Pharmacokinet.* **28:**223-232.

Yan Z, Caldwell GW, Gauthier D, Leo GC, Mei J, Ho CY, Jones WJ, Masucci JA, Tuman RW, Galemmo RA, Jr., and Johnson DL (2006) N-glucuronidation of the platelet-derived growth factor receptor tyrosine kinase inhibitor 6,7-(dimethoxy-2,4-dihydroindeno[1,2-C]pyrazol-3-yl)-(3-fluoro-phenyl)-amine by human UDP-glucuronosyltransferases. *Drug Metab Dispos.* **34:**748-755.

Yin H, Bennett G, and Jones JP (1994) Mechanistic studies of uridine diphosphate glucuronosyltransferase. *Chem Biol Interact.* **90:**47-58.

Zamek-Gliszczynski MJ, Hoffmaster KA, Nezasa K, Tallman MN, and Brouwer KL (2006) Integration of hepatic drug transporters and phase II metabolizing enzymes: mechanisms of hepatic excretion of sulfate, glucuronide, and glutathione metabolites. *Eur J Pharm Sci.* **27:**447-486.

Zenser TV, Lakshmi VM, and Davis BB (1998) N-glucuronidation of benzidine and its metabolites. Role in bladder cancer. *Drug Metab Dispos.* **26:**856-859.

Zenser TV, Lakshmi VM, Hsu FF, and Davis BB (2002) Metabolism of N-acetylbenzidine and initiation of bladder cancer. *Mutat Res.* **506-507:**29-40.

Zhang D, Chando TJ, Everett DW, Patten CJ, Dehal SS, and Humphreys WG (2005) In vitro inhibition of UDP glucuronosyltransferases by atazanavir and other HIV protease inhibitors and the relationship of this property to in vivo bilirubin glucuronidation. *Drug Metab Dispos.* **33:**1729-1739.

Zhang D, Zhao W, Roongta VA, Mitroka JG, Klunk LJ, and Zhu M (2004) Amide N-glucuronidation of MaxiPost catalyzed by UDP-glucuronosyltransferase 2B7 in humans. *Drug Metab Dispos.* **32:**545-551.

Zhou J, Zhang J, and Xie W (2005a) Xenobiotic nuclear receptor-mediated regulation of UDP-glucuronosyl-transferases. *Curr Drug Metab.* **6:**289-298.

Zhou S, Chan E, Duan W, Huang M, and Chen YZ (2005b) Drug bioactivation, covalent binding to target proteins and toxicity relevance. *Drug Metab Rev.* **37:**41-213.